Energy Advances

ROYAL SOCIETY OF CHEMISTRY

REVIEW ARTICLE

View Article Online
View Journal | View Issue

Cite this: *Energy Adv.*, 2025, 4, 1075

Unlocking catalytic longevity: a critical review of catalyst deactivation pathways and regeneration technologies

Ifeanyi Michael Smarte Anekwe * and Yusuf Makarfi Isa

Catalyst deactivation remains a fundamental challenge in heterogeneous catalysis, compromising performance, efficiency, and sustainability across numerous industrial processes. This review critically examines the principal deactivation pathways including coking, poisoning, thermal degradation, and mechanical damage and evaluates the breadth of regeneration strategies developed to restore catalytic activity. Traditional methods such as oxidation, gasification, and hydrogenation are assessed alongside emerging approaches like supercritical fluid extraction (SFE), microwave-assisted regeneration (MAR), plasma-assisted regeneration (PAR) and atomic layer deposition (ALD) techniques. The environmental implications and operational trade-offs associated with each regeneration method were evaluated. By integrating recent scientific advancements with bibliometric analysis, this study identifies prevailing research trends and exposes key knowledge gaps in catalyst regeneration. Unlike prior reviews, this work offers a holistic perspective that spans multiple deactivation mechanisms and regeneration routes. Insights into process optimization and environmental impact reduction are presented to guide future innovation in sustainable catalytic system design. By contrasting current progress with unexplored potential, this study provides a basis for promoting innovation and management of sustainable catalysts. It serves as a strategic roadmap for enhancing catalyst longevity and performance in next-generation industrial applications.

Received 15th January 2025,
Accepted 23rd July 2025

DOI: 10.1039/d5ya00015g

rsc.li/energy-advances

1. Introduction

Heterogeneous catalysts are crucial in facilitating numerous chemical processes, such as the conversion of hydrocarbons and carbohydrates in various industries. They enable the efficient utilisation of limited feedstocks, which can be either renewable (*e.g.* biomass and municipal waste) or non-renewable (*e.g.* crude oil, coal, natural gas). They are used either to accelerate the reaction rate or to specifically produce the target products.[1,2] However, a notable disadvantage of using industrial catalysts is their inevitable deactivation over time, which occurs during continuous operation. While the traditional definition of catalysts implies that they cannot be consumed in chemical reactions, they are not immune to degradation. Deactivation of solid catalysts is a common consequence of various chemical and physical processes, including metal sintering, poisoning and structural deterioration, such as the dealumination of zeolites and framework collapse, which are usually the main cause of this phenomenon.[3,4] In addition, carbon deposits can form that obstruct the catalyst pores or access to the catalytic sites and originate from various compounds.[5] This deactivation results in a decline in catalytic efficiency and product selectivity, which requires careful consideration to ensure the effective design and operation of catalytic activities. The knowledge of catalyst deactivation is crucial for the development of strategies to mitigate deactivation and extend the life of the catalyst, ultimately ensuring the efficiency and sustainability of catalytic processes. Therefore, catalyst deactivation is a critical area of research being pursued in both academia and industry.

Coke generation is not only about the coke deposition in the catalyst pores and on the outer surfaces,[6] but also about the chemical processes involved in its formation. Research has been conducted to comprehend the mechanisms responsible for coke formation.[7–9] In general, three stages are distinguished in coke formation: hydrogen transfer at acidic sites, dehydrogenation of adsorbed hydrocarbons and gas polycondensation.[7] Theoretically, coke has the potential to affect the performance of the catalyst in two ways: active site poisoning (leading to overcoating of the active sites) and clogging the pores (making the active sites inaccessible to the reactants).[10] The specific kind of coke produced is dependent on both the catalyst used and the reaction parameter; therefore, methods for regeneration vary depending on the catalytic processes involved.[6] Considerable efforts have been made to prevent coke formation and extend catalyst life.[6,11,12] Nevertheless, catalyst deactivation is inevitable and

School of Chemical and Metallurgical Engineering, University of the Witwatersrand, Johannesburg, 2050, South Africa. E-mail: anekwesmarte@gmail.com

can occur rapidly, as in fluidised catalytic cracking (FCC), or gradually over several years, as in NH_3 synthesis.[13] In addition, the time required for the regeneration of a particular catalyst is largely influenced by the rate of coke formation. Continuous regeneration of the catalyst becomes economically imperative when coke formation proceeds rapidly.[14]

Regeneration of deactivated catalysts to restore their activity is both practically and economically valuable, as the deactivation of catalysts in industrial catalytic processes is a constant challenge.[14] Therefore, the interest lies in the development of reliable, effective and cost-efficient technologies for the regeneration of catalysts. Given the great concern about the deactivation of catalysts due to coke fouling, especially in the petrochemical sector, our study aims to investigate different regeneration techniques. The resuscitation of the catalytic performance of a completely deactivated catalyst using conventional regeneration methods is a major challenge. Fortunately, the deactivation of catalysts by coke buildup is frequently reversible. Coke can be readily eliminated through oxidation using oxygen or air.[10,15] In many industrial processes, coke is burnt with air to revive used catalysts. However, the exothermic nature of coke combustion presents difficulties as it can lead to hot spots localised temperature gradients and ultimately destroy the catalyst.[14,16,17] Various advanced regeneration techniques can eliminate coke at mild temperatures and thus increase regeneration efficiency while minimising catalyst damage. For example, coked ZSM-5 catalysts can be regenerated at low temperatures with ozone (O_3).[18]

The science of catalyst deactivation and regeneration during biomass conversion has seen significant advancements over the years, resulting in a growing body of literature on this critical topic.[19–24] Many studies highlight that coke formation is a prevalent deactivation pathway in industrial processes involving organic compounds and heterogeneous catalysts. Vogt *et al.*[24] delved into the role of carbon species deposited from various feedstock molecules or formed over time during catalytic processes, shedding light on their contribution to deactivation. Zheng *et al.*[25] systematically analyzed the primary causes of catalytic deactivation while evaluating corresponding regeneration strategies. Similarly, Hatta *et al.*[26] conducted in-depth research on catalyst deactivation and regeneration, particularly focusing on CO methanation reactions. In addition, Wu *et al.*[27] reviewed advances in understanding poisoning mechanisms of alkali metals in selective catalytic reduction (SCR) catalysts, with a comprehensive discussion on various catalyst systems, including vanadium-based, manganese-based, and cerium-based catalysts. Liu *et al.*[28] explored the effects of toluene feeding time and iron concentration on catalytic performance and deactivation characteristics while examining regeneration properties. Furthermore, Liu *et al.*[29] combined *in situ* electrochemical infrared spectroscopy and density functional theory (DFT) calculations to investigate deactivation and regeneration processes of Pt surfaces during oxygen reduction reactions (ORR) in the presence of SO_2 and NO.

Despite these valuable contributions, existing studies often focus on specific catalysts or regeneration methods, leaving gaps in comprehensively addressing coke formation, its prevention, and the environmental implications of regeneration techniques. This study builds upon previous work to bridge these gaps by presenting an integrated critical review of coke formation, catalyst deactivation, and regeneration. To this end, this study contributes uniquely to the field by first conducting a bibliometric review to trace research trends and highlight developments in catalyst deactivation and regeneration. It then provides an in-depth examination of coke formation mechanisms, causes of deactivation, and preventive strategies. Additionally, conventional regeneration techniques, including oxidation (using air/O_2, O_3, and NO_x), gasification (using CO_2 and H_2), and hydrogenation (using H_2), are systematically reviewed, while discussing emerging regeneration methods. Importantly, the study emphasizes the environmental impacts of these regeneration methods, a dimension often overlooked in previous research. Finally, it addresses challenges in coke attenuation and offers insights into optimizing catalyst design and processes. By combining bibliometric analysis, technical evaluation, and environmental assessment, this study aims to provide a holistic understanding of catalyst deactivation and regeneration, advancing the field toward sustainable and efficient catalytic systems.

2. Method

The data for the bibliometric analysis was collected *via* Web of Science (WoS). The methodology flowchart is shown in Fig. 1 and illustrates the individual steps. The search was conducted for 2 days in March 2024 and was limited to the years 2000–2024 and subject areas such as materials science, engineering, chemistry, chemical engineering, energy, environmental science and related fields. The search was further refined by document type (article) and language (English). The search was divided into three categories: (i) catalyst coke, (ii) catalyst stability and deactivation, and (iii) catalyst regeneration, to determine the

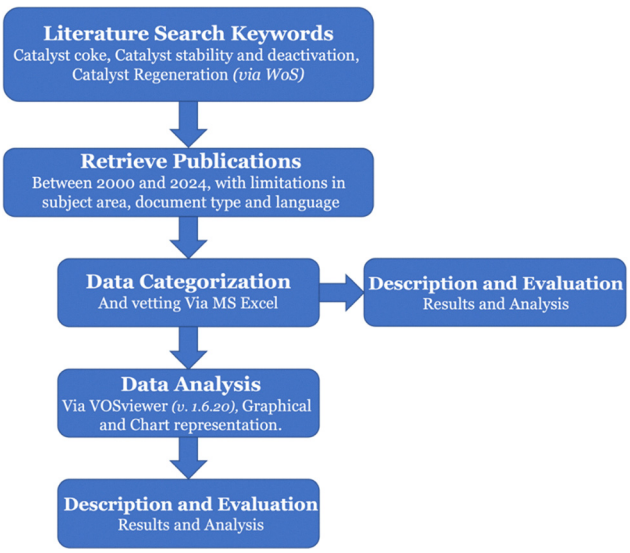

Fig. 1 Methodology flowchart for the bibliometric analysis.

number of research articles in each category. For catalyst coke, seven keywords were used in the initial search (''coke'', ''coking'', ''coke deposition'', ''coke deposit'', ''coke formation'', ''coke resistance'', ''carbon deposition''). Five keywords were used for catalyst stability and deactivation (including ''catalyst deactivation'', ''catalyst stability'', ''deactivation'', ''deactivation mechanism''), while five keywords were used for catalyst regeneration (including ''catalyst regeneration'', ''catalytic regeneration'', ''continuous catalyst regeneration'', ''*in situ* regeneration'', ''regeneration of catalysts''). The number of publications for each category after the application of each limitation was recorded.

Publication data were exported from Web of Science as a ''tab-delimited file'' and checked for completeness by searching for the presence of keywords in the title, abstract, keywords and article. Duplicate publications were removed, and the remaining publications were grouped by focus keywords, countries and regions. A list of keywords based on each parameter (tab-delimited file) was employed for visualisation analysis with VOSviewer (version 1.6.20). VOSviewer is a free software tool for creating and visualising bibliometric networks developed by Nees Jan van Eck and Ludo Waltman at the Centre for Science and Technology Studies at Leiden University. Network maps were created to visualise the keyword analysis based on the three keywords and their relationships to other keywords, with the size of the circle representing the volume of work, study or publication in the focus area.

In addition, a critical review of research on catalyst coke formation, deactivation, and regeneration methods was conducted, capturing a broad spectrum of scientific efforts and providing valuable insights into the evolution of knowledge, methodologies, and persistent challenges in the field.

3. Bibliometric review analysis of research trend on catalyst coke, stability, deactivation and regeneration from 2000–2024 – results and discussion

This section presents the results of a bibliometric analysis covering three key areas: catalyst coke (CC), catalyst stability and deactivation (CSD) and catalyst regeneration (CR) from 2000 to 2024 using Web of Science (WoS) publication data. A total of 30 873, 44 834 and 1987 research articles were considered for ''catalyst coke'', ''catalyst stability and deactivation'', and ''catalyst regeneration'', respectively, all of which were published in English. This section focuses on several factors, including the output of publications from the three focus areas by year (2000–2024), country, region and keywords. The data for 2024 was collected from January to May and cannot be actively used for comparison.

3.1. Publication trend (2000 – May 2024)

The analysis shows a steady upward trend in publications in all focus areas, with the number of publications increasing from 432, 669 and 18 publications in 2000 to 2413, 3083 and 180 publications for CC, CSD and CR, respectively, in 2023, representing significant growth rates of 82.1%, 78.3% and 90% for CC, CSD and CR respectively in the period from 2000 to 2023 (Fig. 2a). Forecasts indicate that total output in 2024 will exceed that of 2023. It is noteworthy that research on CC and CSD has been more extensive compared to CR, with over 92% and 94% more work, respectively than CR over the last 24 years. This emphasises the need for a stronger focus on catalyst regeneration, which is crucial for effective heterogeneous catalysis. Fig. 2b shows the 23 countries actively involved in CC, CSD and CR research, with China in the lead, followed by the USA, Germany and Japan. These four countries together contribute to 54.7% of the total publications, while other countries account for the rest. While studies on CCS and CSD are extensive, research on CR is still relatively limited. Furthermore, the regional distribution of publications on CC, CSD and CR shows that the Asia-Pacific region is leading, followed by Europe and North America (see Fig. 3A–C). On average, these regions make the highest contributions, while Africa makes the smallest contribution. The trend follows Asia-Pacific > Europe > North America > South America > Oceania and Australia > Africa. While China continues to lead the way in heterogeneous catalysis research in the Asia-Pacific region, Europe and North America (Fig. 3D) are also actively contributing to the advancement of heterogeneous catalysis research to promote sustainable energy alternatives.

The results of the VOS analysis show that the keywords catalyst ''coke'', ''deactivation'' and ''regeneration'' have remained constantly present over the last two decades, with their occurrence either doubling or tripling. Using VOSviewer, the minimum number of keyword occurrences was set to 25. Of the 6033 keywords generated, 115 met this threshold. Each node is represented by a specific colour based on year of publication, with different sizes indicating the frequency of occurrence. Larger circles represent more frequent use of the term, while smaller circles represent less frequent use.[30] The links between the keywords represent their co-occurrence. They show how often pairs of keywords occur together in the data set and thus reveal the relationships and patterns between the keywords. The analysis revealed that the terms catalyst coke and catalyst deactivation are studied more intensively compared to catalyst regeneration, which is reflected in the smaller size of the nodes for the latter (Fig. 4a). The different colours show the distribution of the keywords over the last two decades. This observation confirms previous findings, which emphasise that relatively little attention is paid to research on catalyst regeneration in this area. Fig. 4b illustrates the citation analysis of the most frequently cited authors. The entries included 1860 publications, with 326 publications meeting the threshold of 50 citations. Out of the 326 publications, 229 showed the largest set of linked items. The term ''links'' refers to the number of connections an author has with other authors. Specifically, in the context of citation links between researchers, the ''links'' attribute means the number of citations link a researcher has with others. The size of a node corresponds to the frequency of citations, with larger nodes indicating more

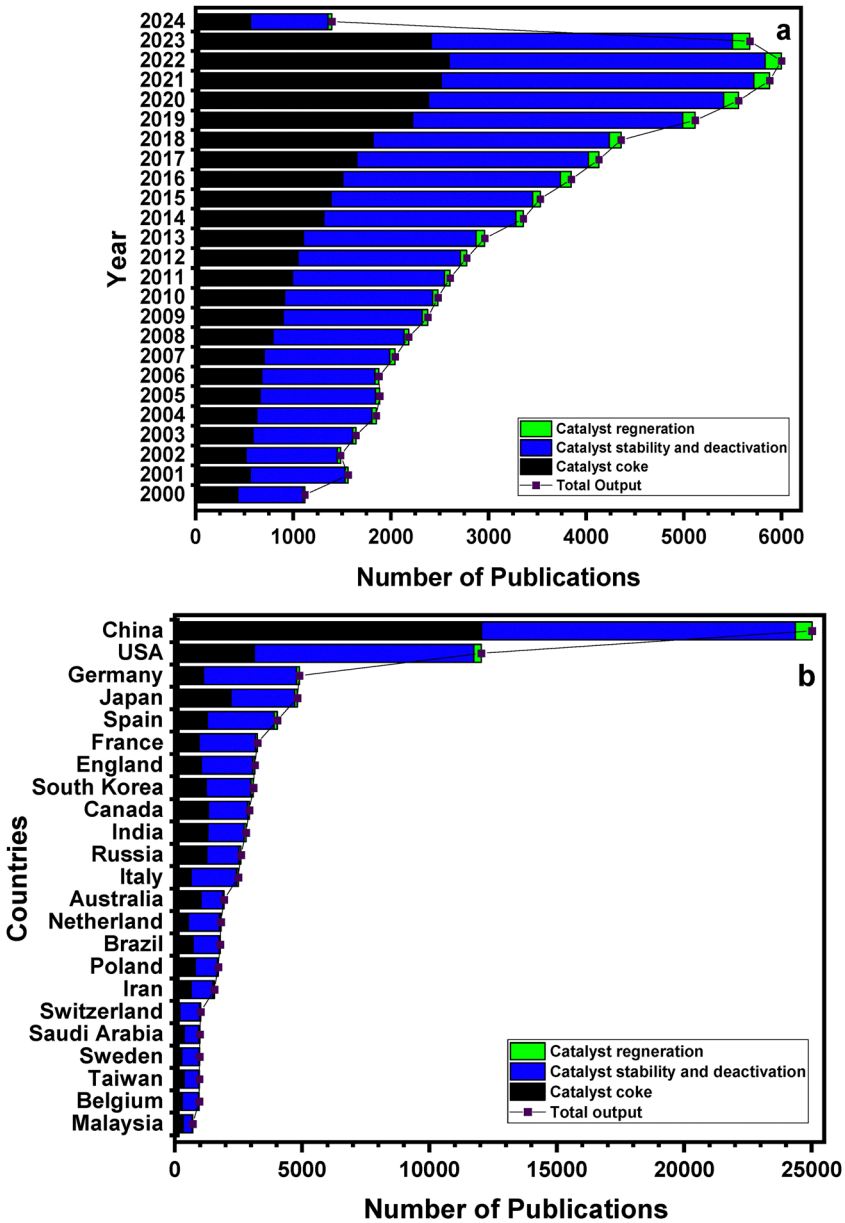

Fig. 2 (a) Publication based on focused keywords for 2000–2024 and (b) most productive countries in CC, CSD and CR research from 2000 to 2024 (Data source: Web of Science).

citations than smaller ones. Fig. 4b not only illustrates the citation analysis of selected authors but also provides valuable insights into the collaborative dynamics of research in this field in the period from 2000 to 2024. The following section looks at the advances in catalyst coke, deactivation mechanisms and regeneration techniques over the last two decades.

4. Catalyst deactivation – coke formation and catalyst deactivation mechanism

The deactivation of catalysts, which is characterised by a gradual decrease in catalytic performance and specificity over time, continues to be a major issue in the field of industrial catalytic processes. Every year, catalyst replacement and process downtime cost the industry billions of dollars. The time frame for the deactivation of catalysts varies greatly. For example, the lifetime of cracking catalysts can be only a few seconds, while iron catalysts in ammonia synthesis can remain active for five to ten years. Nevertheless, the degradation of any catalyst is unavoidable. Various intrinsic mechanisms contribute to catalyst deactivation, which can be broadly categorised into five main types: (1) catalyst poisoning by chemisorption of some species at active sites; (2) fouling by coke deposition; (3) sintering or thermal degradation; (4) vapour–solid or solid–solid reactions; and (5) mechanical failure. Since mechanisms 1 and 4 are primarily chemical, while mechanisms 2 and 5 are

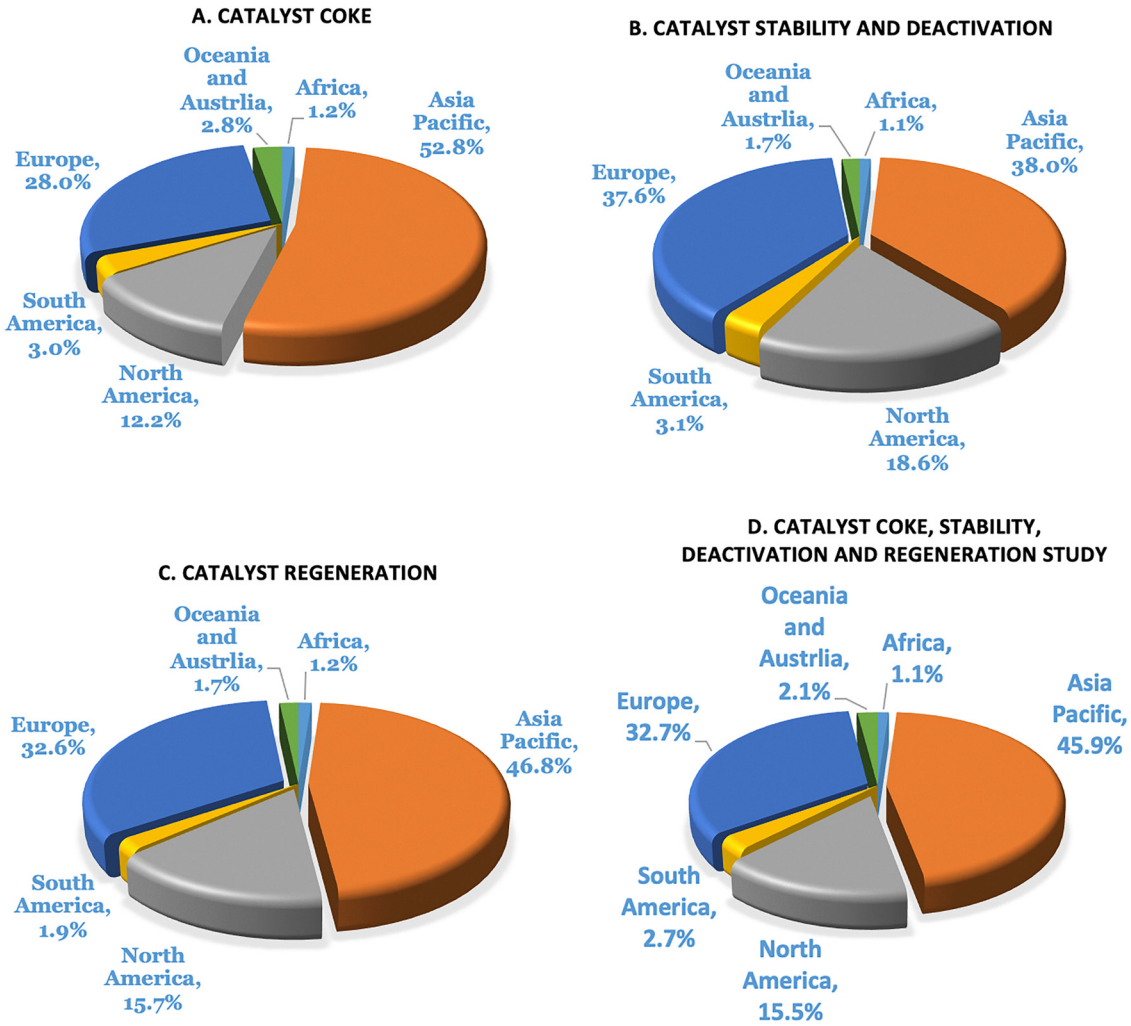

Fig. 3 Publication analysis of the focus keywords (A) catalyst coke, (B) catalyst stability and deactivation, (C) catalyst regeneration according to regions and (D) average regional contribution for these keywords.

mechanical, the causes of deactivation can be divided into three categories: chemical, mechanical and thermal. These deposits can originate from a variety of compounds.[4] While some of these pathways may result in irreversible deactivation, others may cause only a reversible loss of catalytic performance. In the past, the mechanisms responsible for the deactivation of catalysts have been studied in detail, and the complicated processes involved have been elucidated. Table 1 briefly explains each of these five basic mechanisms. The following subsections provide a more detailed examination, focussing on these mechanisms.[4]

4.1. Catalyst poisoning

The deactivation of a catalyst by a chemical substance, whether partial or complete, is known as catalyst poisoning. Poisoning is a particular form of catalyst degradation that is due to chemical factors and differs from other degradation mechanisms such as thermal decomposition or physical damage. Although usually undesirable, poisoning can occasionally lead to improved selectivity of the catalyst despite its generally unfavourable nature. Poisoning, which is characterised by the strong chemisorption of reactants, products or impurities at catalytic sites, is of great importance in catalysis.[31–33] The effectiveness of a species as a poison is dependent on its adsorption strength compared to other competing species for catalytic sites. Adsorbed toxins have the potential to cause variations in the electrical or geometric framework of the surface and physically block the adsorption sites.[32,34] Poisoning can manifest as either temporary or permanent, based on the conditions. An example of reversible poisoning can be observed in fluidized catalytic cracking catalysts, where N_2 compounds in the feed temporarily deactivate the acidic sites. Despite the potential severity, these effects usually disappear within hours to days after the source of N_2 has been removed from the feedstock. A similar scenario occurs when nitrogen compounds are added to the synthesis gas of the cobalt Fischer–Tropsch catalyst, although it takes several weeks to months for the activity to be restored.[35] Conversely, most poisons bind

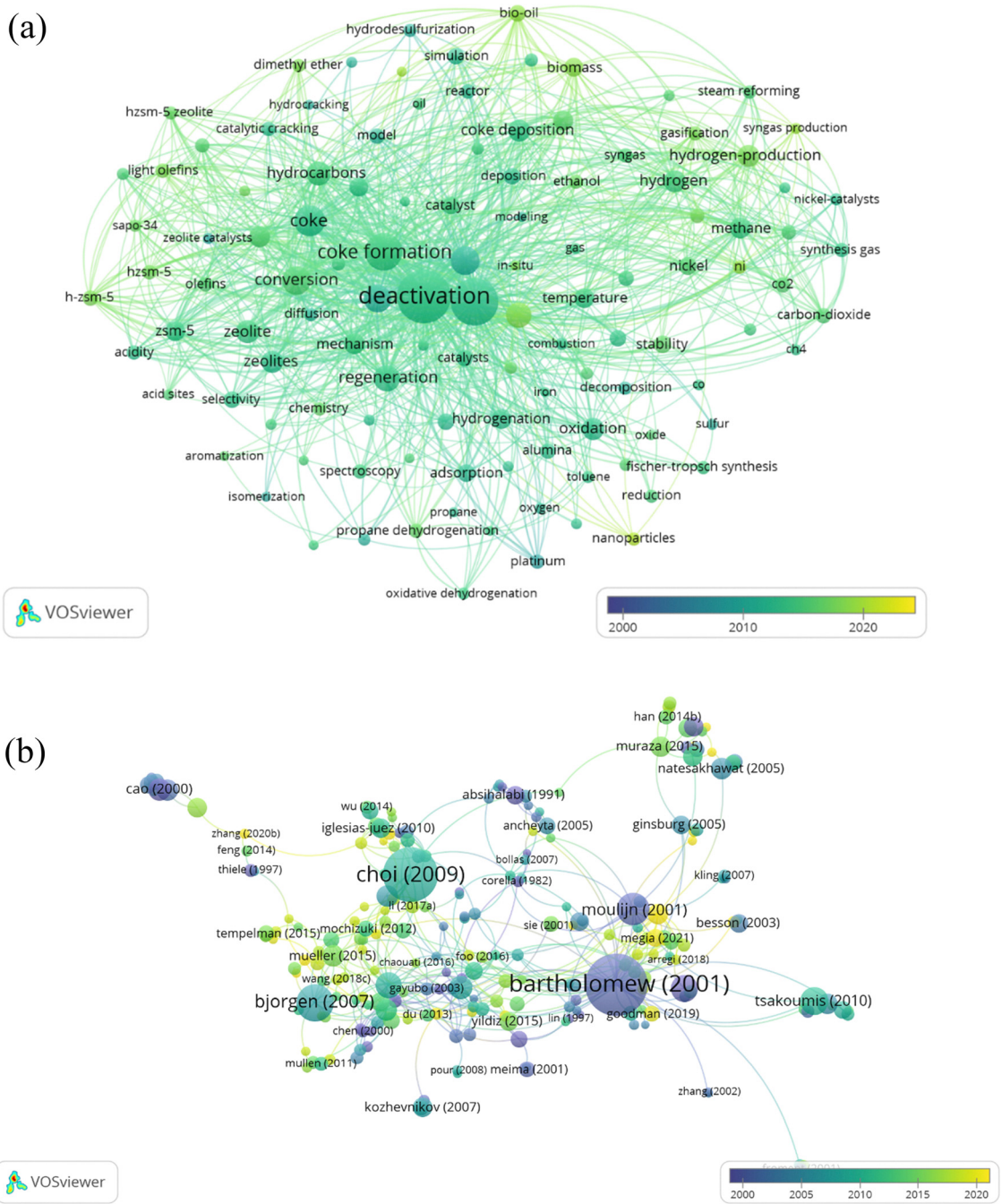

Fig. 4 (a) Network visualisation of publication analysis of keywords co-occurrence. The size of the nodes indicates the number of publications associated with each keyword. The intensity of the links between the nodes reflects the total number of publications between them. These links do not have a specific direction. The colouring of the nodes indicates the links between the keywords and their co-occurrence within the cluster from 2000–2024. (b) Analysis of citations from various authors who have worked on the three focal points in the last two decades. The interconnectedness of the authors is assessed based on their publications and citations. In this analysis, the size of the nodes correlates with the number of citations by an author. A link (line) between two nodes represents a co-citation relationship, indicating that the authors have been cited together in other publications. The thickness of the link reflects the total number of co-citations between the authors. Thicker links represent a stronger citation relationship, suggesting a closer intellectual or thematic connection. In addition, the colour of the nodes indicates the average year of publication of each author.

irreversibly to catalytic surfaces, such as sulphur, on most metals, leading to permanent deactivation effects regardless of reversibility.[36] In addition, poisons are intentionally introduced for two purposes: to improve product performance for subsequent catalytic reprocessing or to reduce the activity and alter the selectivity of fresh catalysts. For example, additives such as zinc and phosphorus in lubricating oils are used to enhance lubricating characteristics and stability but turn into poisons when reprocessed in a hydrotreater or fluidised catalytic cracking unit.[4]

Table 1 Catalyst deactivation mechanisms

Catalyst deactivation mechanisms	Attributes	Effect on catalyst and reaction
Catalyst poisoning	Temporary or permanent deactivation of a catalyst by a chemical substance	A decreased number of active sites; can also lead to improved selectivity of the catalysts
Fouling, carbon or coke deposition	Substances deposition from the liquid phase on the catalyst surface mechanically	Reduced performance due to clogging of sites or pores, which can disintegrate catalyst particles and blockage of reactor crevices
Sintering or thermal deactivation	Sintering occurs when the catalyst near the pores partially melts, hindering access to oxygen for the combustion of coke.	Reduction in the active surface area, reduced activity of the catalyst and a deterioration in the overall activity of the catalyst.
Gas/vapor–solid and solid-state reactions	Chemical pathways are crucial in the deactivation of catalysts by various mechanisms, including reactions between gases or vapours and solid catalysts.	Formation of inert phases differs from poisoning because they do not result in the presence of strongly adsorbed substances but in the formation of completely new phases.
Mechanical failure	The pellet or granular disintegration, breakdown, attrition, decrease of catalyst granules or pellets	Uneven heat and fluid distribution and pressure drop

The effects of Na_2SO_4 poisoning on $Fe_2O_3/MoO_3/TiO_2$ and V_2O_5–WO_3/TiO_2 catalysts during the NH_3-SCR reaction is shown in Fig. 5. Alkali poisoning, particularly from Na^+ ions, is a major deactivation pathway, as these ions block surface acid sites critical for NH_3 adsorption and reaction.[37] In the case of V_2O_5–WO_3/TiO_2 (Fig. 5a), Na^+ accumulation significantly reduces activity by inhibiting NH_3 and NH_4^+ adsorption on acid sites. Conversely, $Fe_2O_3/MoO_3/TiO_2$ (Fig. 5b) shows strong resistance to Na_2SO_4 poisoning due to the protective role of the MoO_3 layer, which preferentially interacts with Na^+, shielding Fe_2O_3 active sites. Na^+ intercalates into the MoO_3 structure, maintaining surface acidity and SCR activity. Even with slight changes in reducibility, overall NH_3 conversion efficiency remains stable, indicating that MoO_3 effectively mitigates alkali-induced deactivation. This highlights the $Fe_2O_3/MoO_3/TiO_2$ catalyst's suitability for SCR applications in Na_2SO_4-rich environments.[37]

4.2. Fouling, carbon and coke deposition

Fouling, which is characterised by the mechanical deposition of substances from the liquid phase on the catalyst surface, leads to reduced performance due to pore clogging, which can result in the catalyst breakdown and clogging of reactor crevices. Notable examples include carbon and coke deposits in porous catalysts. However, the formation of carbon and coke also involves the chemisorption of various carbons or condensed hydrocarbons, which can become catalyst poisons. The definitions of carbon and coke are somewhat arbitrary and based on their regions of origin. Carbon is often a by-product of the disproportionation of carbon monoxide, whereas coke, which consists mainly of polymerised heavy hydrocarbons, is formed by the degradation of hydrocarbons or by condensation on catalyst surfaces. Nevertheless, the conditions during coke formation and ageing can lead to different forms, ranging from heavy molecular weight HCs to graphite. Numerous books and reports deal with the buildup of carbon and coke on catalysts and the subsequent deactivation of the catalyst. The chemical structure of carbons or coke produced during catalytic processes changes depending on the type of reaction, catalyst and conditions.[5,38,39] Menon[39] proposed a classification of catalytic events leading to carbon or coke formation as coke-sensitive or coke-insensitive (similar to Boudart's categorisation into structure-sensitive and structure-insensitive reactions). In reactions that are affected by coke (coke-sensitive), inactive coke accumulates at the active sites and reduces their activity. Conversely, in reactions that are not affected by coke, the more reactive precursors of the coke can be quickly removed using the aid of hydrogen or alternative gasification agents.

4.2.1. Coke formation mechanisms. Several researchers have proposed different mechanisms to explain the formation of coke during steam reforming processes. These mechanisms describe the formation and modification of various intermediate and stable carbon-based compounds.[5] They include different types characterised by their structure and reactivity. These include (i) C_α, which represents atomic carbon adsorbed on the metal surface (surface metal carbide) and is typically formed at

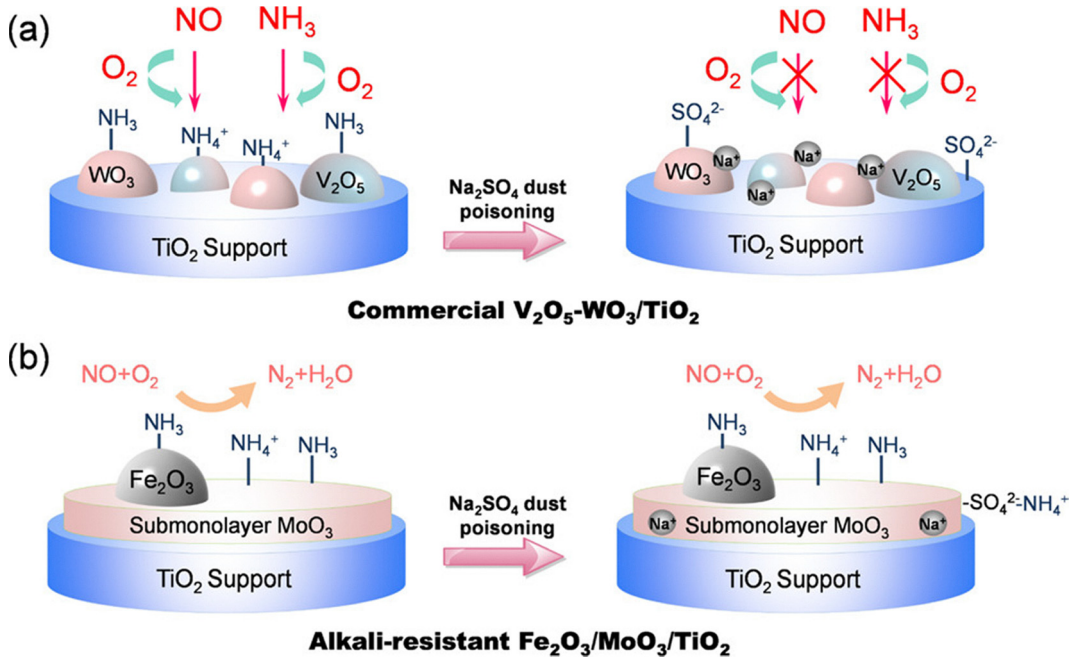

Fig. 5 Presents schematic models illustrating the effects of Na_2SO_4 poisoning on $Fe_2O_3/MoO_3/TiO_2$ and $V_2O_5–WO_3/TiO_2$ catalysts during the NH_3-SCR reaction. Alkali poisoning, particularly from Na^+ ions, is a major deactivation pathway, as these ions block surface acid sites critical for NH_3 adsorption and reaction. In the case of $V_2O_5–WO_3/TiO_2$ (a), Na^+ accumulation significantly reduces activity by inhibiting NH_3 and NH_4^+ adsorption on acid sites. Conversely, $Fe_2O_3/MoO_3/TiO_2$ (b) shows strong resistance to Na_2SO_4 poisoning due to the protective role of the MoO_3 layer, which preferentially interacts with Na^+, shielding Fe_2O_3 active sites. Na^+ intercalates into the MoO_3 structure, maintaining surface acidity and SCR activity. Even with slight changes in reducibility, overall NH_3 conversion efficiency remains stable, indicating that MoO_3 effectively mitigates alkali-induced deactivation. This highlights the $Fe_2O_3/MoO_3/TiO_2$ catalyst's suitability for SCR applications in Na_2SO_4-rich environments. Reproduced from ref. 37 with permission from American Chemical Society (ACS), copyright 2020.

temperatures between 200 and 400 °C; (ii) C_γ, which represents bulk metal carbide and is formed at 150 to 250 °C; (iii) C_β, which indicates the formation of polymeric amorphous films and occurs between 250 and 500 °C; (iv) C_v, which represents filamentary coke formed in the temperature range of 300 to 1000 °C; and (v) C_c, which indicates the formation of graphitic platelets or films and typically occurs at temperatures around 500 to 550 °C. According to this proposed mechanism, highly reactive and amorphous carbonaceous species such as C_α and C_β tend to adsorb on metal sites at lower temperatures. However, as temperatures increase, these species transform into less reactive, graphitic and condensed forms, namely C_v and C_c.[4,5] Consequently, carbon dioxide (C_v) and carbon monoxide (C_c) are the most stable carbonaceous species on the catalyst surface at higher temperatures commonly used in reforming reactions (between 600 and 850 °C). The development of the latter species is primarily favoured by the diffusion of graphitic layers within the metal particles and their subsequent maturation.[40] The structural forms of carbon species generated by different kinds of carbon species generated by CO decomposition on Ni catalysts are shown in Fig. 6.

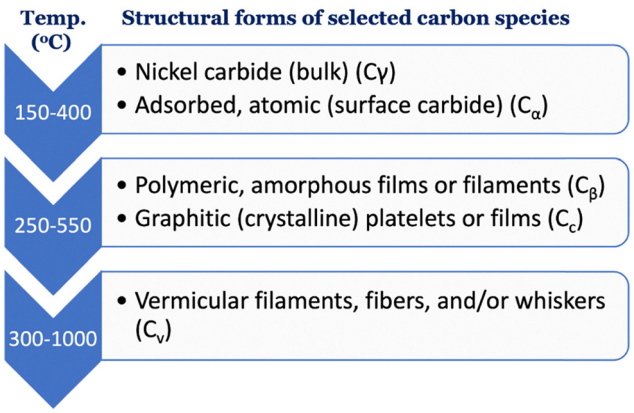

Fig. 6 Structural forms of different kinds of carbon species generated by CO decomposition on Ni catalysts. Carbon classifications: C_γ: metal carbide, C_α: adsorbed atomic carbon, C_β: polymeric carbon film, C_c: amorphous and graphitic carbon, C_v: vermicular carbon. Modified from ref. 5.

Coke formation in hydrocarbon reactions takes place both on active sites and on non-catalytic supports and is catalysed by acidic sites. The process begins with the adsorption of coke precursors such as olefins or light aromatics and involves inter- and intramolecular reactions. At low temperatures (<200 °C), condensation and rearrangement reactions yield mainly co-oligomers and polymers. This "light" coke can be reversible under specific conditions. At high temperatures (>350 °C), additional reactions such as hydrogen transfer led to "heavy" coke, which is difficult to remove due to its stability and size. At medium temperatures, a mixture of mechanisms occurs (Fig. 7), with light coke transforming into aromatics and

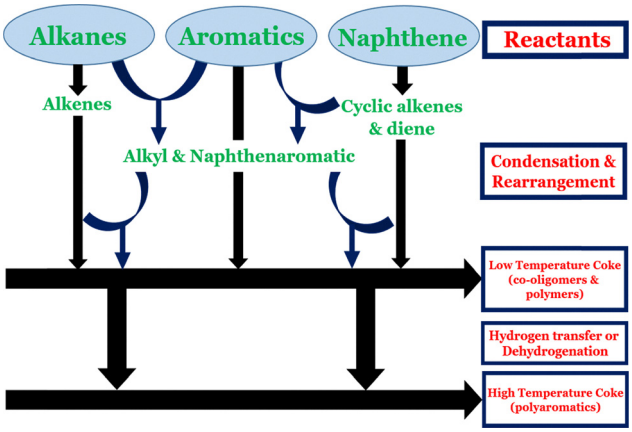

Fig. 7 Basic outline of the formation of coke from hydrocarbons and molecular coke on an acidic zeolite catalyst. Modified and reproduced from ref. 6 with permission from Elsevier, copyright 2009.

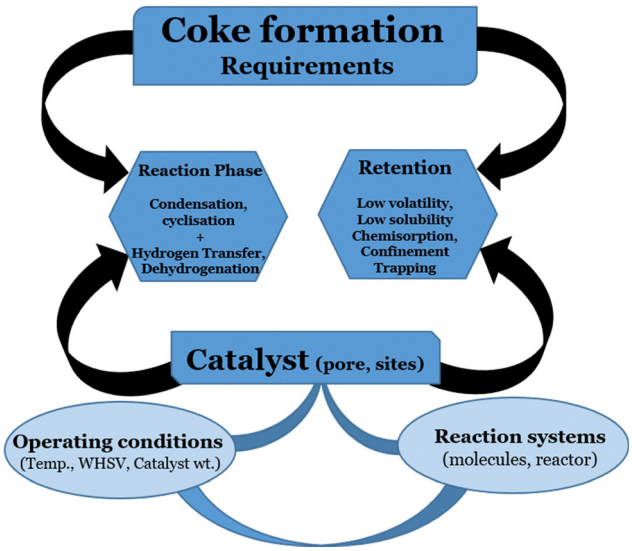

Fig. 8 Essential prerequisites for catalyst-induced coke formation and key influencing factors. Modified and reproduced from ref. 6 with permission from Elsevier, copyright 2009.

eventually into polynuclear aromatics that condense into coke molecules. Polynuclear carbocations sustain molecular growth until termination reactions occur, leading to heavy polyaromatic structures and potential encapsulation and filamentous coke mechanisms.[6] Fig. 8 summarises the most important conditions and factors that contribute to coke formation. The type of reaction, the operating variables and the properties of the catalyst investigated are decisive for the type, distribution and rate of coke formation and thus influence the underlying mechanisms. In general, the classification of coke into three different morphologies (Table 2) – encapsulating, filamentous and pyrolytic – is underpinned by extensive research into the reforming of CH_4, HCs and biomass-derived oxygenates.

4.2.1.1. Coke composition. Coke, a carbonaceous deposit formed during catalytic reactions, is a major cause of catalyst

Table 2 Comparison (summary) of coke types based on morphology and framework[54–59]

Attributes	Encapsulation coke	Filamentous coke	Pyrolytic coke
Formation temp.	<500	>400	>600
Contribution/effects	Significant catalyst deactivation	Hardly noticeable unless there's massive filament growth leading to the breakdown of the catalyst and increasing ΔP	Encapsulation of catalyst particle; deactivation and increasing ΔP
Precursor(s)	Ethoxy ions, secondary rxn products: ethylene, acetone, or acetaldehyde	CO by Boudouard rxn, and CH_4 decomposition	C precursors
Formation mechanism or causes	Adsorption on metal sites, condensation or polymerization of precursors	The process involves (i) the attachment of coke precursor molecules to metal sites and their transformation into atomic carbon, (ii) the movement of carbon through the metal particle, both within its bulk and on its surface, (iii) the formation of carbon clusters, and (iv) the depositing of carbon either on the metal's surface or within its structure.	Thermal cracking of HC, followed by the deposition of carbon precursors onto a catalyst.
Structure	Less evolved structure	Have a more graphite and condensed nature	Have a more condensed and graphitic nature
Component ratios	Higher H/C and/or O/(C ratio)	(Higher aromatics-to-aliphatics ratio)	(Higher aromatics-to-aliphatics ratio)
Key parameters	Low T °C, low H_2O/C_nH_m, low H_2/C_nH_m, aromatic feed	Elevated T °C, low H_2O/C_nH_m, no enhanced H_2O adsorption, low activity, aromatic feed	Elevated T °C, high void fraction, low H_2O/C_nH_m, high pressure, acidic catalyst
Elimination technique	Gasification/combustion	Gasification/combustion	Gasification/combustion
Elimination temp.	Less	Higher	Higher

deactivation, particularly in hydrocarbon processing. Its composition varies depending on the feedstock, reaction conditions, and catalyst type, and typically includes polyaromatic hydrocarbons, amorphous carbon, aliphatic residues, and partially hydrogenated carbon species. Coke can be broadly classified into soft coke (easily oxidizable, often found on external surfaces) and hard coke (more graphitic, resistant to oxidation, often located within micropores).[41] The accumulation of coke blocks active sites and pores, reducing surface area, catalyst acidity, and overall activity. Understanding the nature and composition of coke is essential for developing targeted regeneration strategies and improving catalyst longevity.

The FTIR spectra of the metal doped HZSM-5 spent catalysts from the catalytic conversion of C_1–C_3 alcohols to hydrocarbon revealed various functional groups and species, including adsorbed water, silanol groups, and coke deposits[42] (Fig. 9a and b). Despite coke formation following C_1–C_3 alcohol conversion, the functional groups on the spent catalysts were largely retained. FTIR spectroscopy enabled the identification of bond vibrations between the catalyst surface and adsorbed hydrocarbons. Coke deposits were characterized by distinct hydrocarbon-related spectral bands, notably within the 1300–1700 cm^{-1} and 2800–3100 cm^{-1} ranges, as shown in Fig. 9b, which spans 1300–3800 cm^{-1}. The lower frequency region is linked to polycondensed aromatics, conjugated olefins, and aliphatic bending, while the higher range corresponds to aliphatic C–H stretching and single-ring aromatic compounds. To interpret each vibration, the spectra of the spent catalysts were identified by characteristic peaks: 1390 cm^{-1} (terminal –CH_3), 1450 cm^{-1} (aliphatic/alkyl aromatics), 1595 cm^{-1} (polycondensed coke aromatics), 1620 cm^{-1} (C═C or olefinic groups), 2850 cm^{-1} (–CH_2), and 2960 cm^{-1} (–CH_3).[43–46] These values are approximate and may vary slightly due to experimental conditions. Compared to the undoped catalyst, Anekwe *et al.*[42] reported that Fe/HZSM-5 and Co/HZSM-5 showed more pronounced CH_2 and CH_3 bands in the 2800–3100 cm^{-1} range, implying a greater presence of long or naphthenic aliphatic chains in the coke. Notably, the intensity of CH_3 groups exceeded that of CH_2, with the trend observed as Fe/HZSM-5 > Co/HZSM-5 > Ni/HZSM-5 > HZSM-5, suggesting metal dopants influence the type and structure of coke formed.

The relatively weak intensity observed in the 2800–3100 cm^{-1} region indicates that the coke formed is predominantly unsaturated in nature. In contrast, the band at 1625 cm^{-1} within the 1300–1700 cm^{-1} range appears more pronounced in metal-doped catalysts compared to the undoped sample, suggesting a higher presence of olefinic or double-bonded hydrocarbons. These results align with earlier studies,[43,44,46] indicating that metal species facilitate the formation of olefins and long-chain aliphatics in coke *via* secondary reactions such as aromatization and oligomerization. Product trends support typical behaviour for C_1–C_3 alcohol conversion,[46–48] where olefins act as intermediates and heavier aliphatic and aromatic compounds represent the final products, consistent with the established C_1–C_3 alcohol reaction pathway.[48]

Fig. 10 presents a schematic summary of the formation of two distinct types of coke: soft coke and hard coke on different active sites within the Fe-ZSM-5 catalyst during reaction. Soft coke, typically composed of less condensed, hydrogen-rich carbon species, forms predominantly on the Brønsted acid sites of the zeolite.[41] While it affects product selectivity particularly by reducing benzene yield its impact on overall catalyst deactivation is relatively moderate and it can often be removed under mild regeneration conditions. In contrast, hard coke consists of highly condensed, graphitic carbon species that form mainly on the metal sites. This type of coke strongly adheres to the catalyst surface, leading to significant blockage of active sites and severe loss of catalytic activity. Hard coke is more resistant to removal and requires harsher regeneration

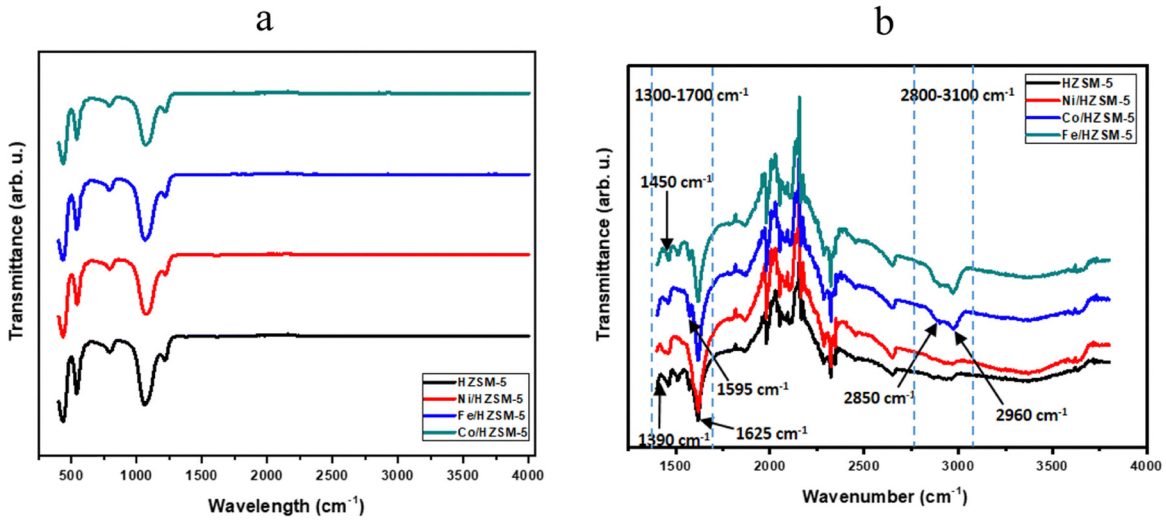

Fig. 9 FTIR spectra of coked metal doped HZSM-5 catalyst after the conversion of C_1–C_3 alcohols to hydrocarbons at 350 °C and WSHV = 7 h^{-1}: (a) full spectral range (400–4000 cm^{-1}) showing overall functional group vibrations; (b) expanded region (1300–3800 cm^{-1}) highlighting characteristic bands associated with coke formation, including aliphatic, olefinic, and aromatic hydrocarbon species. Reproduced from ref. 42 with permission from Royal Society of Chemistry (RCS), copyright 2024.

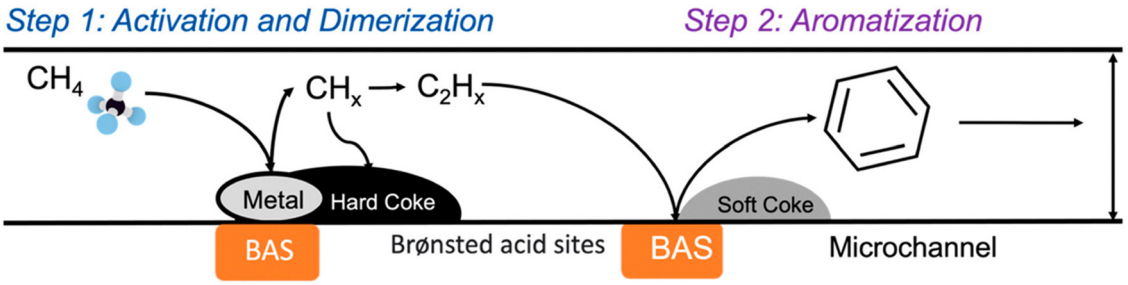

Fig. 10 Diagram depicting the formation of various coke types: soft and hard coke on different catalyst active sites. Reproduced from ref. 41 with permission from MDPI, copyright 2024.

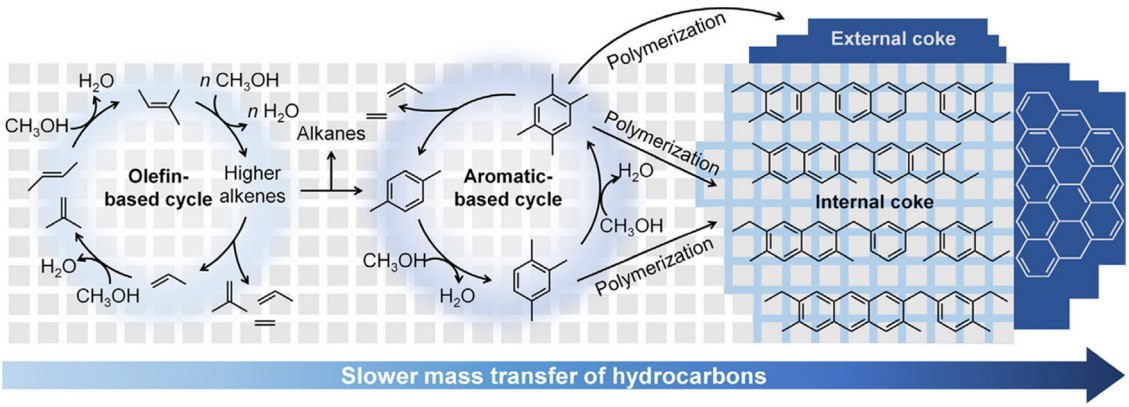

Fig. 11 Proposed pathways for reaction progression and coke formation mechanism during the methanol-to-hydrocarbons (MTH) conversion process. Reproduced from ref. 52 with permission from Elsevier, copyright 2019.

treatments.[41,49] The schematic in Fig. 8 thus highlights the site-specific nature of coke formation and its distinct implications for catalyst performance and regeneration.

Recent studies have increasingly focused on distinguishing between internal and external coke formation mechanisms,[50–52] as illustrated in Fig. 11. Lee and Choi[52] reported that internal coke primarily consists of smaller, methylated aromatic molecules such as methylated acenes linked by methyl bridges. This type of coke typically exhibits a higher hydrogen-to-carbon (H/C) ratio of 1.26 and a density around 1.0 g cm^{-3}. In contrast, external coke is composed of larger, more condensed polyaromatic hydrocarbons, characterized by a lower H/C ratio of 0.28 and a higher density of approximately 1.5 g cm^{-3}. The formation and accumulation of these coke types are heavily influenced by the zeolite's microporous architecture and the specific reaction conditions. Additionally, the extent to which each coke type contributes to catalyst deactivation is also governed by these structural and operational variables.[53]

4.2.2. Coke and carbon formation on selected catalysts

4.2.2.1. Zeolites. The acidity and the pore structure of the catalyst are influential factors which, in conjunction with the HC framework and the process parameters, affect both the nature and the degree of coke deposition. High acid strength and concentration generally increase the degree of coke formation, which is particularly evident with zeolites where shape selectivity significantly influences coke formation, with coke decreasing with decreasing pore size (at constant acid strength and concentration). For instance, the coke yield in catalytic fluidised bed cracking is limited to 0.4% for ZSM-5, which is characterised by smaller pore sizes of 0.54 × 0.56 nm, while it is 2.2% for Y-faujasite with a larger opening diameter of 0.72 nm.[60] Conversely, even a relatively small amount of coke can trigger a significant decrease in activity in pores with a molecular size. The extent of coke formation can change significantly in the internal pores of a catalyst particle or along a catalyst bed, based on the influence of primary and deactivation processes by the mass transport of the film and the diffusion resistance of the pores, so these aspects must be considered. Several recent investigations have delved into coking during HC reactions within zeolites,[60–66] examining diverse facets such as the intricate chemistry of coke precursors and molecules generated within zeolite pores and pore junctions, alongside the comparative importance of adsorption at acidic sites *versus* pore obstruction. The most important findings from these investigations include: (1) coke formation and subsequent deactivation of zeolite catalysts are both shape-dependent reactions, (2) deactivation is primarily driven by the formation and retention of large aromatic clusters in the pores and pore intersections. (3) Acid poisoning and pore plugging contribute to deactivation, with acid poisoning being more pronounced at low coking rates, low coke content (*e.g.* Y zeolite below 2 wt%) and high temperatures, while pore plugging is

more dominant at high reaction rates, high coke content and low temperatures. Consequently, pore size and morphology likely outweigh acid strength and density in industrial processes. Indeed, deactivation is often faster in zeolites with small pores or one-dimensional structures.[67]

Fig. 12 illustrates the coke formation pathways during methane conversion over a Mo_2C/HZSM-5 catalyst. Initially, CH_4 decomposes to CH_x species on Mo_2C sites (Path 1), which couple to form C_2H_4. This ethylene can either undergo aromatization within the zeolite channels to form benzene and naphthalene (Path 2), or it can oligomerize and crack on external surfaces to form coke (Coke-I) (Path 3). Aromatics formed may also further polymerize to coke (Coke-II) (Path 4). Besides the polycondensation of aromatics on Brønsted acid sites, significant coke formation and catalyst deactivation in the studied reaction can also result from the thermal and/or catalytic oligomerization and cracking of C_2H_4, as illustrated in path (3).[68] The formation of external coke (Coke I) has been shown to significantly contribute to catalyst deactivation by blocking pore entrances, thereby hindering reactant access to active sites. This blockage leads to a decline in the conversion of ethylene (C_2H_4) to aromatics, resulting in increased C_2H_4 levels. Thermodynamic data suggest that under these conditions, C_2H_4 remains near its equilibrium concentration, promoting competing pathways such as benzene formation and coke deposition. Despite the accumulation of coke, benzene selectivity often remains high, indicating that coke predominantly forms on external surfaces rather than within the micropores.[69–71]

4.2.2.2. Metal-based, bifunctional metal oxide and sulfide catalysts. The possible impact of carbon (or coke) formation on the operation of supported metal catalysts depends on the reaction or operating conditions. Carbon can (1) strongly chemisorbate as a monolayer or physically adsorb in multilayers, hindering reactant access to metal surface sites. (2) It can completely coat a metal particle, rendering it completely inactive. (3) Carbon can block micropores and mesopores, preventing reactants from entering many contained crystallites.[4] Finally, under severe conditions, robust carbon filaments can gather in the pores and stress and break the support material, causing the catalyst pellet to disintegrate and fill the reactor crevice. Consequently, the carbon filaments can detach from the support by a thermal or mechanical shock and irreversibly deactivate the catalyst. However, the behaviour is complex, as the filaments can emerge from the surface of the metal particles under different conditions and with different metals. The carbon can also penetrate the metal and produce carbides.[4,72] With conventional Selective molecular rearrangement (SMR) catalysts such as Ni/$MgAl_2O_4$, the production of alkene is generally regarded as the main source of coke.[73] In catalysts such as Ni/La_2O_3, carbon forms at the junction between the active metal and the support, hindering access of the active phase to the support.[74] SMR for hydrogen production leads to coke formation and the deposition of carbon on metal catalysts from CO and HCs such as CH_4. These reactions produce different forms of carbon and coke, each with a different structure and reactivity. For example, the dissociation of carbon monoxide (CO) on metals produces C_α, an adsorbed atomic carbon that can react further with C_β, a polymeric carbon film. Amorphous forms of carbon, including C_α and C_β, exhibit higher reactivity at lower temperatures but transform into less reactive graphitic forms with time at higher temperatures.[72]

Similar to the deactivation of metals on supports by coke, the deactivation of oxide and sulphide catalysts also occurs by various mechanisms, which have both chemical and physical causes. However, there are clear nuances in the chemistry. The adsorption of coke molecules on acidic sites primarily accounts for the loss of chemical activities in oxides and sulphides. However, strongly acidic sites are also crucial in the formation of coke precursors, which later condense and form heavy polynuclear aromatic molecules that physically coat the catalytic surfaces. The accumulation of coke is accompanied by a physical loss of activity, which ultimately leads to temporary or permanent clogging of the pores, similar to metal catalysts on supports. In the isomerisation of *cis*-butene on SiO_2/Al_2O_3.[75] For example, rapid and selective poisoning of the strong acids results in catalyst deactivation. The coke formed initially in this reaction is soluble in dichloromethane and pyridine and has low aromatic properties. Considering the wide mesopores of SiO_2/Al_2O_3, blocking the active sites appears to have negligible effects on the catalyst porosity or surface area.

Montero *et al.*[76] investigated the origin and characteristics of coke formed on Ni/La_2O_3–α-Al_2O_3 catalysts during ethanol steam reforming. Using Scanning electron microscopy (SEM), which provides high-resolution images of sample surface revealing intricate morphology, textures and microstructures,[77] the structure of carbon deposits was identified, including encapsulating, filamentous and graphitic types. Encapsulating coke was primarily attributed to the cracking and polymerization of ethanol, acetaldehyde, and ethylene, while filamentous and partially graphitic coke originated from CH_4 and CO through decomposition and the Boudouard reaction. Since filamentous coke forms away from active metal sites, it has limited impact on catalyst deactivation. In contrast, catalyst activity loss was mainly due to encapsulating coke, which directly covers and deactivates metal centres. Notably, filamentous carbon contributed to metal–support separation without obstructing the active sites (Fig. 13).

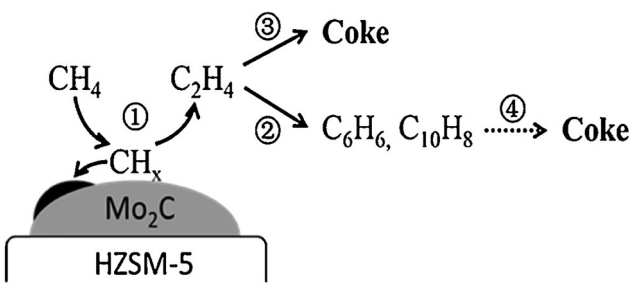

Fig. 12 Schematic diagram of coking pathways during CH_4 conversion over Mo_2C/HZSM-5 catalyst. Reproduced from ref. 68 with permission from Elsevier, copyright 2014.

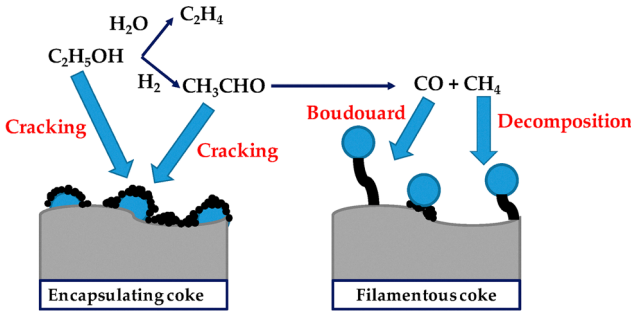

Fig. 13 Formation mechanism and characteristics of coke deposits on Ni/La_2O_3–α-Al_2O_3 catalyst. Reproduced from ref. 78 with permission from MDPI, copyright 2020.

4.2.3. Effect of carbon deposits or coking on different reactions and operating conditions. It should be emphasised that certain types of carbon deposits influence the decrease in catalytic activity, while others do not contribute to this decrease. For example, condensed polymer or β-carbon films can coat the surfaces of methanation and steam-reforming catalyst metals at temperatures of less than 300 to 375 °C. At higher temperatures of more than 650 °C, graphitic carbon films can exhibit similar effects.[5] In steam reforming at higher temperatures (500–900 °C), deactivation can occur through the precipitation of atomic carbon or carbidic carbon dissolved in Ni surface layers deeper than 50–70 nanometres.[39] Adsorbed atomic carbon can deactivate the metal sites for adsorption and reaction, regardless of temperature. When the accumulation of carbon on the free surface is large enough to cause encapsulation by a carbon layer, filament growth stops. However, encapsulation of metal particles is not possible if H/C or H/HC ratio is sufficiently high.[79] Therefore, the occasional formation of carbon filaments during CO hydrogenation or hydrocarbon steam reforming does not lead to a loss of catalyst performance unless the filaments block the pores or metal loss occurs during regeneration. In addition, regions with carbon formation potential during steam reforming must be avoided in practice to prevent catastrophic pore blockage and catalyst failure within hours to days.[80]

The deactivation rate of a particular catalyst and reaction depends on the reaction parameters, especially the temperature and composition of the reactant. For reactions that are insensitive to coke on metals, such as methanation, Fischer–Tropsch production, steam reforming, catalytic reforming and methanol synthesis, the deactivation rate relies on the discrepancy between the formation of carbon/coke precursors and the gasification rates. This means that the deactivation rate is equal to the difference between the rates of formation and gasification of carbon/coke precursors. If the gasification rate (r_g) is equal to or greater than the formation rate (r_f), the rate of deposition (r_d) of carbon and coke is prevented ($r_d = r_f - r_g$). Although both the production and gasification rates of the precursors increase exponentially with temperature, their difference varies considerably due to variations in pre-exponential factors and activation energies. These processes are temperature dependence, hence, the formation of carbon and coke can be avoided in temperature ranges in which the gasification rate of the precursors exceeds the deposition rate. Bartholomew[72] investigated the formation and hydrogenation rates of C_α and C_β species on nickel during CO methanation. The study found that below 327 °C, the gasification rate of the C_α species exceeds its formation rate, thereby inhibiting carbon deposition. However, when the temperature exceeds 327 °C, the formation rate of C_α exceeds its gasification rate, leading to its accumulation and subsequent conversion into a polymeric C_β chain or film between 327 and 427 °C. At 427 °C, the hydrogenation rate of C_β exceeds its formation rate and prevents deactivation. Thus, temperature ranges below 327 °C and above 427 °C serve as "safe" zones for methanation, preventing carbon-induced deactivation. However, these ranges can vary depending on the amount of reactant and catalyst activity. Similar principles apply to steam reforming, where operation at temperatures above a certain threshold is critical to prevent deactivation due to polymer film formation.[81]

4.2.4. Factors that influence catalysts deactivation due to coke deposition. The variables that affect catalyst deactivation due to coke deposition are complex and multifaceted. Since it is difficult to identify the primary coke precursors and associated mechanisms in several catalytic processes, such as low alcohol upgrading, steam reforming of bio-oil, and other hydrocarbon reactions, research efforts are primarily focused on investigating the operating parameters and their effects on coke deposition and subsequent process deactivation.

Temperature is proving to be a critical factor in mitigating the deactivation of most catalysts, such as nickel-based catalysts, during hydrocarbon reactions. For example, the steam reforming of crude bio-oil, aqueous bio-oil fractions, and bio-oil/bioethanol blends. In the temperature range of 650–700 °C, it showed that the reforming reactions are favoured, and coke gasification is improved without sintering of the nickel, thus promoting sustained catalytic activity.[82,83] However, studies by Ochoa *et al.*[84] emphasise the significant influence of coke morphology on deactivation during the catalytic process, which is primarily determined by reaction temperature and space-time. At low temperatures (550 °C), strongly deactivating, encapsulating coke, which originates from oxygenates in the reaction medium, predominates. At higher temperatures (700 °C), conversely, filamentous coke tends to be deposited, which has less impact on catalyst performance. Interestingly, the coke content, which is largely influenced by the steam-to-carbon ratio, appears to have a less pronounced effect on deactivation than its composition and morphology, which are primarily determined by temperature.

Secondly, space-time, as an important parameter in catalytic reactions, influences the composition of the deposited coke. Space time (τ), defined as the ratio of catalyst weight to reactant flow rate, significantly influences coke formation during catalytic reactions. It represents the residence time of the reactants in the catalyst bed, that is, how long the reactants are in contact with the catalyst under flow conditions. Lower space-time values increase the proportion of encapsulating and filamentous

fractions, while higher space-time values reduce the production of encapsulating coke.[82] Considering the role of steam in promoting coke and precursor gasification, Valle *et al.*[85] advocate a molar steam-to-carbon feed ratio of above 4 at high temperatures (700 °C) and high space-times (0.38 g catalyst h $(gbio\text{-}oil)^{-1}$). This strategy results in an initial H_2 yield of 87%, which is maintained at 70% after five hours of on-stream operation. This demonstrates the effectiveness of steam in containing coke and maintaining catalytic performance.

In addition, emphasis is placed on the morphology, composition, and distribution of the coke and not just its presence. A higher degree of deactivation is usually achieved by increasing the proportion of amorphous and encapsulated coke.[84] Coke formation in catalytic processes is influenced by both the structure and surface properties of the catalyst. Pore size plays a crucial role, with smaller pores leading to pore blockage due to the bulky nature of the resulting coke molecules. Industrial observations suggest that pore size and structure are more influential than the catalyst's acidity.[4] Diffusion limitations and secondary deactivation reactions shape the coking process. Catalyst acidity, determined by the Si/Al ratio, affects the reactivity of coke precursors. Higher acidity generally accelerates chemical reactions and enhances coke molecule binding. However, quantifying these effects is challenging due to the difficulty in obtaining zeolites with independently adjustable acidity levels and pore structures.[86]

Metal incorporation enhances the catalyst's vulnerability to coking and deactivation, as reported in a study by Anekwe *et al.*[87] on ethanol transformation to HCs. According to the results of thermogravimetric differential thermal analysis (TG-DTA) (Fig. 14a), three decoking stages were identified: first, the combustion of soft coke at 200–400 °C, which has a lower mass loss at 0.5%Ni and Co compared to Fe and unmodified catalysts. Secondly, the burning of hard coke at 400–600 °C, shows a significant mass loss, especially when doped with 10% Fe and Ni. Thirdly, the reduced mass loss observed between 600–800 °C is indicative of the presence of non-volatile coke deposit or laid coke.[88] The sequence of total mass loss (between 200–600 °C) is as follows: HZSM-5 (pure) (1.6 wt%) < 0.5Co (4.5) < 0.5Ni (4.6) < 10Co (6.2) < HZSM-5 (used) (6.7) < 0.5Fe (6.8) < 10Ni (8.6) < 10Fe (12.1) (Fig. 14a). This indicates that coke formation increases with increasing metal concentration. Higher metal doping correlates with increased coke deposition attributed to the increased acidity of the catalyst, especially at 10 wt% Co, Fe and Ni, which exhibit considerable coke deposit. Conversely, lower metal doping leads to less coke formation and reduced mass loss, due to fewer strong acid sites.

Pure HZSM-5 shows the lowest mass loss due to minimal coke accumulation. To clarify, these mass loss values do not reflect the intrinsic stability of the spent catalysts but rather quantify the amount of coke deposited and subsequently burned off. This is consistent with the results of Xu *et al.*,[89] who reported that Fe doping promotes coke formation on ZSM-5, with deposition increasing with metal content. In contrast, Weckhuysen *et al.*,[90] suggest that metal doping suppresses coke deposition. This emphasises the complex relationship between metal doping, catalyst acidity, and coke deposition. Fig. 14b shows the results of the differential thermal analysis, which indicate a pronounced tendency towards coke formation in metal-doped catalysts, especially those with a higher metal content (10 wt%), which is consistent with the results of the TGA analysis. The summary of factors affecting the formation of coke is presented in Table 3.

4.3. Sintering and thermal decomposition

The reduction of the catalytic surface area attributed to crystallite growth within the catalytic phase, the collapse of the support surface and the pore collapse at the crystallites within the active phase all contribute significantly to thermally induced catalyst deactivation. In addition, chemical conversion from catalytic phases to non-catalytic phases can exacerbate this phenomenon, commonly referred to as "sintering". Three primary mechanisms atomic migration (Ostwald ripening), crystallite migration (particle migration & coalescence) and vapour transport at extreme temperatures have been proposed to describe the formation of metal crystallites.[4] Atomic migration

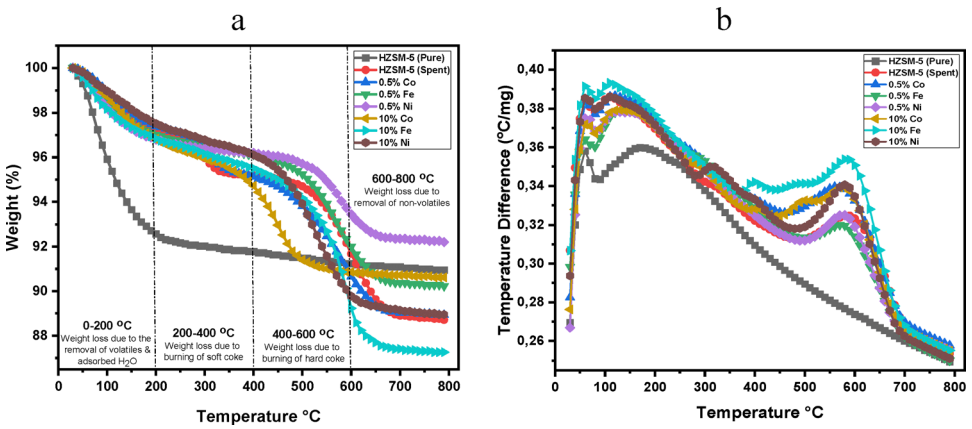

Fig. 14 present the TGA (a) and DTA (b) of spent metal-doped HZSM-5 catalysts. Reproduced from ref. 87 with permission from Elsevier, copyright 2024. The data indicate that increasing metal loading from 0.5 to 10 wt% correlates with higher mass loss, primarily attributed to enhanced coke deposition on the HZSM-5 surface.

Table 3 Summary of factors influencing coke formation[91]

Factors	Effects
Reaction system	– Certain molecules, often referred to as coke precursors, initiate the formation of coke through subsequent reactions. – The identity and characteristics of these precursors vary based on the reaction under investigation and are influenced by the phase in which the reaction takes place.
Temperature	– Temperature significantly impacts the properties of coke, which results in its categorisation into low- and high-temperature types. – Low temperatures prevent the formation of polyaromatic coke and only allow condensation and rearrangement reactions. – Conversely, high temperatures promote hydrogen transfer and dehydrogenation reactions, leading to the abundant formation of polyaromatic molecules with a low H/C ratio.
Reaction time	– The duration of the reaction also affects coke formation, as prolonged contact with deactivating substances promotes the extensive growth of coke structures. – This can result in the formation of long olefin chains or an increase in the amount of aromatic nuclei in polyaromatic compounds.
Space-time	– The amount of coke fractions increases with low space-time and decreases with higher space-time.
Catalyst framework and surface	– The deactivation of zeolites due to coking is mainly influenced by the pore structure of the catalyst, which controls the formation of large aromatic clusters. – The catalyst geometry is decisive for where and how large the coke deposits are, as it regulates the diffusion and accessibility of coke precursors within the catalyst framework.
Metal modification	– Metal doping increases the susceptibility of catalysts to coking – Increased metal doping leads to increased coke formation

comprises the detachment of metal atoms or molecular clusters from the smaller crystallites, their movement along the support's surface, and eventual incorporation into larger crystallites (Fig. 15a). Crystallite migration, on the other hand involves the entire relocation of smaller crystallites across the support's surface, subsequent collision, and merging to larger particles aiming thermodynamic stability (Fig. 15b).[4,54,92] These sintering mechanisms lead to the growth of larger particles as smaller ones shrink or vanish. To this effect, Monte Carlo simulations are used to improve particle size prediction and better understand sintering kinetics.[93,94] In addition, Ostwald ripening significantly contributes to catalyst deactivation during CO methanation.[71] Moreover, Hansen *et al.*[93] identified three sintering stages (Fig. 15c): an initial rapid loss of activity or surface area (Phase I), followed by slower sintering (Phase II), and eventual stabilization of catalyst performance (Phase III).

Conversely, redispersion, the opposite of crystallite growth, may involve the formation of volatile metal oxide or metal chloride complexes or oxide particles or films that promote the formation of small crystallites during reduction. In particular, the temperature, the environment, the kind of metal, the dispersion, the promoters, the impurities and the properties of the carrier have a major influence on the sintering and redispersion rates. For example, sintering rates increase exponentially with temperature, with metals sinking faster in O_2 than in H_2. However, redispersion can be enhanced by exposure to O_2 and Cl at elevated temperatures and subsequent reduction, which has been observed particularly with platinum/alumina catalysts. Water vapour also accelerates the sintering of metals on supports, probably by chemically assisted mechanisms.[4]

The sintering of support materials or carriers has been investigated, with processes such as surface diffusion, solid-state diffusion, evaporation/condensation, grain boundary diffusion and phase transitions identified as mechanisms for the sintering of single-phase oxide supports. The different phase behaviour of Al_2O_3 depending on the temperature and the preparation methods is an example of the phenomenon of sintering of substrates triggered by phase transformations. Al_2O_3 has a number of stable or metastable phases, including boehmite, γ-alumina and α-alumina.[95] These phases are important components among several others. As the temperature increases, boehmite, a form of alumina rich in hydrate or hydroxyl groups, successively transforms into γ-alumina at temperatures between 300 and 450 °C, followed by δ-alumina at around 850 °C, θ-alumina at around 1000 °C and finally α-alumina at around 1125 °C. Further phase transitions are conceivable, whereby the specific temperatures are based on the crystal size and the original moisture content of the material.[95,96]

4.4. Gas/vapor–solid and solid-state reactions

Apart from poisoning, chemical pathways also contribute to the deactivation of catalysts through various mechanisms, including reactions between gases or vapours and solid catalysts. These reactions can lead to the formation of inactive phases, which differ from poisoning in that they do not involve strongly adsorbed species but the development of completely new phases. Notable examples of such vapour-induced chemical changes leading to inactive phases are the formation of $RhAl_2O_4$ in Pt–Rh/Al_2O_3 catalysts during high-temperature process in automotive exhaust, Fe oxidation during ammonia synthesis or regeneration, the dealumination of Y zeolite during catalytic cracking and regeneration, SO_3 reaction with alumina support to form aluminium sulphate, oxidation of Fe_5C_2 and Co metal to corresponding oxides or surface aluminates/silicates during Fischer–Tropsch synthesis and formation of $NiAl_2O_4$ during Ni/Al_2O_3 reaction and vapour regeneration. These reactions emphasise the importance of the chemical transformations that lead to deactivation of the catalyst.[95,97,98] In addition, gases and vapours can react with solids to produce volatile compounds, including metal carbonyls, oxides, sulphides and halides (Fig. 16). While the direct vaporisation of metals is usually considered insignificant, the formation of volatile compounds can lead to significant metal loss,

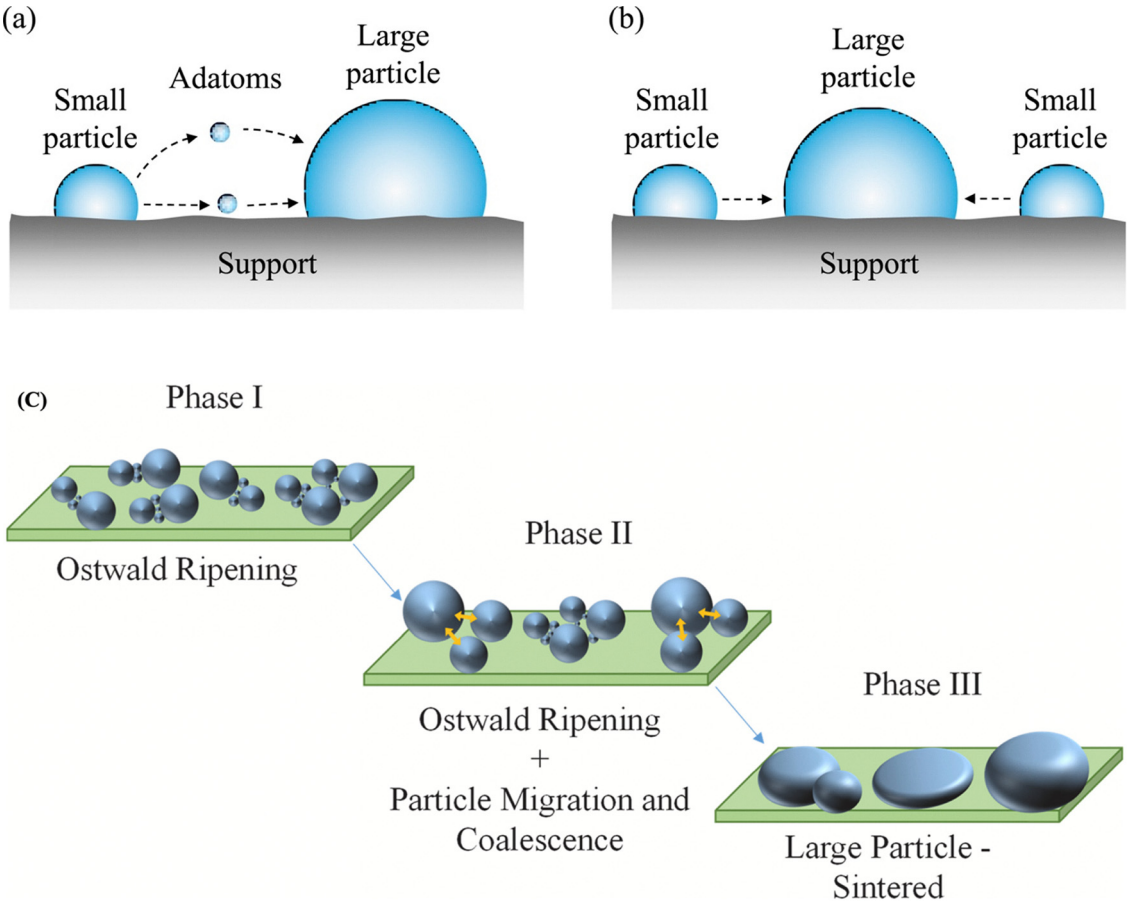

Fig. 15 Illustrates the two primary sintering mechanisms of metal particles: (a) Ostwald ripening, and (b) migration and coalescence of particles, while (c) show the schematic representations of the different sintering pathways in CO methanation. Reproduced from ref. 54 (a and b) and ref. 26 (c) with permission from Elsevier, copyright 2020 and 2023 respectively. Larger metal particles form at the expense of smaller ones, reducing the catalyst's active surface area. Since smaller particles offer more active sites, their loss leads to decreased reactivity in CO methanation. As the reaction progresses, the accumulation of larger, less active particles results in overall catalyst deactivation.

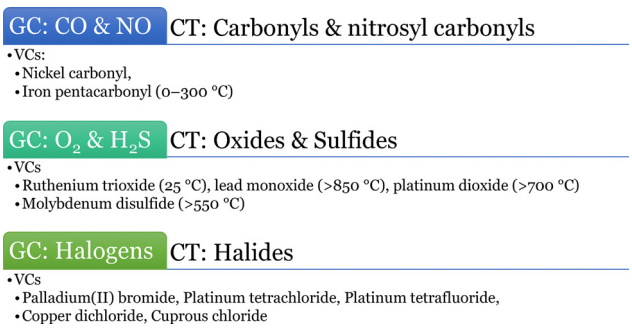

Fig. 16 Volatile compounds produced in catalytic processes at different gaseous conditions. GC: gaseous condition, CT: compound type, VCs: volatile compounds, *T* (°C): temperature of vapour formation. Modified and reproduced from ref. 4 with permission from MDPI, copyright 2015.

especially in environments rich in carbon monoxide, hydrogen sulphide or halogens. For example, carbonyl compounds are produced at relatively low temperatures and under high pressure, while halides are formed at low temperatures and low halogen concentrations. The formation of volatile oxides varies depending on the metal, with RuO_3 forming at ambient temperature and PtO_2 requiring temperatures above about 500 °C to achieve significant formation rates.[95,97,98] These reactions illustrate the diverse chemical interactions that contribute to the catalyst deactivation.

4.5. Mechanical failure of catalysts

The mechanical breakdown of catalysts manifests itself in various forms depending on the reactor type. These include the breakdown of granular, pellet or monolithic catalyst structures under fixed bed loading; attrition, which is characterised by the reduction or disintegration of catalyst granules or pellets into fines, particularly in liquid or slurry beds; and erosion of catalyst particles or monolithic coatings at elevated liquid velocities, regardless of reactor design. Wear can be recognised by an observable reduction in particle size or smoothing of the catalyst particles, which can be seen under a light or electron microscope. Meanwhile, the loss of the washcoat can be recognised by examining honeycomb channel cross-sections under an optical or electron microscope. The susceptibility of commercial catalysts to mechanical failure is largely due to

their formation process.[4] The mechanical failure of catalyst agglomerates primarily occurs through two mechanisms: fragmentation of agglomerates into smaller units ranging from approximately $0.2d_0$–$0.8d_0$ in size and erosion or abrasion from the surface of agglomerates by aggregates of primary particles measuring between 0.1 and 10 μm in diameter.[99] While erosion results from mechanical stresses, fracture can be induced by mechanical, thermal, and/or chemical stresses. Mechanical stresses causing fracture or erosion in fluidized, or sludge beds can stem from particle collisions with each other or with reactor walls or from shear forces generated by turbulent eddies or collapsing bubbles (cavitation) at high liquid velocities. Thermal stresses arise during rapid heating or cooling of the catalyst particles, compounded by temperature gradients between particles and differing coefficients of thermal expansion at interfaces of different materials, such as those between the catalyst coating and the monolith. Chemical stresses occur when phases of different densities form in the catalyst particles due to chemical reactions, leading to strains that can break these particles.[100] In addition, mechanical failure can occur in metal catalysts on supports when the pores of the catalyst become clogged with filamentous carbon, resulting in enormous pressure that can break the original particles and agglomerates.

5. Catalysts regeneration

The decrease in catalytic activity is an inevitable event in most processes despite all efforts to mitigate it. When the activity of a catalyst drops to a critical level, there are four possible courses of action: regeneration/restoration of the catalyst's activity, reuse of the catalyst for another application, recovery and recycling of valuable or high-cost catalytic components, or disposal of the catalyst. Regeneration and reuse, the first option, are usually favoured, with disposal of the catalyst being the last resort, especially considering environmental aspects.[101] The capacity to restore a catalyst is based on the reversibility of the process responsible for its deactivation. For instance, the formation of carbon and coke can be easily reversed by gasification with H_2, H_2O or O_2. Conversely, sintering is usually irreversible. With certain precious metal systems, however, redispersion of the metal can be achieved under certain conditions. Selective removal of some poisons or impurities can be achieved by chemical washing, mechanical treatments, heat treatments or oxidation.[4,101]

5.1. Convention methods of catalyst regeneration

Conventional catalyst regeneration methods have long been employed to restore the activity of deactivated catalysts, particularly in industrial applications. These techniques primarily target the removal of coke, poisons, or surface deposits that hinder catalytic performance. Common methods include thermal oxidation, steam treatment, gasification, and chemical reduction. Each approach varies in temperature, atmosphere, and effectiveness depending on the catalyst type and deactivation mechanism. Despite their widespread use, these methods often involve high energy consumption and may risk damaging catalyst structure. As such, they serve as a foundation for exploring more advanced regeneration strategies. However, some methods cannot be used to remove them without further deactivating or damaging the catalyst. The most common methods of catalyst regeneration include combustion, oxidation, gasification and hydrogenation (Fig. 17).

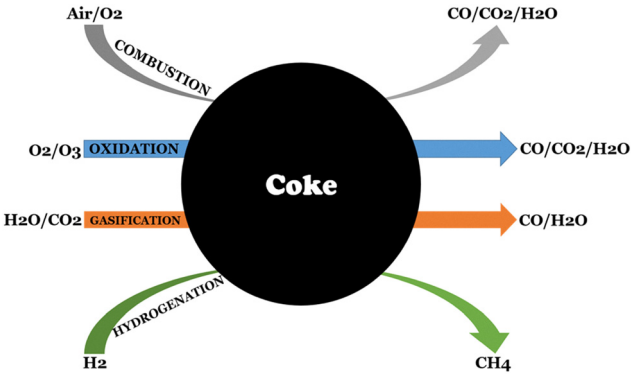

Fig. 17 Catalyst regeneration methods and gaseous products (emissions). Modified and reproduced from ref. 18 with permission from Elsevier, copyright 2020.

5.1.1. Combustion method (air and oxygen). The most common method for rejuvenating coked catalysts is oxidation with air or oxygen.[101] This approach is used in various industrial processes, including FCC,[102] hydrotreating,[103] catalytic reforming[104] and methanol to olefins (MTO).[105] In general, coke oxidation reactions, illustrated by eqn (1)–(4),[18,106] are an exothermic process that produces flue gases consisting mainly of hydrogen peroxide, carbon dioxide or carbon monoxide. The heat generated, particularly in processes such as FCC, helps to maintain a favourable heat balance within the reactor–regenerator system, thus offsetting the heat requirements of the endothermic cracking process. In processes such as MTO, on the other hand, handling the excess heat from methanol conversion and coke oxidation proves difficult due to their exothermic nature, which can lead to catalyst dealumination due to thermal and hydrothermal instability.[106] This aspect is particularly relevant in fixed-bed reactors due to the limited heat transfer possibilities, which can lead to temperature excursions.[107]

$$2H(s) + \tfrac{1}{2}O_2(g) \rightarrow H_2O(g) \quad -121\ \text{kJ mol}^{-1} \qquad (1)$$

$$(s) + O_2(g) \rightarrow CO_2(g) \quad -395\ \text{kJ mol}^{-1} \qquad (2)$$

$$C(s) + \tfrac{1}{2}O_2(g) \rightarrow CO(g) \quad -110\ \text{kJ mol}^{-1} \qquad (3)$$

$$CO(g) + \tfrac{1}{2}O_2(g) \rightarrow CO_2(g) \quad -285\ \text{kJ mol}^{-1} \qquad (4)$$

The degree of coke removal during air combustion relies on the kind of catalyst and the operating conditions. Magnoux and Guisnet[108] found that HY and H-mordenite catalysts had significantly higher coke oxidation rates compared to HZSM-5. They attributed this difference to variations in the pore framework that affect oxygen diffusion and, thus contact between coke and oxygen, leading to shape specificity in coke oxidation.

Similarly, the HFAU catalyst achieves complete coke removal at 550 °C, while HEMT requires a temperature of 600 °C for complete coke oxidation. When the coke content is low (equal to or less than five per cent by weight), the (Al/Al + Si) ratio in the framework also decreases. As a result, the acidity of the framework decreases, which makes coke removal more difficult.[108,109] Furthermore, acidic sites play a crucial role in the removal of coke during regeneration. Jong *et al.*[110] found that the removal of coke from intracrystalline channels near Brønsted acid sites preceded removal from the outer surface. This led to the conversion of certain carbonaceous compounds into more compact structures before the coke was completely oxidised back to its original state upon oxidation with air or a mixture of 0.5% oxygen and nitrogen. Moljord *et al.*[111] demonstrated that the density of the acid sites, which is equivalent to the density of the aluminium atoms of the HY framework, can affect the rate of coke oxidation. The properties of the coke, including its H/C ratio, also influence the oxidation rate. The H/C ratio in the coke has a considerable influence on the activation energy required for coke combustion. Aguayo *et al.*[112] demonstrated that the H/C ratio of deactivated HZSM-5 catalysts decreased after sweeping with He, with a corresponding increase in activation energies during regeneration by air combustion compared to non-swept deactivated catalysts. Similar trends were observed with SAPO-34 catalysts exposed to different reaction conditions, and the coked catalyst was subsequently treated with air combustion. The mesopores recover before the micropores, especially during strong deactivation, indicating a selective recovery of the pore structure.[113] The slower recovery of acidity compared to the surface area indicates that coke deposited at active sites burns more slowly than inert coke, probably due to active sites hindering combustion mechanisms.

Fig. 18 show the images of fresh, spent (coked) and regenerated – unmodified (Z5) and Ni-doped (NiZ) HZSM-5 catalysts regenerated *via* combustion method. The catalysts were regenerated after a 96 h time-on-stream (TOS) stability test conducted during the catalytic conversion of ethanol to fuel blendstock.[114] Specifically, HZSM-5 and Ni/HZSM-5 catalysts were treated in an 80 mL min^{-1} airflow at 550 °C for 5 hours to remove coke deposits formed during the reaction. This regeneration aimed to restore catalytic activity and enable reuse in subsequent cycles. Post-regeneration images revealed a visual resemblance to the fresh catalysts; however, further characterization such as surface area analysis, acidity profiling, and structural integrity assessment is essential to verify the effectiveness of the regeneration process.

5.1.2. Oxidation method (ozone/oxynitride). Ozone (O_3) has been shown to be effective in the removal of coke from catalysts at much lower temperatures, typically between 50 and 200 °C,[17,18,115] due to its strong oxidising capabilities. For example, Copperthwaite *et al.*[116] have shown that regeneration with ozone-enriched O_2 (O_3/O_2 molar ratio of 0.05) can restore the catalytic performance of deactivated ZSM-5 catalysts at 150 °C within 90 minutes. However, compared to reactivation with oxygen (O_2), the initial methane yield may be lower, but the lifetime may be slightly longer. Mariey *et al.*[117] found that coke accumulated on HY catalysts can be eliminated by O_2 at temperatures of 180 °C or less, while O_2 regeneration requires temperatures above 500 °C. Hutchings *et al.*[118] successfully regenerated deactivated HY catalysts with ozone-enriched O_2 at 250 °C without risking hydrothermal decomposition, although coke remained inside the extrudates attributed to limited pore diffusion and high O_2 dissociation. Repeated regeneration by combustion of air at high temperatures often leads to metal segregation and sintering in metal catalysts. Coke elimination at low temperatures by O_3 oxidation is effective and has minimal risks in terms of hydrothermal decay, dealumination and metal sintering.[119] Therefore, coke removal

Fig. 18 Images of the fresh catalyst (Z5 and NiZ) spent (Z5 (S) and NiZ (S)) and regenerated (Z5 (R) and NiZ (R)) zeolite catalysts. Reproduced from ref. 114 with permission from Elsevier, copyright 2024.

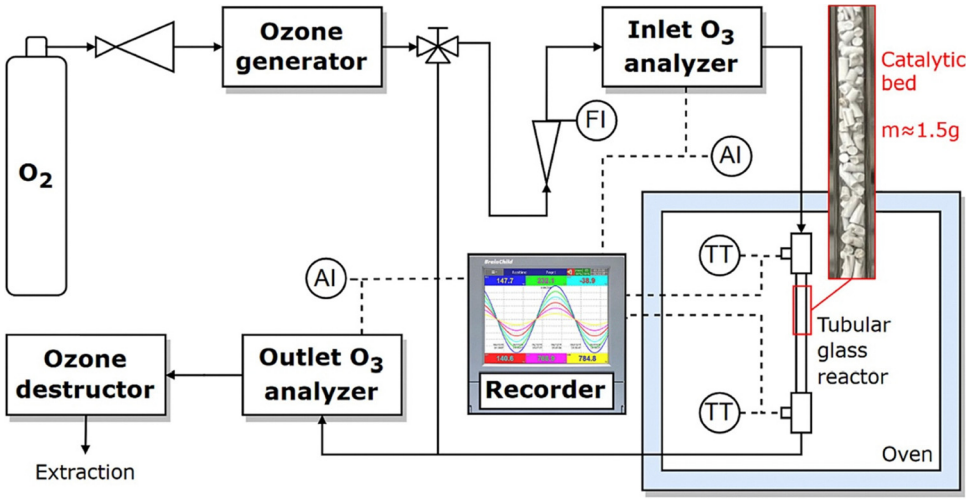

Fig. 19 Laboratory-scale setup for the regeneration of coked catalyst *via* ozonation as proposed by ref. 122. Reproduced from ref. 122 with permission from Elsevier, copyright 2023.

at low temperatures is preferred to ensure the stability of the catalyst during regeneration. However, oxygen oxidation also has disadvantages. For example, it is challenging to eliminate coke from the particle centres due to rapid O_2 dissociation. In addition, the use of oxygen in industry is restricted to avoid damage to the atmosphere. Nitrogen oxides (NO_x) are potential low-cost oxidising agents for coke removal at low temperatures. Ivanov *et al.*[120] found N_2O to be more effective than O_2 in eliminating coke from ZSM-5 deposited during the oxidation of benzene to phenol, while Barbera *et al.*[121] used NO_2 to reactivate ZSM-5 catalysts from the conversion of methanol to HCs. Despite its effectiveness, NO_2 regeneration can lead to catalyst instability due to the redistribution of aluminium atoms and irreversible degradation, indicating the need for further research in this area (Fig. 19). Schematic representation of the laboratory-scale experimental setup designed for the regeneration of coked or deactivated catalysts through ozone-assisted treatment.

5.1.3. Catalyst regeneration by gasification. Gasification is an alternative to the predominant method of coke oxidation for the rejuvenation of inactive industrial catalysts. Coke oxidation, while widely used, results in the release of significant carbon dioxide, a greenhouse gas responsible for environmental problems, including global warming. About 45–55% of CO_2 emissions from refineries come from the regeneration of spent catalysts by air combustion in FCC plants.[123] Another strategy to reduce CO_2 emissions is to regenerate spent catalysts by gasification with water or carbon dioxide.[124–127]

5.1.3.1. CO_2 gasification. The use of carbon dioxide as a feedstock has garnered attention due to its positive effect on the global carbon balance. The reaction between CO_2 and coke is referred to as the Reverse Boudouard (RB) process, which is characterised by the presence of a weak oxidant.[128,129] The coked catalyst regeneration by CO_2 gasification offers potential benefits for the carbon balance as carbon dioxide is reduced to carbon monoxide. Carbon dioxide gasification has been used for coal, biomass and sewage sludge, although these materials are not described in detail here. The highly endothermic nature of CO_2 gasification occurs at >700 °C.[130] However, these high temperatures present challenges. However, these high temperatures pose a challenge as they can potentially damage the catalyst structure or lead to sintering. The main challenges for catalyst renewal by CO_2 gasification are the limited reactivity of CO_2 and the elevated temperatures required.[131] Despite these challenges, CO_2 gasification offers advantages over steam gasification. Unlike steam, carbon dioxide as a gas does not have to be vaporised before gasification. Moreover, at high temperatures, steam can affect the Al–O bond of the catalyst, which can lead to the breakdown of the catalytic structure. This problem is not observed in CO_2 gasification.[132–134] Santos *et al.*[135] studied coked FCC catalyst regeneration in CO_2 and H_2 environments using a temperature-programmed reaction from 25–1000 °C. Their results emphasised the significant influence of coke type on gasification rates. Species with aliphatic and poly-substituted aromatic properties were more likely to react with carbon dioxide. The gasification of CO_2 was efficiently modelled using a first-order kinetic model at temperatures from 600 to 940 °C.[135] Despite the higher reactivity of O_2 compared to CO_2, gasification of CO_2 can also occur in the presence of O_2, possibly dominating the initial stages of catalyst regeneration depending on the partial pressure of CO_2. Tian *et al.*[136] investigated gasification reactivity with CO_2 at temperatures between 800 and 900 °C to regenerate coked catalysts used in the upgrading of heavy petroleum feedstocks. Their results indicate that higher temperature improved gasification rates, although rates beyond 50% coke conversion decreased significantly. Santos *et al.*[135] observed that the removal of coke from the catalyst surface precedes the removal of coke present in the pores. In this scenario, Knudson diffusion gradually becomes dominant, leading to a lower gasification rate as the reaction progresses.

5.1.3.2. Steam gasification. The use of steam as a gasification agent in regeneration processes only reduces the accumulation of CO_2 and also generates synthesis gas consisting of H_2 and CO. Steam gasification, a widely recognised method suitable for both coal and biomass, is commonly used. However, when steam is used to eliminate accumulated coke from catalysts at elevated temperatures, there is a risk of disrupting the structure of the catalyst, which can lead to permanent deactivation. It is, therefore, essential that the catalyst has a high hydrothermal stability. Eqn (5) can be used to describe the process of coke gasification with steam.[137–139]

$$C(s) + H_2O(g) \rightarrow CO(g) + H_2(g) \quad +131 \text{ kJ mol}^{-1} \qquad (5)$$

As Tian *et al.*[136] found, the rate of coke gasification with steam (H_2O) is 2 to 5 times higher than that with CO_2 for different coke types. In the elimination of coke from catalysts used in the cracking of heavy oil, the reactivity of steam gasification at temperatures between 800 and 900 °C was about three to five times higher than that of carbon dioxide.[136] High temperatures of 700 to 900 °C are required for the vapour gasification of graphitic or less reactive coke types. However, the hydrothermal instability of the catalysts at these temperatures limits the commercial application of steam gasification. According to Zhang *et al.*,[140] the steam gasification rate for FCC spent catalysts utilised for vacuum residue cracking was relatively low, with catalyst regeneration possible at temperatures below 700 °C, although a higher temperature of 800 °C resulted in an increased coke removal rate. Regardless of the gasification temperature, the resulting gas retained an unchanged composition of 87 vol% H_2 and CO.[140] Initially, the steam gasification rate increased but eventually peaked at coke conversions between 5% and 20% before gradually decreasing.[141] A correlation between the initial pore volume and the maximum vapour gasification rate was observed by Sahimi and Tsotsis.[142] Since coke can be deposited both on the outer surfaces and in the inner pores of the catalysts, the steam reacts with the surface coke, resulting in higher gasification rates attributed to the increased contact area between steam and coke. However, if the coke content decreases during the process, the gasification rate also decreases.[140] Similar to the oxidation of O_2 and the gasification of CO_2, steam gasification can also be improved by the addition of metal or metal oxide additives. Corma *et al.*[126] found that the coke deposited on standard FCC catalysts has a relatively low reactivity during steam gasification. By modifying FCC catalysts with metals including La, Ce, Zn, Ti and Mn, the gasification rate can be increased by 50 to 100%. Despite the high reaction rate of this novel steam gasification compared to CO_2 gasification, it is rarely used industrially due to the required hydrothermal stability of the catalysts. Lowering the temperature of steam gasification is possible using metal-doped catalysts and oxygen-steam gas mixtures as regeneration agents but requires further research.

5.1.4. Regeneration by hydrogenation. The removal of coke can also be achieved by non-oxidative methods, including pyrolysis with inert gas[143] or hydrocracking with H_2 or alkanes (eqn (6)).[144] Schulz and Wei[145] found that coke accumulation on HZSM-5 catalysts could be entirely removed by treating them with inert gas at 287 °C. However, treatment at higher temperatures (327 to 377 °C) only partially removed the coke. Similarly, Magnoux *et al.*[146] observed that while N_2 treatment could partially eliminate coke on USHY catalysts, it led to increased residual aromaticity in the coke and resulted in catalyst deactivation.[146] However, it remains uncertain whether the catalytic activity can be fully restored after exposure to high-temperature inert gas treatment. Therefore, this section will primarily focus on the catalyst regeneration by hydrocracking with hydrogen.

$$C(s) + 2H_2(g) \rightarrow CH_4(g) \quad -75 \text{ kJ mol}^{-1} \qquad (6)$$

Marecot *et al.*[147] observed methane as the only product in the regeneration of industrially coked Pt/Al_2O_3 catalysts by temperature-controlled reactions under a hydrogen atmosphere.[147] Walker Jr *et al.*[148] found that at 800 °C, the relative coke removal rate followed the order $O_2 > H_2O > CO_2 > H_2$, indicating the relatively low activity of H_2 in coke regeneration, which requires a lot of time and energy.[148] Bauer *et al.*[149] reported that a spent HZSM-5 used in processes to convert methanol to hydrocarbons could be partially reactivated by heating to 420 °C and treatment with hydrogen and alkanes, resulting in increased activity recovery and improved hydrogen-to-carbon ratio in the residual coke due to hydrogenation and hydrocracking reactions facilitated by acidic zeolites.[149] Aguayo *et al.*[143] reported that the catalytic performance of coked HZSM-5 was restored after treatment with H_2, with a small increase in the H/C ratio indicating reduced dehydrogenation of coke. However, Jong *et al.*[150] demonstrated that even at temperatures of 900 °C, complete removal of coke that had accumulated on HZSM-5 could not be achieved with H_2 as a regeneration gas. They observed that internal coke removal near Brønsted acid sites was more effective than external coke removal at the surface, indicating the significant role of Brønsted acid sites in H_2 regeneration.[150] In addition, Bauer *et al.*[151] found that propane selectively removed coke from spent catalysts and that the combination of hydrogen and alkane treatment reactivated active sites in the material.[151] The effectiveness of the regeneration gas in removing coke from spent USHY catalysts for the conversion of *m*-xylene at 500 °C follows the order of air > hydrogen > nitrogen.[152] Benamar *et al.*[152] found that the amount of coke removed by H_2 treatment relies on the initial coke concentration on the deactivated catalyst, with lower removal percentages observed for samples with higher coke concentrations.[152] Table 4 provides a comparative evaluation of various conventional regeneration methods, while Table 5 summarizes the regeneration strategies applied to different catalysts across a range of heterogenous processes.

5.2. Emerging catalyst regeneration techniques

As catalytic processes evolve to meet the demands of sustainability and efficiency, conventional regeneration methods often fall short in restoring full catalyst activity. Emerging techniques are being developed to address challenges such as severe deactivation, structural degradation, and selectivity loss. These innovative approaches leverage advanced technologies,

Table 4 Comparison of different conventional catalyst regeneration methods[18]

Attributes	Air (O_2)	Ozone (O_3/NO_x)	CO_2 gasification	Steam gasification	Hydrogenation
Oxidising/gasification capacity	Strong	Moderate	Limited CO_2 reactivity	2 to 3 times CO_2 reactivity at 800 to 900 °C	Effective/strong
Temperatures	>300–600 °C	50–400 °C	>700 °C	700–900 °C	>400–900 °C
Time	Less treatment time	Less treatment time	Moderate treatment time	Moderate treatment time	Time-consuming
Stability	May affect catalyst stability if the regeneration temp. Is above calcination temp. for zeolite catalyst	Catalyst stability during regeneration	Uncertain at extreme gasification temperature	Result in catalyst instability	Catalyst stability is ensured
Delamination and hydrothermal degradation tendency	Medium	Low	High, attributed to high temp. process	Hydrothermal degradation	Moderate
Heat effect	Exothermic	Exothermic	Endothermic	Endothermic	Exothermic
Pressure	Atmospheric	Atmospheric	Atmospheric	Atmospheric	Elevated pressure
Gaseous product	CO_2/CO/H_2O	CO_2/H_2O/NO_x	CO	CO/H_2	CH_4
Other associated risks/challenges	Metal segregation and sintering in metal catalysts and CO_2 emission	Harmful gases and CO_2 emission	High temp. can lead to sintering	Steam can affect the Al–O bond, hence the breakdown of the catalytic framework	High temperature or pressure

including supercritical fluid extraction, plasma treatment, microwave-assisted regeneration, *etc.* Such methods offer improved regeneration efficiency, reduced environmental impact, and greater adaptability across catalytic systems.

5.2.1. Supercritical fluid extraction (SFE). Supercritical fluid extraction (SFE) is a promising green technology for the regeneration of deactivated catalysts, especially those contaminated with organic compounds or coke.[163–165] The process uses supercritical fluids (SCFs) typically supercritical CO_2 which possess unique physicochemical properties between those of gases and liquids, such as low viscosity, high diffusivity, and high solvating power. These properties enable SCFs to penetrate catalyst pores effectively and dissolve surface-bound contaminants without causing thermal damage or altering the catalyst's structure.[163,164] In SFE-based regeneration, the deactivated catalyst is exposed to a supercritical solvent (*e.g.*, CO_2) at controlled temperatures (above 31 °C for CO_2) and pressures (above 73 atm). The SCF diffuses through the porous catalyst structure, solubilizing organic foulants like coke precursors, polymers, or heavy hydrocarbons. This mass transfer process is governed by fluid–catalyst interactions and is enhanced by the adjustable density and polarity of the SCF, which can be fine-tuned with co-solvents such as ethanol or methanol to increase extraction efficiency.[163] Once dissolved, the contaminants are carried out of the system with the exiting SCF stream, and the purified catalyst is recovered. Compared to conventional thermal or oxidative regeneration, SFE operates at lower temperatures, avoiding sintering, metal particle agglomeration, and destruction of acid sites. The process is non-destructive, environmentally friendly, and potentially recyclable, making it suitable for sensitive catalysts like zeolites, enzymes, or precious metal–supported systems.[163,164] A typical SFE setup is presented in Fig. 20.

Different studies have highlighted the effectiveness of supercritical fluid extraction (SFE) for catalyst regeneration. Gumerov *et al.*[163] showed that supercritical CO_2, aided by co-solvents, can remove deactivating deposits from metal-based catalysts without damaging their structure. Gumerov *et al.*[164] emphasized that employing supercritical CO_2 extraction for catalyst regeneration not only enhances energy efficiency but also allows for more regeneration cycles, thereby improving the overall sustainability and cost-effectiveness of the process. A broader review on SFE reinforced its advantages, including low energy use and mild operating conditions, making it a promising method for preserving catalyst activity while ensuring efficient contaminant removal.[165]

5.2.2. Plasma-assisted regeneration. Plasma-assisted regeneration is an emerging and highly effective technique for regenerating catalysts deactivated by coke deposition. Unlike conventional thermal regeneration, which requires high temperatures and can lead to catalyst sintering or metal particle agglomeration, plasma-assisted regeneration operates at lower temperatures, reducing thermal damage and extending catalyst life.[167] The process involves exposing the coked catalyst to a non-thermal plasma (NTP), typically generated using dielectric barrier discharge (DBD), microwave, or radiofrequency methods.

Table 5 Summary of regeneration strategies for different catalyst

Catalyst	Reaction/process	Regeneration conditions	Inference	Ref.
HY, H-mordenite and HZSM-5	Regeneration of zeolites	5 h catalyst pretreatment under N_2 (40 cm^3 min^{-1}) at 500 °C and cooling at 150 °C, O_2 (10 cm^3 min^{-1}) treatment temp. of 250–500 °C and time: 30 min to 1 hour	The choice of zeolite has a considerable effect on the oxidation rate of coke, whereby clear differences can be observed between the different types. For example, HY and H-mordenite zeolites have significantly faster oxidation rates for coke compared to HZSM-5. The observed differences in oxidation rates cannot be attributed solely to the several compositions of the coke present in these samples.	108
HEMT and HFAU zeolites	Comparative study	T = 350–600 °C, under O_2 at 25 °C (5 °C min^{-1}) for 1 h	HFAU catalysts showed much higher coke oxidation rates than HEMT catalysts regardless of the framework composition, which can be due to the external deposition of coke on the surface of HFAU catalysts, making it more accessible to oxygen	153
HZSM-5	Ethylbenzene conversion catalyst	Air, 0.5% O_2 in N_2 and H_2 at 500 °C	Coke oxidation with air or a mixture of O_2 and N_2 led to the conversion of certain carbon compounds into more compact structures, followed by complete coke oxidation. Meanwhile, the external coke was partially cracked when exposed to hydrogen.	110
HY zeolites	Propene transformation at 450 °C.	O_2 environment at 25–550 °C	The presence of additional aluminium species outside the framework or minimal amounts of sodium (below 0.15 wt%) in the zeolites did not affect the coke oxidation and removal process.	111
HZSM-5	Effects of sweeping with each one on both coke hydrogenation and coke gasification.	Combustion in air at 550 °C	Hydrogen during sweeping prevents the dehydration of coke but removes some of the coke and leads to a secondary reaction that gradually deactivates the catalyst. Steam, on the other hand, removes coke and irreversibly deactivates the catalyst.	112
SAPO-34	Regeneration of SAPO-34 for MTO conversion	30–60 min ageing treatment at 500–600 °C Regeneration: gas flow: 0–10 mol $g_{catalyst}^{-1}$ min^{-1}; time: 0–3 h. Temp: 200–375 °C	The H/C ratio in the coke has a considerable influence on the activation energy required for coke combustion. The mesopores recover before the micropores, especially during strong deactivation, indicating a selective recovery of the pore structure.	113
ZSM-5	Regeneration of ZSM-5 catalyst for MTG process	Oxygen flow at 5 °C min^{-1} from 200 to 550 °C.	Precise temperature control during combustion in the reactor is essential to prevent the catalyst from sintering. Therefore, the use of this coke equilibrating technique for regeneration in industrial adiabatic fixed bed processes is necessary to prevent the sintering of the catalyst.	154
H-ZSM-5/H-mordenite ZSM-5/MOR	ZSM-5/MOR derived from the cracking of *n*-heptane	Combustion temperature (500–700 °C) at a rate of 50 °C min^{-1} under a nitrogen flow of 100 mL min^{-1},	In contrast to the catalyst deactivated by coking with water steam, the presence of two different types of coke was observed in the coked catalyst deactivated by catalytic cracking without water steam. These various forms of coke exhibited several kinetic combustion models.	155
MFI-type zeolite	MFI-type zeolite from *n*-hexane catalytic cracking	Temp.: 650 °C, airflow was 0.1 MPa at 200 mL min^{-1}.	Most of the coke on the MFI zeolite was predominantly located on the outer surface. The rates of carbon and hydrogen combustion in the coke were found to agree with the Arrhenius equation, showing activation energies of 156 kJ mol^{-1} and 140 kJ mol^{-1}, respectively.	156
HZSM-5	HZSM-5 for ethanol dehydration reaction	Calcination at 550 °C for 6 h under air (100 mL min^{-1})	Catalysts still maintained 90% ethanol conversion for 400 h TOS even after successive catalyst regeneration.	157
Zn/ZSM-5	Zn/ZSM-5 for ethylene aromatization	Air (O_2 content: 20%) at 550 °C (0.5 °C min^{-1}) for 10 h.	The crystallinity, pore volume, surface area, and total acidity of the regenerated Zn/ZSM-5 were fully restored after the removal of carbon deposits during regeneration.	158
ZSM-5	ZSM-5 from catalytic fast pyrolysis (CFP) of biomass	4% O_2 at temperatures between 500–700 °C	The study shows that higher regeneration temperatures (650 °C and 700 °C) for 20 minutes effectively regenerate a ZSM-5 catalyst used in the catalytic fast pyrolysis of biomass. Lower temperatures (550 °C and 600 °C) may require a longer regeneration time. Regeneration at 500 °C and 20 minutes may not completely remove coke deposits, resulting in incomplete recovery of catalyst activity.	159
HZSM-5, Hβ and HY zeolites	Catalysts from biomass pyrolysis	Airflow at 450 °C for	The disappearance of the adsorbed hydrocarbon bands and the appearance of hydroxyl and silanol group bands in the FTIR spectrum is evidence that the catalysts have been regenerated.	160
MFI zeolite (Fe–Ga–Si zeolites)	MFI zeolites from oxidative dehydrogenation of propane by N_2O	450 °C for 90 min in air	The initial propylene production of fresh and regenerated Fe–Ga–Si zeolites was identical, but the regenerated sample was deactivated faster. This is attributed to changes in the iron composition after the first reaction-regeneration cycle.	161
Zeolite	Zeolite from isobutane/butene alkylation	Regeneration was carried out every 7 h, at an H_2 pressure of 15 bar and 300 °C	Regeneration of the catalyst under suitable conditions can fully restore its activity for the alkylation reaction with 100% conversion of 1-butene	162

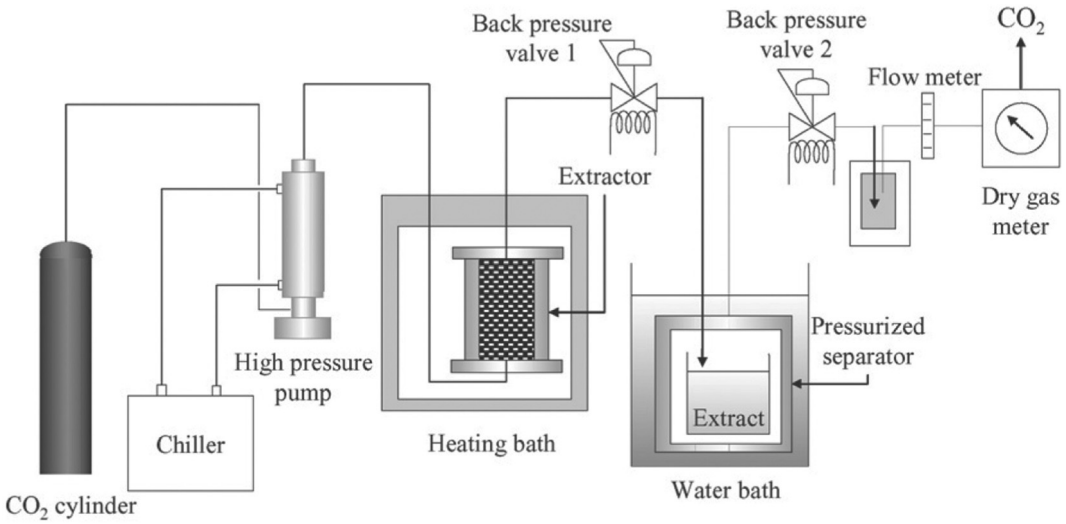

Fig. 20 Schematic diagram of supercritical fluid extraction (SFE) set-up. Reproduced from ref. 166 with permission from Elsevier, copyright 2006.

In this environment, an electrical field energizes gas molecules (*e.g.*, O_2, N_2, CO_2, or air), producing reactive plasma species such as atomic oxygen, ozone, and excited radicals. These highly reactive species selectively oxidize and gasify coke deposits on the catalyst surface at low bulk temperatures, forming CO and CO_2 without significantly heating the catalyst structure. The regeneration is highly surface-specific, minimizing damage to internal pores and active sites. This method is particularly suited for delicate catalysts like zeolites and metal oxides and offers enhanced control over coke removal. Studies have shown that plasma treatment can restore up to 90–100% of original catalyst activity depending on coke type and operating conditions.[167]

Metal catalysts deactivated through oxidation can be effectively regenerated by treatment in a reducing atmosphere at suitable temperatures. The introduction of plasma during this reduction process can alter the reduction environment, enhancing regeneration efficiency. In a study by Kim *et al.*,[168] the plasma-assisted regeneration of an oxidized Cu catalyst (CuO/ZnO supported on γ-alumina beads) was examined and compared with conventional thermal reduction. Using a packed-bed reactor and a 4 vol% H_2 stream (Fig. 21), they observed that plasma-assisted reduction enabled complete conversion of CuO/ZnO to Cu/ZnO at lower temperatures and in a shorter time than thermal treatment. Temperature programmed reduction (TPR) profiles (Fig. 22) revealed a significant shift to lower reduction temperatures under plasma conditions at a discharge power of 1.61 W and a peak voltage of 7 kV. Notably, both methods produced regenerated catalysts with comparable physicochemical properties, including surface area and pore size distribution, demonstrating that plasma-assisted regeneration is a viable and potentially more energy-efficient alternative to traditional thermal reduction methods.[167]

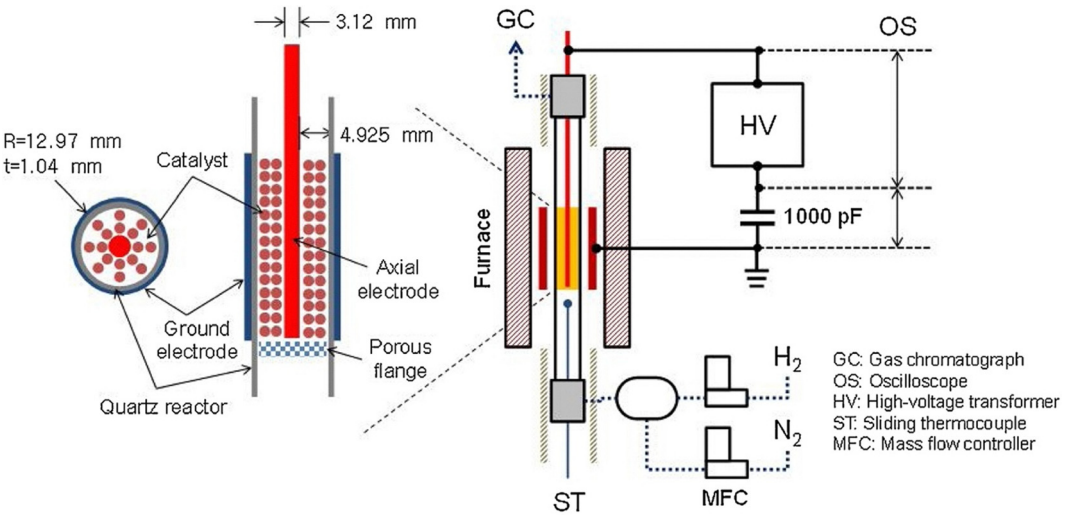

Fig. 21 Illustrates the experimental configuration of the packed-bed reactor employed by ref. 168. Reproduced from ref. 167 with permission from Elsevier, copyright 2019.

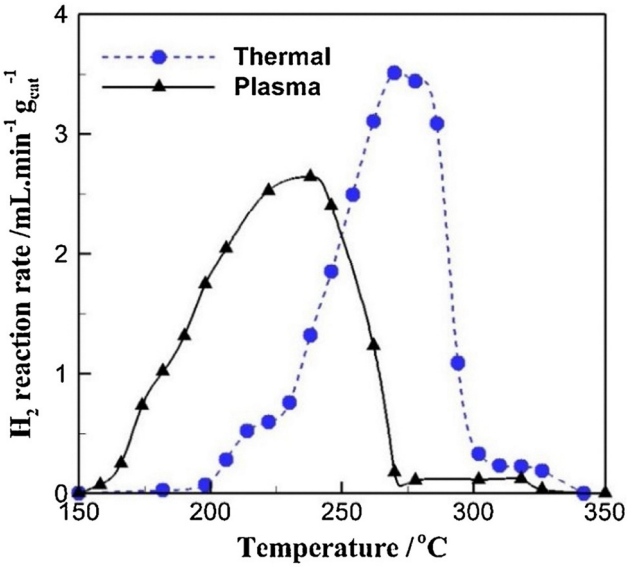

Fig. 22 H_2 temperature-programmed reduction (TPR) profiles comparing thermal and plasma-assisted reduction methods. Reproduced from ref. 168 with permission from John Wiley and Sons, copyright 2016.

5.2.3. Microwave-assisted regeneration. Microwave-assisted regeneration is presented as a highly effective and energy-efficient technique for restoring the adsorption capacity of spent activated carbon. This method uses microwave radiation to rapidly and selectively heat the carbon material, thereby desorbing or decomposing adsorbed organic compounds, including coke-like residues. The regeneration process involves placing the spent activated carbon in a microwave reactor, where it is exposed to electromagnetic radiation typically at 2.45 GHz.[169,170] Microwaves interact directly with the carbon matrix, causing dipolar rotation and ionic conduction within the material. This leads to volumetric and internal heating, which contrasts with conventional surface-based thermal methods. The rapid and uniform heating generates sufficient thermal energy to desorb and thermally decompose the adsorbed species, restoring active adsorption sites. Studies by Xin-hui *et al.*[171] and Nor *et al.*[172] demonstrated that parameters such as microwave power, regeneration time, and moisture content significantly influence regeneration efficiency. Under optimized conditions, the regenerated carbon retained high adsorption capacity with minimal structural damage.

5.2.3.1. Microwave-assisted regeneration (conventional). Findings from the study by Amornsin *et al.*[173] demonstrate that, compared to conventional heating (Fig. 23a), microwave-assisted regeneration (Fig. 23b) of zeolite 13X used as a sorbent in the CO_2 capture process consistently achieves higher efficiency at lower temperatures (90 °C, 120 °C, and 300 °C), as illustrated in Fig. 24. This is attributed to its direct and selective energy delivery through Na^+ ion vibration.[174,175] At 150 °C and 350 °C temperatures associated with key CO_2 desorption stages both methods exhibit comparable performance. Microwave regeneration is significantly faster requiring 5–10 minutes compared to 30 minutes for conventional methods and consumes substantially less energy. For instance, at 350 °C, microwave regeneration used 0.06 kWh *versus* 0.62 kWh for conventional heating, with similar trends across other temperatures.[176,177] However, initial CO_2 adsorption was higher in the conventional method, possibly due to moisture uptake during extended storage of samples used in microwave testing.[178] Improved sample preparation or purging could mitigate this.

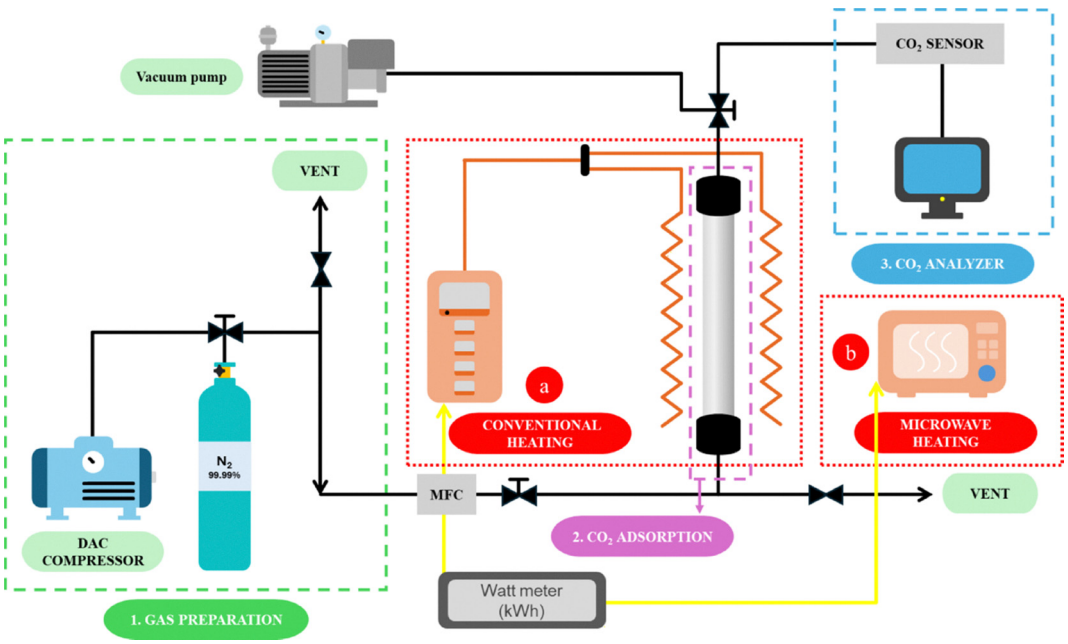

Fig. 23 Illustration of the direct air CO_2 capture process in a fixed-bed reactor: (a) regeneration through traditional thermal heating, and (b) regeneration utilizing microwave-assisted heating. Reproduced from ref. 173 with permission from Springer Nature, copyright 2025.

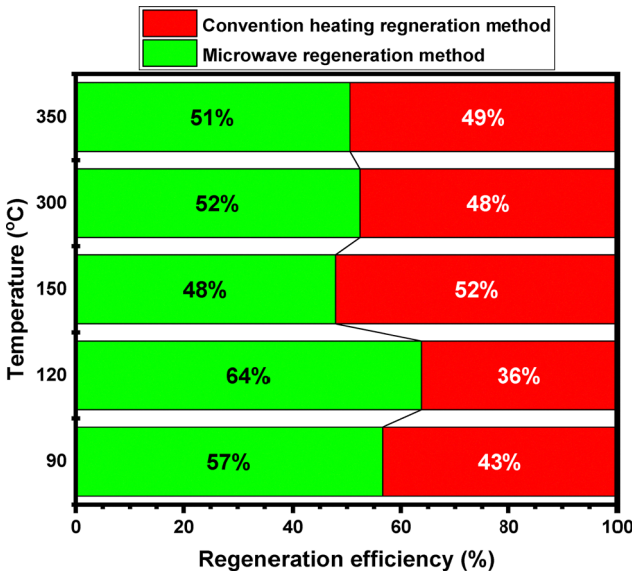

Fig. 24 Comparison of regeneration performance between microwave-assisted and conventional heating methods across different regeneration conditions. Modified and reproduced from ref. 173 with permission from Springer Nature, copyright 2025.

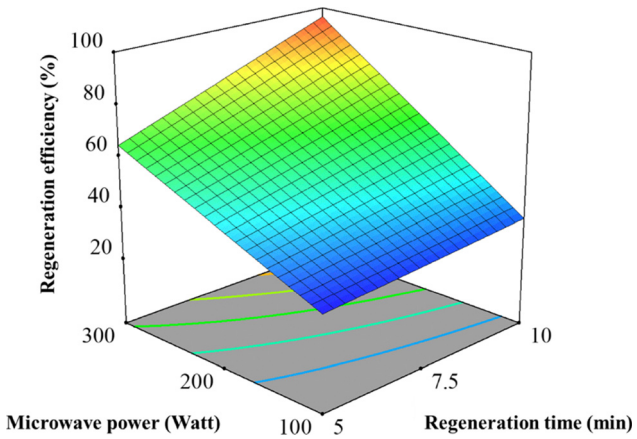

Fig. 25 Three-dimensional surface plot showing the interaction between experimental variables and the efficiency of regeneration. Reproduced from ref. 173 with permission from Springer Nature, copyright 2025.

Additionally, while the conventional method uses N_2 purging to enhance desorption, the microwave system achieved higher efficiency without it, highlighting the superior influence of dielectric heating.[179,180] This effect is further supported by Fig. 25, which illustrates the interaction between the experimental variables and regeneration efficiency. The data show that regeneration efficiency tends to improve with increases in both microwave power and regeneration time. Among these, microwave power has the most significant impact, as demonstrated by the sharp gradients and colour variations in the graphs. These patterns are consistent with the trends previously discussed by Amornsin *et al.*[173] regarding how microwave power and regeneration time affect CO_2 adsorption capacity and overall regeneration performance. It can be inferred that microwave-assisted regeneration demonstrates clear advantages in energy savings, regeneration speed, and long-term performance.

5.2.3.2. Microwave and ultrasonic spray assisted regeneration (improved). Lin *et al.*[181] conducted a study on the regeneration of spent catalysts using microwave heating combined with ultrasonic spray (US) assistance. Under optimized experimental conditions, the spent activated carbon (AC) was regenerated in three distinct atmospheric environments: carbon dioxide (AC-CO_2), nitrogen (AC-N_2), and ultrasonic spray (AC-US). Nitrogen adsorption analysis, including isotherms, pore volume, and pore size distribution (Fig. 26a–c), revealed that AC-ultrasonic spray exhibited the highest adsorption isotherm, suggesting enhanced pore development. This sample also showed the greatest micropore volume, covering a wide range from narrow micropores to large mesopores. Compared to the other regeneration atmospheres, the AC-ultrasonic spray demonstrated significantly improved textural properties, including higher total pore volume, BET surface area, and micropore volume. These findings confirm the effectiveness of ultrasonic spray-assisted microwave regeneration. Notably, AC-ultrasonic spray achieved a BET surface area of 1263 $m^2\ g^{-1}$, making it a promising material for industrial applications in adsorption and pollutant removal.[181] The study highlights ultrasonic spray as a highly efficient regeneration method for spent catalysts.

To support the results presented by Amornsin *et al.*,[173] Table 6 provide relevant evidence. It presents the pore structure properties of regenerated activated carbons derived from various spent materials using either microwave or conventional heating methods. Among them, the activated carbon regenerated using the ultrasonic spray method under microwave heating exhibited superior characteristics compared to the others.

5.2.4. Atomic layer deposition (ALD). Atomic layer deposition (ALD) is a vapor-phase technique that enables the deposition of ultra-thin, conformal films with atomic-level precision. This method is particularly effective for catalyst repair and regeneration, as it allows for the restoration of active sites, prevention of sintering, and enhancement of catalyst stability. ALD operates through sequential, self-limiting surface reactions. In a typical ALD cycle, the substrate is exposed to a gaseous precursor that reacts with available surface sites, forming a monolayer. After purging excess precursor and by-products, a second precursor is introduced, reacting with the first to form a thin film. This cycle is repeated to achieve the desired film thickness. The self-limiting nature of these reactions ensures uniform and conformal coatings, even on complex and porous structures.[186] In catalyst repair, ALD can deposit protective layers that prevent sintering and leaching of active metal nanoparticles. For instance, coating nickel-based catalysts with ALD-grown Al_2O_3 layers has been shown to suppress sintering and reduce coke formation, thereby enhancing catalyst stability. Additionally, ALD can be used to introduce new active sites or modify existing ones, tailoring the catalyst's activity and selectivity. The precision and versatility of ALD make it a valuable tool in extending catalyst longevity and

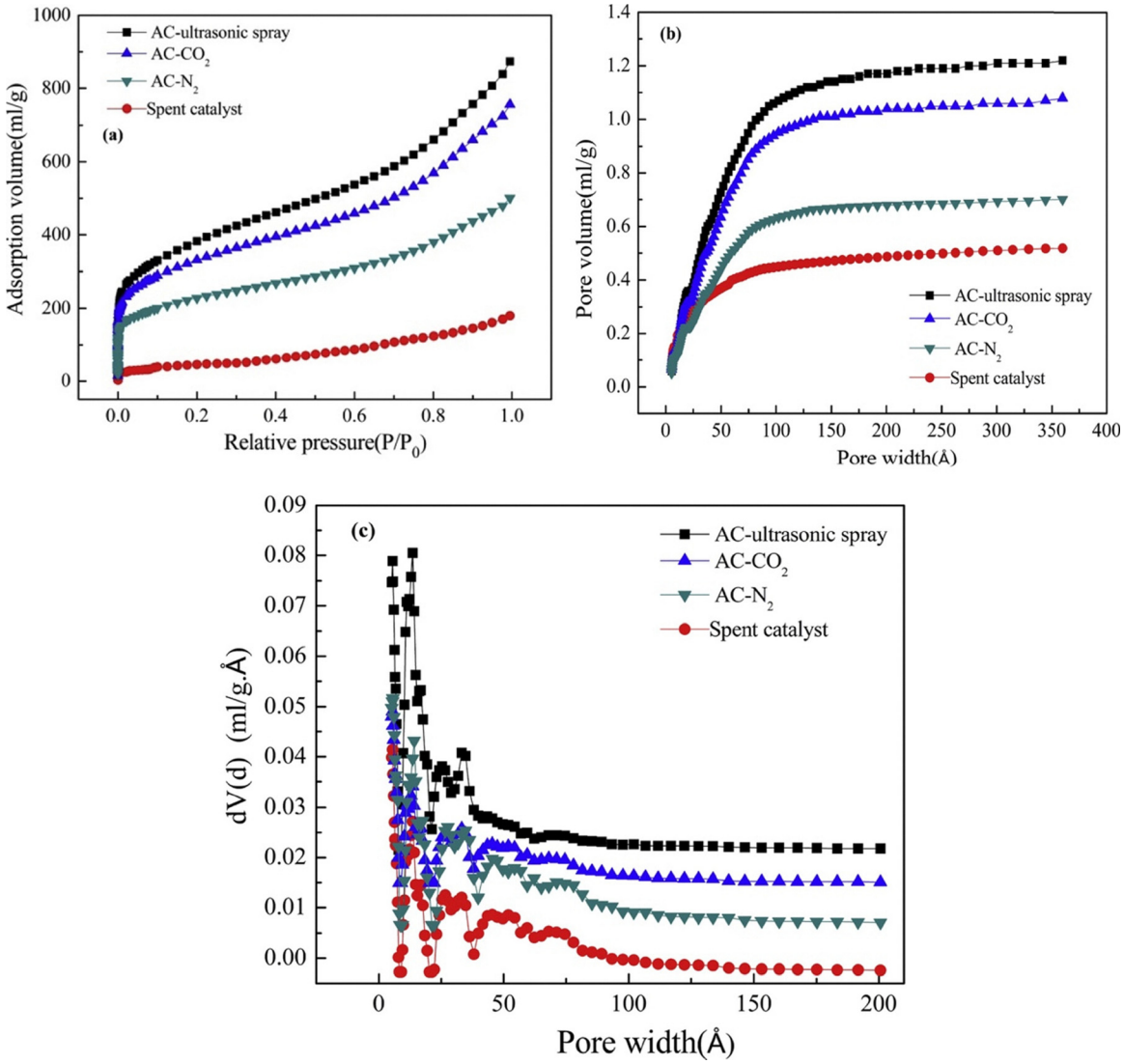

Fig. 26 Properties of regenerated activated carbon under various atmospheric conditions, along with the spent catalyst: (a) nitrogen adsorption isotherms, (b) total pore volume, and (c) pore size distribution profiles. Reproduced from ref. 181 with permission from Elsevier, copyright 2018.

Table 6 Pore structure comparison of activated carbon regenerated from different spent catalysts. reproduced from ref. 181 with permission from Elsevier, copyright 2018

Regeneration/heating method	Heating temp. (°C)	Time (s)	Activation agent	BET surface area (S_{BET}, $m^2\ g^{-1}$)	Micropore volume (V_{mic}, mL g^{-1})	Ref.
Microwave heating	878	840	Ultrasonic spray	1263	0.42	181
Microwave heating	1000	1500	CO_2	1255	0.50	182
Microwave heating	850	240	N_2	1083	0.20	183
Conventional heating	983	8100	Steam	1233	0.53	184
Conventional heating	850	240	CO_2	1064	0.19	185

improving performance. Its ability to engineer catalysts at the atomic level opens avenues for designing catalysts with enhanced durability and tailored functionalities.[187,188]

Zhang *et al.*[189] utilised ALD to rejuvenate aged Pt/CeO_2 catalysts and effectively restore their catalytic performance. This dual approach, which serves as both a catalyst regeneration and preparation method, targets metal-supported systems and is in line with broader catalyst restoration and enhancement strategies. In particular, the method is aimed at the regeneration of supported platinum-based three-way catalysts in the field of precious metal catalysis.[189] The process involves using a commercial Pt/CeO_2 catalyst, which is first subjected to thermal aging in a muffle furnace at 800 °C for 5 hours to simulate sintering-induced deactivation.[189] The deactivated

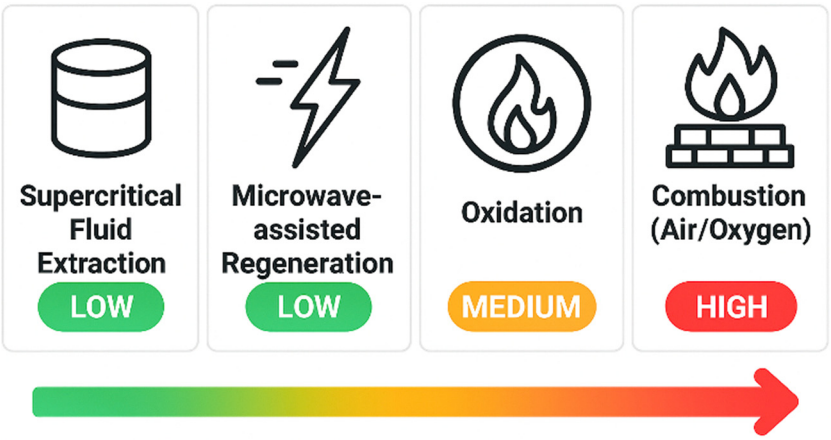

Fig. 27 Severity of emissions from different regeneration methods.

catalyst is then treated using atomic layer deposition (ALD) to apply various oxide coatings. This approach effectively regenerates the sintered catalyst, enabling it to regain a portion of its original catalytic activity. While Fig. 27 highlights the severity of emissions associated with various regeneration methods, Table 7 presents a comparative evaluation of emerging catalyst regeneration techniques.

6. Challenges in catalyst deactivation and regeneration

Several factors can influence or hinder the regeneration of a deactivated catalyst. Some of the challenges for effective regeneration of these catalysts are presented below:

6.1. Complete removal of deactivants and preservation of catalyst structure and activity

Ensuring the complete removal of foulants, such as coke, tar, or contaminants, from the catalyst surface is challenging. Even small amounts left behind can continue to deactivate the catalyst during subsequent reaction cycles. In addition, regeneration processes can alter the catalyst structure and chemistry, potentially reducing its activity or selectivity. Regeneration treatments, such as high temperatures or harsh chemical reactions, can cause catalyst degradation, including sintering, phase changes, or surface area loss.[4] Minimizing these undesirable changes while effectively removing deactivants is a significant challenge. Balancing the removal of deactivants with the preservation of active sites and surface properties is crucial for maintaining or restoring catalyst performance.

6.2. Safety concerns of catalyst regeneration methods

Although coke deposited on catalysts can be eliminated by oxidation, gasification and hydrogenation, air is commonly used in industry for the regeneration of catalysts as it provides a mild regeneration temperature. Nevertheless, both ozone and oxynitride offer alternatives for lowering regeneration temperatures, but their use is limited due to safety concerns and strict emission regulations. Conventional methods often involve high temperatures, flammable gases, or corrosive chemicals, posing significant operational risks. Gasification of coke with carbon dioxide or steam offers the possibility of converting low-grade coke into syngas, adding value while reducing carbon dioxide emissions. However, coke gasification is an extremely endothermic process that requires high temperatures, which can compromise the integrity of the catalyst structure.[4,18] In addition, hydrogen can be used at elevated temperatures or pressures to remove coke from the substrates. Emerging techniques, while potentially safer, may introduce hazards related to novel energy sources (*e.g.*, microwaves, plasma) and unfamiliar process dynamics. Proper safety protocols and risk assessments are essential for both approaches.

6.3. Cost and scale-up implementation of catalyst regeneration technologies

There are several obstacles and considerations in the regeneration of catalysts. The cost and time associated with regeneration are important factors, as regeneration processes can require specialised equipment and a significant amount of labour, potentially increasing the overall process cost. In addition, the duration of regeneration can affect the overall performance, efficiency and cost of the process. There is also a risk of damage during regeneration, particularly with techniques including thermal treatment or the addition of chemicals, which can cause physical changes that result in reduced activity or stability of the catalyst. Conventional regeneration methods are often cost-effective and widely implemented at scale, but they may suffer from inefficiencies and catalyst degradation over time. In contrast, emerging techniques offer improved selectivity and lower environmental impact but face challenges in scalability, infrastructure demands, and high initial costs. Balancing economic feasibility with long-term performance remains crucial. Strategic investment in technology adaptation and process optimization is essential for industrial adoption. Transitioning from laboratory-scale regeneration processes to industrial-scale applications can present challenges in terms of equipment design, process scalability, and economic feasibility.[191] Ensuring that regeneration methods are practical and cost-effective at large scales is essential for industrial implementation.

Table 7 Comparative evaluation of emerging catalyst regeneration techniques, highlighting their applications, performance, and key considerations

Technique	Application	Performance	Operating temp.	Advantages	Limitations	Ref.
Supercritical fluid extraction (SFE)	Regeneration of coked/poisoned catalysts (*e.g.*, zeolites, activated carbon)	Moderate to high recovery of activity; selective coke/impurity removal	Low-temp. (depending on fluid type)	Low-temperature, non-destructive, eco-friendly	Limited to organics; less effective on graphitic coke	163
Plasma-assisted regeneration	Coke removal from metal catalysts and zeolites	High coke removal efficiency; preserves catalyst structure	Low-temp. (depends on plasma type)	Low-temp, fast activation, surface-specific	Requires special plasma reactors; scale-up challenges	167
Microwave-assisted regeneration	Regeneration of activated carbon and zeolites	Fast and efficient coke decomposition; selective heating	Low temp. (depending on material)	Uniform internal heating; reduced energy/time	Risk of non-uniform heating or hot spots, depends on dielectric properties	170 and 173
Atomic layer deposition (ALD)	Repair and stabilization of supported metal catalysts	Enhances stability, reduces sintering, restores selectivity	Low to high (depends on material and precursor)	Atomic-level control, uniform coatings, catalyst life extension	High cost, slow deposition, specialized equipment required	188–190

6.4. Energy consumption and environmental impact

Some effective catalyst regeneration methods often demand high temperatures, pressures, or chemical treatments, amplifying energy consumption and environmental repercussions. These methods, while essential for rejuvenating catalysts, can lead to elevated carbon footprints, resource depletion, and hazardous waste generation. Current regeneration techniques may not be sustainable or appropriate for all catalyst kinds or may not be efficient for certain deactivation processes.[192] Therefore, there is an urgent need to develop new, sustainable, more selective, efficient, and cost-effective approaches tailored to different catalysts and deactivation processes. Paramount importance rests on developing regeneration processes that mitigate energy requirements and environmental footprints.

While regeneration is essential for maintaining process efficiency and reducing the costs of catalyst replacement, the energy and environmental implications of different regeneration methods require careful consideration. Despite advancements, both conventional and emerging methods carry environmental trade-offs. Each catalyst regeneration method discussed in the earlier offers distinct advantages and challenges but also produces emissions, generates byproducts, and demands significant energy inputs, impacting air quality, greenhouse gas emissions, water resources, and waste management. Each regeneration technique discussed earlier has unique benefits and constraints, but all contribute directly or indirectly to environmental burdens such as air pollution, carbon emissions, and resource depletion (Table 8). Therefore, a critical evaluation of energy usage, byproduct formation, and waste generation is essential when selecting or designing a regeneration process to ensure sustainable industrial practices.

7. Prospects for effective mitigation of catalyst deactivation and regeneration

Future progress in catalysis hinges on the development of robust strategies that effectively reduce deactivation and improve regeneration efficiency. Advancements in tailored catalyst design, real-time performance monitoring, and environmentally benign regeneration techniques are essential for enhancing catalyst longevity and sustaining high catalytic activity. The integration of these innovations will pave the way for more sustainable, energy-efficient, and economically viable catalytic processes, as detailed in the discussion below.

7.1. Prevention of catalyst deactivation

7.1.1. Understanding the mechanisms of catalyst deactivation. This can enable more effective treatment and prevention strategies. Investigating how each mechanism affects the reaction rate and catalytic activity can provide valuable insights. While some deactivation mechanisms involve only one component, others may consist of several components that contribute to the observed activity, resulting in catalyst deactivation. For instant, poisoning leads to a loss of active sites, sintering leads to crystallite growth and a decrease in active surface area, and fouling leads to surface blockage and pore filling. Poisoning can also reduce intrinsic activity by altering the electronic framework of nearby atoms.[4] It is, therefore, crucial to understand and identify these components, their mechanisms and the processes that lead to each type of deactivation in order to mitigate their occurrence.

7.1.2. Adopting preventive measures. To effectively prevent the deactivation of catalysts, it is often more practical to focus on prevention rather than treatment. This approach is critical in minimising the catalyst deactivation in industrial processes. Significant investments are often made in catalyst stocks, and maximising their effective lifetime is economically crucial. Processes with irreversible or partially reversible deactivation, such as sulfur poisoning or sintering, particularly benefit from extended catalyst lifetimes. Different catalyst types have different lifetimes and are influenced by several deactivation mechanisms.[4] Although it is not possible to completely prevent the deactivation of catalysts, the rates can be reduced in many cases if the mechanisms are understood, and preventive measures are taken. Avoidance or preventive strategies include control of catalyst characteristics, process parameters, feedstock impurities, contacting methods and process design. Strategies to prevent deactivation through chemical degradation, fouling, poisoning, sintering and mechanical damage include the selection of appropriate

Table 8 Environmental implications of catalyst regeneration methods[189,193–197]

Methods	Key emissions	Environmental concerns	Mitigation strategies	Potential benefits
Combustion (air/oxygen)	CO_2, CO, NO_x, particulate matter (PM)	High greenhouse gas emissions (CO_2); air pollution (NO_x, SO_x); release of particulate matter; heat emissions contribute to thermal pollution	Employ emission scrubbers; use energy-efficient systems; optimize combustion for lower emissions	Effective and widely used; simple infrastructure requirements
Oxidation (ozone/oxynitride)	Ozone, NO_x	Secondary pollutants (*e.g.*, NO_x); toxic or corrosive byproducts; ozone leakage risks; high energy demand for oxidant generation	Use renewable energy; ensure safe handling and containment of ozone; treat and dispose of byproducts responsibly	High efficacy in coke removal; potential for controlled reactions
Gasification (steam/CO_2)	CO_2, water usage	High carbon emissions from CO_2 gasification; intensive water consumption; high energy requirements for operation	Capture and reuse syngas; use renewable energy sources; improve water recycling systems	Produces valuable syngas (H_2, CO); potential for circular economy applications
Hydrogenation	Methane (if leaked)	Methane leakage risk (potent greenhouse gas); high carbon footprint if gray hydrogen is used; energy-intensive process	Use green hydrogen; ensure methane capture and reuse; improve energy efficiency	Produces lighter hydrocarbons or methane; minimal air pollution compared to other methods
Supercritical fluid extraction (SFE)	Minimal (mostly CO_2 if vented)	Potential CO_2 release if not recovered or recycled	Use closed-loop CO_2 systems; integrate renewable energy for compression	Low-temperature, solvent-free, reusable CO_2, reduced solid waste
Microwave-assisted regeneration	Possible VOCs or light gases from coke breakdown	Localized heating may generate hot spots and partial oxidation by-products	Employ exhaust gas treatment; optimize power input and time to avoid over-processing	Efficient microwave heating (~30 W) quickly desorbs/decomposes VOCs with minimal heat loss; energy-efficient
Microwave + UV-oxidation				Enhanced mineralization (~50–60%) of persistent organics with limited VOC emission; minimal structural damage to catalysts
Plasma-assisted regeneration	O_3, NO_x, and radicals depending on gas used	Formation of reactive or toxic species in effluent gas	Use gas scrubbers or filters; select inert or low-emission plasma gases	Operates at low temperature, preserves catalyst structure, fast regeneration
Atomic layer deposition (ALD)	Metal–organic precursor vapors, trace solvents	Handling and disposal of hazardous chemicals; energy-intensive precursor synthesis	Use environmentally friendly precursors; ensure proper ventilation and waste treatment	Extends catalyst life, reduces waste, enhances resistance to deactivation

catalysts and process designs, the use of additives to improve stability and the optimisation of reaction conditions to minimise deactivation rates.[4,198]

7.1.3. Selection of suitable catalyst and operating parameters. To prevent sintering, reaction conditions and catalyst qualities that inhibit particle growth must be selected. Lowering the reaction temperatures, reducing the water vapour content and incorporating heat stabilisers into the catalysts can slow down the rate of sintering while adding steam, O_2 or CO_2 to the feedstock to gasify carbon or coke-forming precursors can mitigate these forms of degradation. The prevention of poisoning is aimed at removing impurities in the feedstock that can accumulate strongly on catalysts, making them difficult or impossible to regenerate.[198] The selective poisoning of unwanted metals and the use of guard beds can mitigate the poisoning effects. Strategies such as the use of protective beds, scrubbers and philtres to eliminate various toxins and impurities from the feedstock can be utilised. Avoiding fouling is about reducing the formation and accumulation of carbon or coke on the catalyst surfaces. This can be achieved by adjusting the reaction conditions so that gasification is favoured over formation, by using gasification agents or by using selective membranes. Methods such as supporting metals on different layers or using promoters to maintain high reducibility can also mitigate these problems.[199] To prevent mechanical degradation, carriers and coatings with high fracture resistance must be selected, porosity minimised, and processes designed to minimise turbulence and thermal stresses. Careful selection of support materials, coatings and catalyst particle formation processes can also minimise mechanical damage. Thermal or chemical annealing can strengthen catalyst particles or agglomerates and thus reduce the risks of mechanical degradation. In addition, careful control of process parameters can minimise fouling, thermal degradation and chemical degradation.[13] Regeneration methods must be compatible with the operating conditions of the catalytic process, including temperature, pressure, and feedstock composition. Careful selection of regeneration processes is important to ensure efficiency and minimise further damage to the catalyst.

7.1.4. Development of coke-resistant, stable catalysts. To establish a thriving bio-based and sustainable economy through catalysis, the first and most important step is to recognise the stability challenges associated with the integration of biomass conversion processes into industrial environments. However, this journey has only just begun. Extensive research is still required to understand the causes of these catalyst deactivation problems and to develop innovative techniques to mitigate them. The development of higher quality and more resistant catalysts is probably one of the strategies to mitigate these problems. However, innovative approaches to process design will also be required. These approaches may include developing new purification techniques for the feed, stabilising reactive feed components and intermediates, implementing strategies to prevent fouling, poisoning or destruction of the catalyst, or exploring new ways to regenerate the catalyst cost-effectively and efficiently. Exciting developments in these areas can be expected in the coming decades.[200]

7.2. Advances in catalyst characterization: integrating artificial intelligence (AI) and data-driven approaches

The characterisation of catalyst stability remains a challenge, and the identification of appropriate tools to monitor changes in catalyst properties associated with each deactivation mechanism is critical to the development of remedial methods. Advances in *in situ* and operando characterisation techniques, together with simulations, will provide insight into the dynamic factors contributing to catalyst deactivation. Artificial intelligence (AI) and data-driven approaches are transforming catalyst research by enabling predictive analysis of deactivation mechanisms. By processing large datasets from experimental and operational conditions, machine learning models can identify patterns such as coke formation, poisoning, or sintering. This allows for early detection and informed adjustments to prolong catalyst life. Additionally, AI facilitates the design of more robust catalysts through simulation of structural and performance changes over time. These advancements reduce reliance on trial-and-error methods, enhance regeneration strategies, and accelerate the development of more efficient and sustainable catalytic systems. In addition, improved methods are needed to distinguish and track the behavior of short-lived active site structures with both spatial and temporal precision, particularly those influenced by porosity. These features often change rapidly during reactions and are difficult to observe directly, making their accurate characterization under operando (real-time reaction) conditions a major challenge in catalysis research. Developing such techniques is essential for a deeper understanding of catalyst function and deactivation mechanisms. Furthermore, moving away from the traditional view that assessing stability is less valuable than demonstrating catalytic systems with high performance and selectivity is essential for understanding and mitigating catalyst deactivation.

7.3. Improvement in existing regeneration techniques

Catalyst nature, coke properties, and its distribution significantly influence the effectiveness of regeneration. The use of metals can considerably improve the regeneration performance of certain techniques. However, metals can also act as poisons, rendering catalysts inactive at high temperatures. Despite considerable progress in catalyst regeneration, further research is needed to develop optimal coke removal strategies. Achieving high regeneration efficiency while maintaining catalyst stability and activity requires optimization of existing conventional regeneration conditions, selection of suitable regeneration methods, and minimizing catalyst degradation during regeneration cycles. Emerging regeneration methods such as plasma treatment, microwave-assisted regeneration, and supercritical fluid extraction offer improved efficiency, selectivity, and lower environmental impact compared to conventional approaches. These techniques enable coke removal at lower temperatures and reduce structural damage to catalysts. However, effective regeneration requires accurate monitoring of catalyst performance

and deactivation mechanisms to determine the optimal timing and conditions for regeneration. Developing reliable sensors, diagnostic techniques, and control strategies for real-time monitoring of catalyst conditions is essential. Emerging techniques like plasma and microwave-assisted are increasingly incorporating AI-driven control to optimize process parameters, predict regeneration outcomes, and minimize energy use for enhanced efficiency. This integration supports more reliable and sustainable regeneration strategies.

7.4. Development of more sustainable and less energy-intensive regeneration techniques

The shift toward greener catalysis calls for regeneration methods that minimize energy input and environmental impact. Techniques leveraging renewable energy sources, solvent-free systems, and milder operating conditions are gaining traction. These approaches aim to maintain catalyst performance while supporting sustainable industrial practices. The development of more sustainable and effective regeneration methods is another challenge that needs to be overcome. Strategies may include optimizing regeneration conditions to minimize energy input, exploring alternative regeneration techniques such as microwave or plasma regeneration, or integrating renewable energy sources into regeneration processes. Moreover, adopting green chemistry principles, such as utilizing environmentally benign solvents or catalysts, can mitigate environmental impact. By prioritizing energy efficiency and environmental sustainability in catalyst regeneration, industries can ensure responsible resource utilization while maintaining competitiveness and meeting regulatory requirements. Collaborative efforts across academia, industry, and policymakers are imperative to drive innovation and implement sustainable regeneration practices on a broader scale.[26]

7.5. Future work consideration for catalyst deactivation and effective regeneration

Future investigations should prioritize advancing catalyst regeneration to improve both efficiency and sustainability. Emphasis must be placed on developing targeted strategies that effectively address specific deactivation mechanisms. The following areas are key for future research:

- Develop operando and *in situ* tools to monitor catalyst structure, porosity, and active site changes in real time.
- Design regeneration strategies tailored to specific deactivation pathways (*e.g.*, coking, poisoning, sintering).
- Prioritize development of low-energy, low-emission regeneration techniques such as supercritical fluid extraction, plasma, and microwave-assisted methods.
- Integrate renewable energy sources into regeneration technologies to enhance sustainability and reduce environmental impact.
- Engineer catalysts with improved resistance to deactivation through robust supports, active site stabilization, and surface modification.
- Incorporate real-time sensors and data analytics for early detection of deactivation and adaptive regeneration control.
- Evaluate catalyst performance over multiple regeneration cycles to ensure durability and consistent activity.
- Include life cycle analysis (LCA) and techno-economic evaluation to assess the long-term environmental and cost benefits of regeneration approaches.
- Explore the synergy of combining physical, chemical, and thermal methods to enhance regeneration efficiency.

8. Conclusion and outlook

Catalyst deactivation remains a major challenge in heterogeneous catalysis, reducing activity, selectivity, and long-term operational stability. This review presents a comprehensive analysis of coke formation and catalyst deactivation mechanisms. It further critically evaluates both current and emerging regeneration techniques and outlines key challenges in achieving effective regeneration. A distinctive strength of this work is its multidimensional integration of bibliometric analysis with current research and technological developments, offering a unique perspective on evolving trends, knowledge gaps, and sustainability priorities. The study emphasizes three primary causes of deactivation including chemical, mechanical, and thermal and identifies five degradation pathways: poisoning, fouling, thermal degradation, chemical degradation, and mechanical failure. These differ in reversibility and onset kinetics, underscoring the importance of targeted prevention. Strategies such as limiting coke precursor formation, optimizing process parameters, and encapsulating active metal sites have shown promise in reducing deactivation rates. Despite significant advances, regeneration remains essential for restoring catalyst functionality and extending its operational lifespan.

In parallel, the review evaluates different regeneration technologies, analysing their operating principles, effectiveness, energy demands, and environmental impacts. It covers both conventional methods such as oxidation (air, ozone, oxynitride), gasification (CO_2 and steam), and hydrogenation and emerging approaches, including supercritical fluid extraction (SFE), microwave-assisted regeneration, plasma-enhanced techniques, and atomic layer deposition (ALD). Conventional regeneration methods, while widely adopted for their effectiveness in coke removal, often operate at high temperatures and are energy-intensive, contributing to significant greenhouse gas emissions and potential catalyst degradation. Despite their maturity, these methods are limited by their thermodynamic mismatch with reaction conditions, process inflexibility, and high operational costs particularly in continuous heterogeneous processes. In contrast, emerging techniques such as non-thermal plasma and SFE offer regeneration under milder conditions, substantially reducing thermal damage and environmental burdens. However, scalability, safety protocols, and integration with existing industrial systems remain challenges that warrant further investigation.

Bibliometric analysis reveals that while catalyst deactivation, coking, and stability have been widely studied, regeneration remains underexplored. Continued research and innovation in

catalyst regeneration are vital for enhancing the efficiency and long-term viability of catalytic processes. Future work must focus on developing advanced, data-driven methods, including machine learning, to predict deactivation and optimize regeneration process. Overcoming current challenges requires precision strategies and interdisciplinary collaboration. Emphasis should be placed on environmentally sustainable, low-energy solutions that extend catalyst longevity. These advancements are pivotal for unlocking long-term catalytic performance and support the transition to cleaner, more efficient technologies in a carbon-constrained future.

Author contributions

I. M. S. Anekwe – conceptualization, methodology, software, formal analysis, validation, investigation, data curation, writing – original draft, writing – review & editing, visualization, supervision, project administration. Y. M. Isa – supervision, writing – review & editing.

Consent to Publish

Authors consent to the publication of this manuscript

Conflicts of interest

The authors have no competing interests to declare that are relevant to the content of this article.

List of acronyms

AC	Activated carbon
AEE	Aqueous ethanolic extract
AC-CO_2	Activated carbon regenerated under carbon dioxide atmosphere
AC-N_2	Activated carbon regenerated under nitrogen atmosphere
AC-US	Activated carbon regenerated using ultrasonic spray-assisted method
ALD	Atomic layer deposition
AOP	Advanced oxidation processes
C_γ	Metal carbide
C_α	Adsorbed atomic carbon
C_β	Polymeric carbon film
C_c	Amorphous and graphitic carbon
C_v	Vermicular carbon
CC	Catalyst coke
CH_x	Methane-derived hydrocarbon fragments
CR	Catalyst regeneration
CSD	Catalyst stability and deactivation
DBD	Dielectric barrier discharge
DTA	Differential thermal analysis
FCC	Fluidized catalytic cracking
FTIR	Fourier transform infrared spectroscopy
GC-HRT-MS	Gas chromatography high resolution time-of-flight mass spectrometry
GC-MS	Gas chromatography mass spectrometry
HCs	Hydrocarbons
HZSM-5	Hydrogen-form zeolite socony mobil 5
IC_{50}	Half maximal inhibitory concentration
MAR	Microwave-assisted regeneration
MFI	Mobil five framework zeolite
MOR	Mordenite
MTG	Methanol-to-gasoline
MTH	Methanol-to-hydrocarbons
NiZ	Nickel-doped Z5M-5
NTP	Non-thermal plasma
OECD	Organisation for economic co-operation and development
ORR	Oxygen reduction reaction
PAR	Plasma-assisted regeneration
RB	Reverse Boudouard reaction
SBET	Brunauer Emmett Teller surface area
SCR	Selective catalytic reduction
SEM	Scanning electron microscopy
SFE	Supercritical fluid extraction
SMR	Steam methane reforming
TGA	Thermogravimetric analysis
TPR	Temperature-programmed reduction
TOS	Time-on-stream
WoS	Web of science
Z5	Unmodified zeolite ZSM-5
ZSM-5	Zeolite socony mobil 5

Data availability

Data is available on request from authors.

Acknowledgements

This work was supported by a grant from the Oppenheimer Memorial Trust (OMT), whose generous support was integral to the successful completion of this work.

References

1 S. Mondal, S. Ruidas, S. Chongdar, B. Saha and A. Bhaumik, Sustainable porous heterogeneous catalysts for the conversion of biomass into renewable energy products, *ACS Sustainable Resour. Manage.*, 2024, **1**(8), 1672–1704.
2 I. M. S. Anekwe, S. O. Akpasi, E. K. Tetteh, A. S. Joel, S. I. Mustapha and Y. M. Isa, Progress in heterogeneous catalysis for renewable energy and petrochemical production from biomass, *Fuel Process. Technol.*, 2025, **276**, 108267, DOI: 10.1016/j.fuproc.2025.108267.
3 M. Guisnet and F. R. A. Ribeiro, *Deactivation and regeneration of zeolite catalysts*, 2011.
4 M. D. Argyle and C. H. Bartholomew, Heterogeneous Catalyst Deactivation and Regeneration: A Review, *Catalysts*, 2015,

5(1), 145–269. Available: https://www.mdpi.com/2073-4344/5/1/145.
5 C. H. Bartholomew, Carbon deposition in steam reforming and methanation, *Catal. Rev.: Sci. Eng.*, 1982, **24**(1), 67–112.
6 M. Guisnet, L. Costa and F. R. Ribeiro, Prevention of zeolite deactivation by coking, *J. Mol. Catal. A: Chem.*, 2009, **305**(1–2), 69–83.
7 M. Guisnet and P. Magnoux, Organic chemistry of coke formation, *Appl. Catal., A*, 2001, **212**(1–2), 83–96.
8 S. Gao, *et al.*, Insight into the deactivation mode of methanol-to-olefins conversion over SAPO-34: coke, diffusion, and acidic site accessibility, *J. Catal.*, 2018, **367**, 306–314.
9 A. De Lucas, P. Canizares, A. Duran and A. Carrero, Coke formation, location, nature and regeneration on dealuminated HZSM-5 type zeolites, *Appl. Catal., A*, 1997, **156**(2), 299–317.
10 M. Guisnet and P. Magnoux, Fundamental description of deactivation and regeneration of acid zeolites, *Stud. Surf. Sci. Catal.*, 1994, **88**, 53–68.
11 M. Guisnet and P. Magnoux, Deactivation by coking of zeolite catalysts. Prevention of deactivation. Optimal conditions for regeneration, *Catal. Today*, 1997, **36**(4), 477–483.
12 S. S. Arora, D. L. Nieskens, A. Malek and A. Bhan, Lifetime improvement in methanol-to-olefins catalysis over chabazite materials by high-pressure H_2 co-feeds, *Nat. Catal.*, 2018, **1**(9), 666–672.
13 C. H. Bartholomew, Mechanisms of catalyst deactivation, *Appl. Catal., A*, 2001, **212**(1–2), 17–60.
14 M. Argyle and C. Bartholomew, *Catalysts*, 2015, **5**, 145–269, DOI: 10.3390/catal5010145[Crossref], Google Scholar There is no corresponding record for this reference.
15 I. M. Szilágyi and G. Liptay, *Who is who in thermal analysis and calorimetry*, Springer, 2014.
16 S. Mahamulkar, *et al.*, Formation and oxidation/gasification of carbonaceous deposits: a review, *Ind. Eng. Chem. Res.*, 2016, **55**(37), 9760–9818.
17 C. A. Querini, Isobutane/butene alkylation: regeneration of solid acid catalysts, *Catal. Today*, 2000, **62**(2–3), 135–143.
18 J. Zhou, J. Zhao, J. Zhang, T. Zhang, M. Ye and Z. Liu, Regeneration of catalysts deactivated by coke deposition: a review, *Chin. J. Catal.*, 2020, **41**(7), 1048–1061.
19 M. van Sint Annaland, J. Kuipers and W. P. M. van Swaaij, A kinetic rate expression for the time-dependent coke formation rate during propane dehydrogenation over a platinum alumina monolithic catalyst, *Catal. Today*, 2001, **66**(2–4), 427–436.
20 M. Guisnet, Coke'' molecules trapped in the micropores of zeolites as active species in hydrocarbon transformations, *J. Mol. Catal. A: Chem.*, 2002, **182**, 367–382.
21 F. Lin, M. Xu, K. K. Ramasamy, Z. Li, J. L. Klinger and J. A. Schaidle, Catalyst deactivation and its mitigation during catalytic conversions of biomass, *ACS Catal.*, 2022, **12**, 13555–13599.
22 R. B. Rostami, M. Ghavipour, Z. Di, Y. Wang and R. M. Behbahani, Study of coke deposition phenomena on the SAPO_34 catalyst and its effects on light olefin selectivity during the methanol to olefin reaction, *RSC Adv.*, 2015, **5**(100), 81965–81980.
23 X. Hou, L. Zhao and Z. Diao, Roles of Alkenes and Coke Formation in the Deactivation of ZSM-5 Zeolites During n-Pentane Catalytic Cracking, *Catal. Lett.*, 2020, **150**(9), 2716–2725, DOI: 10.1007/s10562-020-03173-4.
24 E. T. C. Vogt, D. Fu and B. M. Weckhuysen, Carbon Deposit Analysis in Catalyst Deactivation, Regeneration, and Rejuvenation, *Angew. Chem., Int. Ed.*, 2023, **62**(29), e202300319, DOI: 10.1002/anie.202300319.
25 F. Zheng, C. Liu, X. Ma, Z. Zhou and J. Lu, Review on NH_3-SCR for simultaneous abating NO_x and VOCs in industrial furnaces: catalysts' composition, mechanism, deactivation and regeneration, *Fuel Process. Technol.*, 2023, **247**, 107773, DOI: 10.1016/j.fuproc.2023.107773.
26 A. H. Hatta, *et al.*, A comprehensive review on the advancements in catalyst regeneration strategies for enhanced reactivity in CO methanation, *Mater. Today Chem.*, 2023, **33**, 101743, DOI: 10.1016/j.mtchem.2023.101743.
27 P. Wu, X. Tang, Z. He, Y. Liu and Z. Wang, Alkali metal poisoning and regeneration of selective catalytic reduction denitration catalysts: recent advances and future perspectives, *Energy Fuels*, 2022, **36**(11), 5622–5646.
28 H. Liu, *et al.*, Catalytic cracking and catalyst deactivation/regeneration characteristics of Fe-loaded biochar catalysts for tar model compound, *Fuel*, 2023, **334**, 126810, DOI: 10.1016/j.fuel.2022.126810.
29 Y.-X. Liu, *et al.*, Deactivation and regeneration of a benchmark Pt/C catalyst toward oxygen reduction reaction in the presence of poisonous SO_2 and NO, *Catal. Sci. Technol.*, 2022, **12**(9), 2929–2934, DOI: 10.1039/D2CY00141A.
30 D. N. Al Husaeni, A. B. D. Nandiyanto and R. Maryanti, Bibliometric analysis of special needs education keyword using VOSviewer indexed by google scholar, *Indonesian J. Commun. Special Needs Educ.*, 2023, **3**(1), 1–10.
31 J. Oudar, *Deactivation and poisoning of catalysts*, CRC Press, 1985.
32 L. Hegedus and R. McCabe, Catalyst poisoning, *Stud. Surf. Sci. Catal.*, 1980, **6**, 471–505.
33 J. B. Butt, Catalyst poisoning and chemical process dynamics, *Progress in Catalyst Deactivation: Proceedings of the NATO Advanced Study Institute on Catalyst Deactivation*, Springer, Algarve, Portugal, 1982, pp. 153–208.
34 C. H. Bartholomew, Mechanisms of nickel catalyst poisoning, *Stud. Surf. Sci. Catal.*, 1987, **34**, 81–104.
35 J. Inga, P. Kennedy and S. LeViness, Syntroleum Corp. Fischer-Tropsch process in the presence of nitrogen contaminants, *US Pat.*, Application 10/755,942, 2005, https://patents.google.com/patent/US20050154069A1/en.
36 J. Völiter and M. Hermann, Katalytische Wirksamkeit van reinem und von CO-vergiftetem Platin bei der *p*-H_2-Umwandlung, *Z. Anorg. Allg. Chem.*, 1974, **405**(3), 315–328.

37 J. Zhang, Z. Huang, Y. Du, X. Wu, H. Shen and G. Jing, Alkali-Poisoning-Resistant $Fe_2O_3/MoO_3/TiO_2$ Catalyst for the Selective Reduction of NO by NH_3: The Role of the MoO_3 Safety Buffer in Protecting Surface Active Sites, *Environ. Sci. Technol.*, 2020, **54**(1), 595–603, DOI: **10.1021/acs.est.9b06318**.
38 L. F. Albright and R. T. K. Baker, *Coke formation on metal surfaces*, ACS Publications, 1983.
39 P. Menon, Coke on catalysts-harmful, harmless, invisible and beneficial types, *J. Mol. Catal.*, 1990, **59**(2), 207–220.
40 J. M. Ginsburg, J. Piña, T. El Solh and H. I. De Lasa, Coke formation over a nickel catalyst under methane dry reforming conditions: thermodynamic and kinetic models, *Ind. Eng. Chem. Res.*, 2005, **44**(14), 4846–4854.
41 S. Karpe and G. Veser, Coke Formation and Regeneration during Fe-ZSM-5-Catalyzed Methane Dehydro-Aromatization, *Catalysts*, 2024, **14**(5), 292. Available: **https://www.mdpi.com/2073-4344/14/5/292**.
42 I. M. S. Anekwe, B. Oboirien and Y. M. Isa, Performance evaluation of a newly developed transition metal-doped HZSM-5 zeolite catalyst for single-step conversion of C1–C3 alcohols to fuel-range hydrocarbons, *Energy Adv.*, 2024, **3**(6), 1314–1328.
43 H. G. Karge, W. Nießen and H. Bludau, In situ FTIR measurements of diffusion in coking zeolite catalysts, *Appl. Catal., A*, 1996, **146**(2), 339–349.
44 L. Palumbo, F. Bonino, P. Beato, M. Bjørgen, A. Zecchina and S. Bordiga, Conversion of Methanol to Hydrocarbons: Spectroscopic Characterization of Carbonaceous Species Formed over H-ZSM-5, *J. Phys. Chem. C*, 2008, **112**(26), 9710–9716, DOI: **10.1021/jp800762v**.
45 J. Robertson, Diamond-like amorphous carbon, *Mater. Sci. Eng., R*, 2002, **37**(4), 129–281, DOI: **10.1016/S0927-796X(02)00005-0**.
46 J. Valecillos, H. Vicente, A. G. Gayubo, A. T. Aguayo and P. Castaño, Spectro-kinetics of the methanol to hydrocarbons reaction combining online product analysis with UV–vis and FTIR spectroscopies throughout the space time evolution, *J. Catal.*, 2022, **408**, 115–127, DOI: **10.1016/j.jcat.2022.02.021**.
47 J. Valecillos, E. Epelde, J. Albo, A. T. Aguayo, J. Bilbao and P. Castaño, Slowing down the deactivation of H-ZSM-5 zeolite catalyst in the methanol-to-olefin (MTO) reaction by P or Zn modifications, *Catal. Today*, 2020, **348**, 243–256.
48 S. Ilias and A. Bhan, Mechanism of the catalytic conversion of methanol to hydrocarbons, *ACS Catal.*, 2013, **3**(1), 18–31.
49 X. Gao, P. Sun, J. Liao and L. Xia, Advanced characterization techniques for the coking process of zeolites: a comprehensive review, *CrystEngComm*, 2025, DOI: **10.1039/d5ce00156k**.
50 N. Wang, *et al.*, Modulation of b-axis thickness within MFI zeolite: correlation with variation of product diffusion and coke distribution in the methanol-to-hydrocarbons conversion, *Appl. Catal., B*, 2019, **243**, 721–733.
51 D. Rojo-Gama, *et al.*, Structure–deactivation relationships in zeolites during the methanol-to-hydrocarbons reaction: complementary assessments of the coke content, *J. Catal.*, 2017, **351**, 33–48, DOI: **10.1016/j.jcat.2017.04.015**.
52 S. Lee and M. Choi, Unveiling coke formation mechanism in MFI zeolites during methanol-to-hydrocarbons conversion, *J. Catal.*, 2019, **375**, 183–192, DOI: **10.1016/j.jcat.2019.05.030**.
53 D. Wang, X. Su, Z. Fan, Z. Wen, N. Li and Y. Yang, Recent Advances for Selective Catalysis in Benzene Methylation: Reactions, Shape-Selectivity and Perspectives, *Catal. Surv. Asia*, 2021, **25**(4), 347–361, DOI: **10.1007/s10563-021-09337-5**.
54 A. Ochoa, J. Bilbao, A. G. Gayubo and P. Castaño, Coke formation and deactivation during catalytic reforming of biomass and waste pyrolysis products: a review, *Renewable Sustainable Energy Rev.*, 2020, **119**, 109600, DOI: **10.1016/j.rser.2019.109600**.
55 C. Montero, A. Ochoa, P. Castaño, J. Bilbao and A. G. Gayubo, Monitoring Ni^0 and coke evolution during the deactivation of a Ni/La_2O_3–αAl_2O_3 catalyst in ethanol steam reforming in a fluidized bed, *J. Catal.*, 2015, **331**, 181–192.
56 S. Helveg, J. Sehested and J. Rostrup-Nielsen, Whisker carbon in perspective, *Catal. Today*, 2011, **178**(1), 42–46.
57 A. M. Karim, *et al.*, A comparative study between Co and Rh for steam reforming of ethanol, *Appl. Catal., B*, 2010, **96**(3–4), 441–448.
58 P. J. Ortiz-Toral, J. Satrio, R. C. Brown and B. H. Shanks, Steam reforming of bio-oil fractions: effect of composition and stability, *Energy Fuels*, 2011, **25**(7), 3289–3297.
59 D. Rennard, R. French, S. Czernik, T. Josephson and L. Schmidt, Production of synthesis gas by partial oxidation and steam reforming of biomass pyrolysis oils, *Int. J. Hydrogen Energy*, 2010, **35**(9), 4048–4059.
60 C. Naccache, Deactivation of acid catalysts, *Chem. Informationsdienst*, 1986, **17**(16), DOI: **10.1002/chin.198616376**.
61 M. Guisnet and P. Magnoux, Coking and deactivation of zeolites: influence of the pore structure, *Appl. Catal.*, 1989, **54**(1), 1–27.
62 W. Groten, B. Wojciechowski and B. Hunter, On the relationship between coke formation chemistry and catalyst deactivation, *J. Catal.*, 1992, **138**(1), 343–350.
63 A. Bellare and D. Dadyburjor, Evaluation of modes of catalyst deactivation by coking for cumene cracking over zeolites, *J. Catal.*, 1993, **140**(2), 510–525.
64 H. Cerqueira, P. Magnoux, D. Martin and M. Guisnet, Effect of contact time on the nature and location of coke during methylcyclohexane transformation over a USHY zeolite, *Stud. Surf. Sci. Catal.*, **126**, 105–112.
65 T. Masuda, P. Tomita, Y. Fujikata and K. Hashimoto, Deactivation of HY-type zeolite catalyst due to coke deposition during gas–oil cracking, *Stud. Surf. Sci. Catal.*, 1999, **126**, 89–96.
66 M. Uguina, D. Serrano, R. Van Grieken and S. Venes, Adsorption, acid and catalytic changes induced in ZSM-5 by coking with different hydrocarbons, *Appl. Catal., A*, 1993, **99**(2), 97–113.
67 M. Guisnet, P. Magnoux and D. Martin, Roles of acidity and pore structure in the deactivation of zeolites by

carbonaceous deposits, *Stud. Surf. Sci. Catal.*, 1997, **111**, 1–19.

68 Y. Song, Y. Xu, Y. Suzuki, H. Nakagome and Z.-G. Zhang, A clue to exploration of the pathway of coke formation on Mo/HZSM-5 catalyst in the non-oxidative methane dehydroaromatization at 1073K, *Appl. Catal., A*, 2014, **482**, 387–396, DOI: 10.1016/j.apcata.2014.06.018.

69 J. Goetze, *et al.*, Insights into the Activity and Deactivation of the Methanol-to-Olefins Process over Different Small-Pore Zeolites As Studied with Operando UV-vis Spectroscopy, (in eng), *ACS Catal.*, 2017, **7**(6), 4033–4046, DOI: 10.1021/acscatal.6b03677.

70 D. Chen, H. P. Rebo, K. Moljord and A. Holmen, Influence of Coke Deposition on Selectivity in Zeolite Catalysis, *Ind. Eng. Chem. Res.*, 1997, **36**(9), 3473–3479, DOI: 10.1021/ie9700223.

71 A. Zachariou, *et al.*, New Spectroscopic Insight into the Deactivation of a ZSM-5 Methanol-to-Hydrocarbons Catalyst, *ChemCatChem*, 2021, **13**(11), 2625–2633, DOI: 10.1002/cctc.202100286.

72 C. H. Bartholomew, Carbon Deposition in Steam Reforming and Methanation, *Catal. Rev.*, 1982, **24**(1), 67–112, DOI: 10.1080/03602458208079650.

73 J. R. Rostrup-Nielsen, Conversion of hydrocarbons and alcohols for fuel cells, *Phys. Chem. Chem. Phys.*, 2001, **3**(3), 283–288.

74 S. M. de Lima, *et al.*, Evaluation of the performance of Ni/La_2O_3 catalyst prepared from $LaNiO_3$ perovskite-type oxides for the production of hydrogen through steam reforming and oxidative steam reforming of ethanol, *Appl. Catal., A*, 2010, **377**(1), 181–190, DOI: 10.1016/j.apcata.2010.01.036.

75 A. G. Gayubo, J. M. Arandes, A. T. Aguayo, M. Olazar and J. Bilbao, Deactivation and acidity deterioration of a silica/alumina catalyst in the isomerization of *cis*-butene, *Ind. Eng. Chem. Res.*, 1993, **32**(4), 588–593.

76 C. Montero, A. Remiro, B. Valle, L. Oar-Arteta, J. Bilbao and A. G. Gayubo, Origin and nature of coke in ethanol steam reforming and its role in deactivation of Ni/La_2O_3–αAl_2O_3 catalyst, *Ind. Eng. Chem. Res.*, 2019, **58**(32), 14736–14751.

77 I. M. S. Anekwe, S. O. Akpasi, E. M. Enemuo, D. Ashiegbu, S. I. Mustapha and Y. M. Isa, Innovations in catalytic understanding: a journey through advanced characterization, *Mater. Today Catal.*, 2024, **7**, 100061, DOI: 10.1016/j.mtcata.2024.100061.

78 V. Palma, C. Ruocco, M. Cortese and M. Martino, Bioalcohol Reforming: An Overview of the Recent Advances for the Enhancement of Catalyst Stability, *Catalysts*, 2020, **10**(6), 665. Available: https://www.mdpi.com/2073-4344/10/6/665.

79 J. Rostrup-Nielsen and D. L. Trimm, Mechanisms of carbon formation on nickel-containing catalysts, *J. Catal.*, 1977, **48**(1–3), 155–165.

80 K.-J. Marschall and L. Mleczko, Short-contact-time reactor for catalytic partial oxidation of methane, *Ind. Eng. Chem. Res.*, 1999, **38**(5), 1813–1821.

81 J. R. Rostrup-Nielsen, Catalytic steam reforming, *Catalysis: Science and Technology*, Springer, 1984, vol. 5, pp. 1–117.

82 B. Valle, B. Aramburu, M. Olazar, J. Bilbao and A. G. Gayubo, Steam reforming of raw bio-oil over Ni/La_2O_3–αAl_2O_3: influence of temperature on product yields and catalyst deactivation, *Fuel*, 2018, **216**, 463–474.

83 F. Bimbela, J. Ábrego, R. Puerta, L. García and J. Arauzo, Catalytic steam reforming of the aqueous fraction of bio-oil using Ni–Ce/Mg–Al catalysts, *Appl. Catal., B*, 2017, **209**, 346–357.

84 A. Ochoa, *et al.*, Coking and sintering progress of a Ni supported catalyst in the steam reforming of biomass pyrolysis volatiles, *Appl. Catal., B*, 2018, **233**, 289–300.

85 B. Valle, B. Aramburu, P. L. Benito, J. Bilbao and A. G. Gayubo, Biomass to hydrogen-rich gas via steam reforming of raw bio-oil over Ni/La_2O_3–αAl_2O_3 catalyst: effect of space-time and steam-to-carbon ratio, *Fuel*, 2018, **216**, 445–455.

86 D. Bibby, N. Milestone, J. Patterson and L. Aldridge, Coke formation in zeolite ZSM-5, *J. Catal.*, 1986, **97**(2), 493–502.

87 I. M. S. Anekwe, B. Oboirien and Y. M. Isa, Effects of Transition Metal Doping on the Properties and Catalytic Performance of ZSM-5 Zeolite Catalyst on Ethanol-to-hydrocarbons Conversion, *Fuel Commun.*, 2023, 100101.

88 I. M. S. Anekwe and Y. M. Isa, Influence of metal doping on the coke formation of a novel hierarchical HZSM-5 zeolite catalyst in the conversion of 1-propanol to fuel blendstock, *RSC Adv.*, 2025, **15**(6), 3988–3999.

89 Y. Xu, J. Wang, Y. Suzuki and Z.-G. Zhang, Improving effect of Fe additive on the catalytic stability of Mo/HZSM-5 in the methane dehydroaromatization, *Catal. Today*, 2012, **185**(1), 41–46, DOI: 10.1016/j.cattod.2011.09.026.

90 B. M. Weckhuysen, D. Wang, M. P. Rosynek and J. H. Lunsford, Conversion of Methane to Benzene over Transition Metal Ion ZSM-5 Zeolites: I. Catalytic Characterization, *J. Catal.*, 1998, **175**(2), 338–346, DOI: 10.1006/jcat.1998.2010.

91 V. Daligaux, R. Richard and M.-H. Manero, Deactivation and Regeneration of Zeolite Catalysts Used in Pyrolysis of Plastic Wastes—A Process and Analytical Review, *Catalysts*, 2021, **11**(7), 770. Available: https://www.mdpi.com/2073-4344/11/7/770.

92 J. Sehested, Four challenges for nickel steam-reforming catalysts, *Catal. Today*, 2006, **111**(1–2), 103–110.

93 T. W. Hansen, A. T. DeLaRiva, S. R. Challa and A. K. Datye, Sintering of catalytic nanoparticles: particle migration or Ostwald ripening?, *Acc. Chem. Res.*, 2013, **46**(8), 1720–1730.

94 X. Wang and A. Atkinson, Combining densification and coarsening in a Cellular Automata-Monte-Carlo simulation of sintering: methodology and calibration, *Comput. Mater. Sci.*, 2018, **143**, 338–349.

95 C. H. Bartholomew and R. J. Farrauto, *Fundamentals of industrial catalytic processes*, John Wiley & Sons, 2011.

96 S. Raoux, W. Wełnic and D. Ielmini, Phase change materials and their application to nonvolatile memories, *Chem. Rev.*, 2010, **110**(1), 240–267.

97 I. Manson, Self-regenerating diesel exhaust particulate filter and material, *US Pat.*, 6248689, Redem Technologies Inc, 2001, https://patents.google.com/patent/US6248689B1/en.
98 G. W. Huber, C. G. Guymon, T. L. Conrad, B. C. Stephenson and C. H. Bartholomew, Hydrothermal stability of CO/SiO_2 Fischer-Tropsch synthesis catalysts, *Stud. Surf. Sci. Catal.*, 2001, 139, 423–430.
99 H. N. Pham, J. Reardon and A. K. Datye, Measuring the strength of slurry phase heterogeneous catalysts, *Powder Technol.*, 1999, **103**(2), 95–102.
100 D. S. Kalakkad, M. D. Shroff, S. Köhler, N. Jackson and A. Datye, Attrition of precipitated iron Fischer-Tropsch catalysts, *Appl. Catal., A*, 1995, **133**(2), 335–350.
101 D. Trimm, The regeneration or disposal of deactivated heterogeneous catalysts, *Appl. Catal., A*, 2001, **212**(1–2), 153–160.
102 B. Behera and S. S. Ray, Structural changes of FCC catalyst from fresh to regeneration stages and associated coke in a FCC refining unit: a multinuclear solid state NMR approach, *Catal. Today*, 2009, **141**(1–2), 195–204.
103 P. Dufresne, Hydroprocessing catalysts regeneration and recycling, *Appl. Catal., A*, 2007, **322**, 67–75.
104 C. Kern and A. Jess, Regeneration of coked catalysts—modelling and verification of coke burn-off in single particles and fixed bed reactors, *Chem. Eng. Sci.*, 2005, **60**(15), 4249–4264.
105 P. Tian, Y. Wei, M. Ye and Z. Liu, Methanol to olefins (MTO): from fundamentals to commercialization, *ACS Catal.*, 2015, **5**(3), 1922–1938.
106 L. Jia, *et al.*, New routes for complete regeneration of coked zeolite, *Appl. Catal., B*, 2017, **219**, 82–91.
107 M. D. P. Sørensen, The establishment of a coke-burn kinetic model for zeolite catalysts, *Chem. Eng. Sci.*, 2017, **168**, 465–479.
108 P. Magnoux and M. Guisnet, Coking, ageing and regeneration of zeolites: VI. Comparison of the Rates of Coke Oxidation of HY, H-Mordenite and HZSM-5, *Appl. Catal.*, 1988, **38**(2), 341–352.
109 G. D. Nassionou, P. Magnoux and M. Guisnet, Comparative study of coking and regeneration of HEMT and HFAU zeolites, *Microporous Mesoporous Mater.*, 1998, **22**(1–3), 389–398.
110 S.-J. Jong, A. R. Pradhan, J.-F. Wu, T.-C. Tsai and S.-B. Liu, On the regeneration of coked H-ZSM-5 catalysts, *J. Catal.*, 1998, **174**(2), 210–218.
111 K. Moljord, P. Magnoux and M. Guisnet, Coking, aging and regeneration of zeolites: XVI. Influence of the composition of HY zeolites on the removal of coke through oxidative treatment, *Appl. Catal., A*, 1995, **121**(2), 245–259, DOI: 10.1016/0926-860X(94)00211-8.
112 A. T. Aguayo, A. G. Gayubo, J. Ereña, A. Atutxa and J. Bilbao, Coke aging and its incidence on catalyst regeneration, *Ind. Eng. Chem. Res.*, 2003, **42**(17), 3914–3921.
113 A. T. Aguayo, A. G. Gayubo, A. Atutxa, M. Olazar and J. Bilbao, Regeneration of a catalyst based on a SAPO-34 used in the transformation of methanol into olefins, *J. Chem. Technol. Biotechnol.*, 1999, **74**(11), 1082–1088.
114 I. M. S. Anekwe, *et al.*, Stability, deactivation and regeneration study of a newly developed HZSM-5 and Ni-doped HZSM-5 zeolite catalysts for ethanol-to-hydrocarbon conversion, *Catal. Commun.*, 2024, **186**, 106802, DOI: 10.1016/j.catcom.2023.106802.
115 C. Pieck, C. Querini and J. Parera, Influence of O_2 and O_3 regeneration on the metallic phase of the Pt—Re/Al_2O_3 catalyst, *Appl. Catal., A*, 1997, **165**(1–2), 207–218.
116 R. G. Copperthwaite, G. J. Hutchings, P. Johnston and S. W. Orchard, Regeneration of pentasil zeolite catalysts using ozone and oxygen, *J. Chem. Soc., Faraday Trans. 1*, 1986, **82**(3), 1007–1017.
117 L. Mariey, J. Lamotte, T. Chevreau and J. C. Lavalley, FT-IR study of coked HY zeolite regeneration using oxygen or ozone, *React. Kinet. Catal. Lett.*, 1996, **59**(2), 241–246, DOI: 10.1007/BF02068119.
118 G. Hutchings, *et al.*, A comparative study of reactivation of zeolite Y using oxygen and ozone/oxygen mixtures, *Appl. Catal.*, 1987, **34**, 153–161.
119 P. Monneyron, S. Mathé, M.-H. Manero and J.-N. Foussard, Regeneration of high silica zeolites via advanced oxidation processes—a preliminary study about adsorbent reactivity toward ozone, *Chem. Eng. Res. Des.*, 2003, **81**(9), 1193–1198.
120 D. Ivanov, V. Sobolev and G. Panov, Deactivation by coking and regeneration of zeolite catalysts for benzene-to-phenol oxidation, *Appl. Catal., A*, 2003, **241**(1–2), 113–121.
121 K. Barbera, *et al.*, Role of internal coke for deactivation of ZSM-5 catalysts after low temperature removal of coke with NO_2, *Catal. Sci. Technol.*, 2012, **2**(6), 1196–1206.
122 V. Daligaux, R. Richard and M. H. Manero, Regeneration of coked catalysts via ozonation: experimental study of diffusion–reaction mechanisms at pellet and reactor scales, *Chem. Eng. J.*, 2023, **476**, 146446, DOI: 10.1016/j.cej.2023.146446.
123 L. F. de Mello, *et al.*, A technical and economical evaluation of CO_2 capture from FCC units, *Energy Proc.*, 2009, **1**(1), 117–124.
124 L. T. dos Santos, *et al.*, Mechanistic insights of CO_2-coke reaction during the regeneration step of the fluid cracking catalyst, *Appl. Catal., A*, 2008, **336**(1–2), 40–47.
125 S. C. Pereira, F. Franco, F. Ribeiro, N. Batalha and M. M. Pereira, Vanadium-lithium alumina a potential additive for coke oxidation by CO_2 in the presence of O_2 during FCC catalyst regeneration, *Appl. Catal., B*, 2016, **196**, 117–126, DOI: 10.1016/j.apcatb.2016.05.024.
126 A. Corma, L. Sauvanaud, E. Doskocil and G. Yaluris, Coke steam reforming in FCC regenerator: a new mastery over high coking feeds, *J. Catal.*, 2011, **279**(1), 183–195, DOI: 10.1016/j.jcat.2011.01.020.
127 G. Tian, G. Wang, C. Xu and J. Gao, Gasification of the Coke on Spent-Residue-Pretreating Catalysts with Steam and Steam–O_2 Mixtures, *Energy Fuels*, 2014, **28**(2), 1372–1379, DOI: 10.1021/ef402045d.
128 M. B. Ansari and S. E. Park, Carbon dioxide utilization as a soft oxidant and promoter in catalysis, *Energy Environ. Sci.*, 2012, **5**(11), 9419–9437, DOI: 10.1039/c2ee22409g.

129 T. C. Da Silva, R. P. Dos Santos, N. Batalha and M. M. Pereira, Vanadium-potassium-alumina catalyst: a way of promoting CO_2 and coke reaction in the presence of O_2 during the FCC catalyst regeneration, *Catal. Commun.*, 2014, **51**, 42–45, DOI: 10.1016/j.catcom.2014.03.013.

130 J. Hunt, A. Ferrari, A. Lita, M. Crosswhite, B. Ashley and A. E. Stiegman, Microwave-specific enhancement of the carbon-carbon dioxide (Boudouard) reaction, *J. Phys. Chem. C*, 2013, **117**(51), 26871–26880, DOI: 10.1021/jp4076965.

131 M. Mikkelsen, M. Jørgensen and F. C. Krebs, The teraton challenge. A review of fixation and transformation of carbon dioxide, *Energy Environ. Sci.*, 2010, **3**(1), 43–81, DOI: 10.1039/b912904a.

132 S. M. Campbell, D. M. Bibby, J. M. Coddington, R. F. Howe and R. H. Meinhold, Dealumination of HZSM-5 zeolites: I. Calcination and hydrothermal treatment, *J. Catal.*, 1996, **161**(1), 338–349, DOI: 10.1006/jcat.1996.0191Art no. 0191.

133 M. Müller, G. Harvey and R. Prins, Comparison of the dealumination of zeolites beta, mordenite, ZSM-5 and ferrierite by thermal treatment, leaching with oxalic acid and treatment with $SiCl_4$ by ^1H, ^{29}Si and $^{27}A1$ MAS NMR, *Microporous Mesoporous Mater.*, 2000, **34**(2), 135–147, DOI: 10.1016/S1387-1811(99)00167-5.

134 C. S. Triantafillidis, A. G. Vlessidis and N. P. Evmiridis, Dealuminated H-Y zeolites: influence of the degree and the type of dealumination method on the structural and acidic characteristics of H-Y zeolites, *Ind. Eng. Chem. Res.*, 2000, **39**(2), 307–319, DOI: 10.1021/ie990568k.

135 L. T. D. Santos, *et al.*, Mechanistic insights of CO_2-coke reaction during the regeneration step of the fluid cracking catalyst, *Appl. Catal., A*, 2008, **336**(1), 40–47, DOI: 10.1016/j.apcata.2007.10.005.

136 G. Tian, G. Wang, C. Xu and J. Gao, Coproduction of syngas during regeneration of coked catalyst for upgrading heavy petroleum feeds, *Ind. Eng. Chem. Res.*, 2013, **52**(47), 16737–16744, DOI: 10.1021/ie402527t.

137 T. Zhang and M. D. Amiridis, Hydrogen production via the direct cracking of methane over silica-supported nickel catalysts, *Appl. Catal., A*, 1998, **167**(2), 161–172, DOI: 10.1016/S0926-860X(97)00143-9.

138 J. Wang, M. Jiang, Y. Yao, Y. Zhang and J. Cao, Steam gasification of coal char catalyzed by K_2CO_3 for enhanced production of hydrogen without formation of methane, *Fuel*, 2009, **88**(9), 1572–1579, DOI: 10.1016/j.fuel.2008.12.017.

139 H. De Lasa, E. Salaices, J. Mazumder and R. Lucky, Catalytic steam gasification of biomass: catalysts, thermodynamics and kinetics, *Chem. Rev.*, 2011, **111**(9), 5404–5433, DOI: 10.1021/cr200024w.

140 Y. Zhang, D. Yu, W. Li, Y. Wang, S. Gao and G. Xu, Fundamentals of petroleum residue cracking gasification for coproduction of oil and syngas, *Ind. Eng. Chem. Res.*, 2012, **51**(46), 15032–15040, DOI: 10.1021/ie302103m.

141 Y. Zhang, *et al.*, Fundamental study of cracking gasification process for comprehensive utilization of vacuum residue, *Appl. Energy*, 2013, **112**, 1318–1325, DOI: 10.1016/j.apenergy.2012.12.075.

142 M. Sahimi and T. T. Tsotsis, Statistical modeling of gas-solid reaction with pore volume growth: kinetic regime, *Chem. Eng. Sci.*, 1988, **43**(1), 113–121, DOI: 10.1016/0009-2509(88)87132-X.

143 A. T. Aguayo, A. G. Gayubo, J. Ereña, A. Atutxa and J. Bilbao, Coke aging and its incidence on catalyst regeneration, *Ind. Eng. Chem. Res.*, 2003, **42**(17), 3914–3921, DOI: 10.1021/ie030085n.

144 R. Klingmann, R. Josl, Y. Traa, R. Gläser and J. Weitkamp, Hydrogenative regeneration of a Pt/La-Y zeolite catalyst deactivated in the isobutane/n-butene alkylation, *Appl. Catal., A*, 2005, **281**(1–2), 215–223, DOI: 10.1016/j.apcata.2004.11.032.

145 H. Schulz and M. Wei, Deactivation and thermal regeneration of zeolite HZSM-5 for methanol conversion at low temperature (260-290 °C), *Microporous Mesoporous Mater.*, 1999, **29**(1–2), 205–218, DOI: 10.1016/S1387-1811(98)00332-1.

146 P. Magnoux, H. S. Cerqueira and M. Guisnet, Evolution of coke composition during ageing under nitrogen, *Appl. Catal., A*, 2002, **235**(1–2), 93–99, DOI: 10.1016/S0926-860X(02)00242-9Art no. 6108.

147 P. Marecot, S. Peyrovi, D. Bahloul and J. Barbier, Regeneration by hydrogen treatment of bifunctional catalysts deactivated by coke deposition, *Appl. Catal.*, 1990, **66**(1), 181–190, DOI: 10.1016/S0166-9834(00)81636-X.

148 P. L. Walker Jr, S. Matsumoto, T. Hanzawa, T. Muira and I. M. K. Ismail, Catalysis of gasification of coal-derived cokes and chars, *Fuel*, 1983, **62**(2), 140–149, DOI: 10.1016/0016-2361(83)90186-2.

149 F. Bauer, H. Ernst, E. Geidel and R. Schödel, Reactivation of coked H-ZSM-5 by treatment with hydrogen and alkanes, *J. Catal.*, 1996, **164**(1), 146–151, DOI: 10.1006/jcat.1996.0370Art no. 0370.

150 S. J. Jong, A. R. Pradhan, J. F. Wu, T. C. Tsai and S. B. Liu, On the regeneration of coked H-ZSM-5 catalysts, *J. Catal.*, 1998, **174**(2), 210–218, DOI: 10.1006/jcat.1998.1971Art no. Ca981971.

151 F. Bauer, W. H. Chen, Q. Zhao, A. Freyer and S. B. Liu, Improvement of coke-induced selectivation of H-ZSM-5 during xylene isomerization, *Microporous Mesoporous Mater.*, 2001, **47**(1), 67–77, DOI: 10.1016/S1387-1811(01)00318-3.

152 A. Benamar, Z. Bechket, Y. Boucheffa and A. Miloudi, Transformation of *m*-xylene over an USHY zeolite: deactivation and regeneration, *C. R. Chim.*, 2009, **12**(6–7), 706–715, DOI: 10.1016/j.crci.2008.10.019.

153 G. A. Doka Nassionou, P. Magnoux and M. Guisnet, Comparative study of coking and regeneration of HEMT and HFAU zeolites, *Microporous Mesoporous Mater.*, 1998, **22**(1–3), 389–398, DOI: 10.1016/S1387-1811(98)00087-0.

154 J. M. Ortega, A. G. Gayubo, A. T. Aguayo, P. L. Benito and J. Bilbao, Role of Coke Characteristics in the Regeneration of a Catalyst for the MTG Process, *Ind. Eng. Chem. Res.*, 1997, **36**(1), 60–66, DOI: 10.1021/ie9507336.

155 N. Zhu, Y.-Y. Liu, Y. Wang, F.-Q. Chen and X.-L. Zhan, Kinetic Models for the Coke Combustion on Deactivated ZSM-5/MOR Derived from *n*-Heptane Cracking, *Ind. Eng. Chem. Res.*, 2010, **49**(1), 89–93, DOI: 10.1021/ie900855y.

156 Y. Nakasaka, T. Tago, H. Konno, A. Okabe and T. Masuda, Kinetic study for burning regeneration of coked MFI-type zeolite and numerical modeling for regeneration process in a fixed-bed reactor, *Chem. Eng. J.*, 2012, **207–208**, 368–376, DOI: **10.1016/j.cej.2012.06.138**.

157 S. Moon, H.-J. Chae and M. B. Park, Dehydration of Bioethanol to Ethylene over H-ZSM-5 Catalysts: A Scale-Up Study, *Catalysts*, 2019, **9**(2), 186. Available: **https://www.mdpi.com/2073-4344/9/2/186**.

158 R. Geng, *et al.*, Structure Evolution of Zn Species on Fresh, Deactivated, and Regenerated Zn/ZSM-5 Catalysts in Ethylene Aromatization, *ACS Catal.*, 2022, **12**(23), 14735–14747, DOI: **10.1021/acscatal.2c04074**.

159 M. M. Yung, *et al.*, Restoring ZSM-5 performance for catalytic fast pyrolysis of biomass: effect of regeneration temperature, *Catal. Today*, 2019, **323**, 76–85, DOI: **10.1016/j.cattod.2018.06.025**.

160 P. Castaño, G. Elordi, M. Olazar, A. T. Aguayo, B. Pawelec and J. Bilbao, Insights into the coke deposited on HZSM-5, Hβ and HY zeolites during the cracking of polyethylene, *Appl. Catal., B*, 2011, **104**(1), 91–100, DOI: **10.1016/j.apcatb.2011.02.024**.

161 O. Sánchez-Galofré, Y. Segura and J. Pérez-Ramírez, Deactivation and regeneration of iron-containing MFI zeolites in propane oxidative dehydrogenation by N_2O, *J. Catal.*, 2007, **249**(2), 123–133, DOI: **10.1016/j.jcat.2007.04.010**.

162 R. Josl, R. Klingmann, Y. Traa, R. Gläser and J. Weitkamp, Regeneration of zeolite catalysts deactivated in isobutane/butene alkylation: an in situ FTIR investigation at elevated H_2 pressure, *Catal. Commun.*, 2004, **5**(5), 239–241, DOI: **10.1016/j.catcom.2004.02.005**.

163 F. Gumerov, A. Sagdeev, R. Gallyamov, A. Galimova and K. Sagdeev, Regeneration of the Catalysts by Supercritical Fluid Extraction, *Int. J. Anal. Mass Spectrom. Chromatogr.*, 2014, **02**, 1–14, DOI: **10.4236/ijamsc.2014.21001**.

164 F. M. Gumerov, B. Le Neindre, T. R. Bilalov and A. A. Sagdeev, Regeneration of spent catalyst and impregnation of catalyst by supercritical fluid, *Int. J. Anal. Mass Spectrom. Chromatogr.*, 2016, **4**(4), 51–65.

165 S. D. Manjare and K. Dhingra, Supercritical fluids in separation and purification: a review, *Mater. Sci. Energy Technol.*, 2019, **2**(3), 463–484, DOI: **10.1016/j.mset.2019.04.005**.

166 S. Machmudah, A. Sulaswatty, M. Sasaki, M. Goto and T. Hirose, Supercritical CO_2 extraction of nutmeg oil: experiments and modeling, *J. Supercrit. Fluids*, 2006, **39**(1), 30–39, DOI: **10.1016/j.supflu.2006.01.007**.

167 D. H. Lee, Y.-H. Song, K.-T. Kim, S. Jo and H. Kang, Current state and perspectives of plasma applications for catalyst regeneration, *Catal. Today*, 2019, **337**, 15–27, DOI: **10.1016/j.cattod.2019.04.071**.

168 T. Kim, D. H. Lee, S. Jo, S. H. Pyun, K. T. Kim and Y. H. Song, Mechanism of the accelerated reduction of an oxidized metal catalyst under electric discharge, *ChemCatChem*, 2016, **8**(4), 685–689.

169 M. Strobel, M. Erguvan and S. Amini, Microwave-Assisted CO_2 Capture: Adsorption and Regeneration Performance in Monolithic and Fluidized Bed Reactors with Zeolite 13X, *J. Environ. Chem. Eng.*, 2025, 117395, DOI: **10.1016/j.jece.2025.117395**.

170 X. Duan, C. Srinivasakannan, W.-W. Qu, W. Xin, P. Jin-hui and Z. Li-bo, Regeneration of microwave assisted spent activated carbon: process optimization, adsorption isotherms and kinetics, *Chem. Eng. Process.*, 2012, **53**, 53–62, DOI: **10.1016/j.cep.2011.12.011**.

171 D. Xin-hui, C. Srinivasakannan, W.-W. Qu, W. Xin, P. Jin-hui and Z. Li-bo, Regeneration of microwave assisted spent activated carbon: process optimization, adsorption isotherms and kinetics, *Chem. Eng. Process.*, 2012, **53**, 53–62, DOI: **10.1016/j.cep.2011.12.011**.

172 N. M. Nor, M. F. F. Sukri and A. R. Mohamed, Development of high porosity structures of activated carbon via microwave-assisted regeneration for H_2S removal, *J. Environ. Chem. Eng.*, 2016, **4**(4), 4839–4845.

173 P.-o Amornsin, P. Nokpho, X. Wang, P. Piumsomboon and B. Chalermsinsuwan, Investigation of microwave-assisted regeneration of zeolite 13X for efficient direct air CO_2 capture: a comparison with conventional heating method, *Sci. Rep.*, 2025, **15**(1), 18376, DOI: **10.1038/s41598-025-02074-z**.

174 B. Whittington and N. Milestone, The microwave heating of zeolites, *Zeolites*, 1992, **12**(7), 815–818.

175 X. Zhang, D. O. Hayward and D. M. P. Mingos, Effects of Microwave Dielectric Heating on Heterogeneous Catalysis, *Catal. Lett.*, 2003, **88**(1), 33–38, DOI: **10.1023/A:1023530715368**.

176 M. M. Yassin, S. Biti, W. Afzal and C. F. Martín, A systematic analysis of the dynamics of microwave-and conventionally-assisted swing adsorption on zeolite 13X and an activated carbon under post-combustion carbon capture conditions, *J. Environ. Chem. Eng.*, 2021, **9**(6), 106835.

177 Y. Gomez-Rueda, B. Verougstraete, C. Ranga, E. Perez-Botella, F. Reniers and J. F. Denayer, Rapid temperature swing adsorption using microwave regeneration for carbon capture, *Chem. Eng. J.*, 2022, **446**, 137345.

178 K.-M. Lee, Y.-H. Lim and Y.-M. Jo, Evaluation of moisture effect on low-level CO_2 adsorption by ion-exchanged zeolite, *Environ. Technol.*, 2012, **33**(1), 77–84.

179 X. Li, S. Wang and C. Chen, Experimental study of energy requirement of CO_2 desorption from rich solvent, *Energy Proc.*, 2013, **37**, 1836–1843.

180 G. Gecim, Y. Ouyang, S. Roy, G. J. Heynderickx and K. M. Van Geem, Process intensification of CO_2 desorption, *Ind. Eng. Chem. Res.*, 2022, **62**(45), 19177–19196.

181 G. Lin, *et al.*, Process optimization of spent catalyst regeneration under microwave and ultrasonic spray-assisted, *Catal. Today*, 2018, **318**, 191–198, DOI: **10.1016/j.cattod.2017.09.042**.

182 Z. Zhang, *et al.*, Comparison between microwave and conventional thermal reactivations of spent activated carbon generated from vinyl acetate synthesis, *Desalination*, 2009, **249**(1), 247–252.

183 C. Ania, J. Menéndez, J. Parra and J. Pis, Microwave-induced regeneration of activated carbons polluted with

phenol. A comparison with conventional thermal regeneration, *Carbon*, 2004, **42**(7), 1383–1387.

184 D. Xin-hui, C. Srinivasakannan and L. Jin-sheng, Process optimization of thermal regeneration of spent coal based activated carbon using steam and application to methylene blue dye adsorption, *J. Taiwan Inst. Chem. Eng.*, 2014, **45**(4), 1618–1627.

185 C. Ania, J. Parra, J. Menéndez and J. Pis, Effect of microwave and conventional regeneration on the microporous and mesoporous network and on the adsorptive capacity of activated carbons, *Microporous Mesoporous Mater.*, 2005, **85**(1–2), 7–15.

186 V. Cremers, R. L. Puurunen and J. Dendooven, Conformality in atomic layer deposition: current status overview of analysis and modelling, *Appl. Phys. Rev.*, 2019, **6**(2), 021302, DOI: **10.1063/1.5060967**.

187 S. M. Kim, *et al.*, Structural insight into an atomic layer deposition (ALD) grown Al_2O_3 layer on Ni/SiO_2: impact on catalytic activity and stability in dry reforming of methane, *Catal. Sci. Technol.*, 2021, **11**(23), 7563–7577, DOI: **10.1039/D1CY01149A**.

188 B. J. O'Neill, *et al.*, Catalyst Design with Atomic Layer Deposition, *ACS Catal.*, 2015, **5**(3), 1804–1825, DOI: **10.1021/cs501862h**.

189 G. Zhang, Y. Xu, H. He, Z. He and S. Li, A kind of supported platinum-based three-way catalyst regeneration method, *China Pat.*, CN202110294324.0A, Beijing University of Technology, 2021, **https://patents.google.com/patent/CN113058597A/en**.

190 S. M. Kim, *et al.*, Structural insight into an atomic layer deposition (ALD) grown Al_2O_3 layer on Ni/SiO_2: impact on catalytic activity and stability in dry reforming of methane, *Catal. Sci. Technol.*, 2021, **11**(23), 7563–7577.

191 P. Tufvesson, W. Fu, J. S. Jensen and J. M. Woodley, Process considerations for the scale-up and implementation of biocatalysis, *Food Bioprod. Process.*, 2010, **88**(1), 3–11.

192 J. W. Burnett, Z. Sun, J. Li, X. Wang and X. Wang, Comparative life cycle assessment of NAD (P) H regeneration technologies, *Green Chem.*, 2021, **23**(18), 7162–7169.

193 A. M. Rojas Márquez, I. B. Vega Erramuspe, B. K. Via, B. Sastri and S. Banerjee, Regeneration of Spent Desiccants with Supercritical CO_2, *Ind. Eng. Chem. Res.*, 2024, **63**(49), 21154–21157, DOI: **10.1021/acs.iecr.4c03636**.

194 Y. Wang, G. Wu, Y. Zhang, Y. Su and H. Zhang, The deactivation mechanisms, regeneration methods and devices of activated carbon in applications, *J. Cleaner Prod.*, 2024, **476**, 143751, DOI: **10.1016/j.jclepro.2024.143751**.

195 M. J. Sanchez-Montero, J. Pelaz, N. Martin-Sanchez, C. Izquierdo and F. Salvador, Supercritical Regeneration of an Activated Carbon Fiber Exhausted with Phenol, *Appl. Sci.*, 2018, **8**(1), 81. Available: **https://www.mdpi.com/2076-3417/8/1/81**.

196 H. Nigar, I. Julián, R. Mallada and J. Santamaría, Microwave-Assisted Catalytic Combustion for the Efficient Continuous Cleaning of VOC-Containing Air Streams, *Environ. Sci. Technol.*, 2018, **52**(10), 5892–5901, DOI: **10.1021/acs.est.8b00191**.

197 Y. Sun, T. Zheng, G. Zhang, Y. Zheng and P. Wang, Effect and mechanism of microwave-activated ultraviolet-advanced oxidation technology for adsorbent regeneration, *Environ. Sci. Pollut. Res.*, 2018, **25**(1), 290–298, DOI: **10.1007/s11356-017-0320-8**.

198 F. Lin, *et al.*, Catalyst deactivation and its mitigation during catalytic conversions of biomass, *ACS Catal.*, 2022, **12**(21), 13555–13599.

199 C. j Liu, J. Ye, J. Jiang and Y. Pan, Progresses in the preparation of coke resistant Ni-based catalyst for steam and CO_2 reforming of methane, *ChemCatChem*, 2011, **3**(3), 529–541.

200 J. P. Lange, Renewable feedstocks: the problem of catalyst deactivation and its mitigation, *Angew. Chem., Int. Ed.*, 2015, **54**(45), 13186–13197.